Renewables

REVIEW

Received: Apr. 25, 2023 I Accepted: June 20, 2023 I Published: July 25, 2023

Advancements in Seawater Electrolysis: Progressing from Fundamental Research to Applied Electrolyzer Application

Jinfa Chang[1,20] & Yang Yang H,s.[6].

'NanoScience Technology Center, University of Central Florida, Orlando, Florida 32826, 'Faculty of Chemistry, Key Laboratory of Polyoxometalate and Reticular Material Chemistry of Ministry of Education, Northeast Normal University, Changchun 130024, [3]Department of Materials Science and Engineering, University of Central Florida, Orlando, Florida 32826, [4]Renewable Energy and Chemical Transformation Cluster, University of Central Florida, Orlando, Florida 32826, [5]Department of Chemistry, University of Central Florida, Orlando, Florida32826, [6]TheStephen W. Hawking Centerfor Microgravity Research and Education, University of Central Florida, Orlando, Florida 32826

•*corresponding authors: changjinfa@nenu.edu.cn; yangyang@ucfedu*

Cite this: *Renewables* 2023, ,, 415-454
DOI: 10.31635/renewables.023.202300034

Seawater electrolysis (SWE) provides a promising and efficient pathway to produce green hydrogen. However, the current SWE technology confronts a lot of challenges, such as the sluggish reaction kinetics on the anode side, and a lot of impurities and ions in seawater that poison the active sites of the catalyst and block membrane pores. In addition, the existence of chloride ions (cl-) in seawater will strongly compete with oxygen evolution reaction (OER) by the chlorine oxidation/evolution reaction (CIOR/CIER) on the anode side as a result of the extremely similar thermodynamic potentials. Thus, to move SWE much closer to commercialization, it is highly desirable to enhance not only the activity of electrocatalysts but also the selectivity and stability of efficient OER to restrain CIOR/CIER. At the same time, the additive of electrolytes and the unique structural design of the electrolyzer also promote the development of SWE. In this review, the fundamental mechanisms for SWE and water electrolysis are first introduced and compared. Then, the design principles of efficient catalysts, electrolytes, surface/interface engineering, and novelty reaction device are critically, comprehensively summarized and analyzed. Finally, perspectives, challenges, and opportunities to develop and boost SWE technologies are proposed.

Keywords: seawater electrolysis, water oxidation reaction, chlorine oxidation reaction, competing reaction, selectivity

DOI: 1o.31635/renewables.023.202300034
Citation: *Renewables* 2023, 1, 415-454
Link to VoR:https://doi.org/10.31635/renewables.023-202300034

Introduction

Sufficient energy is essential for the rapid development of human society and the economy. Nonrenewable fossil fuels, such as coal, oil, and natural gas, continue to be heavily relied upon for the current energy supply.[1] Currently, these nonrenewable resources account for ~80% of the world's energy.[2,3] The overuse of fossil fuels has resulted in an energy crisis, which has led to severe environmental pollution and global climate change due to the emission of greenhouse gases, specifically carbon dioxide (CO_2).[3] These issues are expected to constrain further development of society and adversely impact normal production and the daily lives of human beings. Governments worldwide have recognized these problems and proposed protocols to address them.[4,5] The concepts of carbon peak and carbon neutrality (the double carbon target) have gained widespread acceptance in the international community.[6-8] The double carbon target requires the development of clean, efficient energy harvesting and storage technologies with net-zero carbon emissions. Fuel cells[9] and water electrolysis (WE)[10] technologies are widely recognized as the most promising options for achieving the double carbon target.

The WE reaction isthe reverse reaction ofH_2-O_2fuel cells.[11,12] In the fuel cell reaction, H_2 and O_2 are fed into the anode and cathode sides, respectively, generating electric energy and water. Fuel cell technology is not subject to the Carnot limit and can effectively extract more energy from hydrogen fuel than traditional internal combustion engines.[13,14] Its high efficiency and zero pollution with zero carbon emissions make fuel cell technology an ideal candidate to replace traditional fossil fuel technology.[15] As the reverse reaction of the fuel cell reaction, WE technology provides a sustainable, clean, effective, and green pathway for hydrogen production compared to the traditional method of fossil fuel disintegration.[16] WE can be driven by renewable but intermittent energy sources (such as the sun, wind, and tides), allowing for the storage of this intermittent energy in chemical form.[13,16-18] When combined with fuel cell and WE technology, the hydrogen/oxygen-water cycle can be easily realized, which is a crucial requirement for the development of renewable energy technologies in the future.[19]

Even though water splitting is a promising technology for producing green hydrogen, currently, over 95% of the hydrogen used in the industrial community still largely relies on steam methane/methanol-reforming and coal gasification.[16] The high cost of **WE** technology, particularly due to the expensive and scarce platinum group metals **(PGMs}**widely used as catalystsin the anode and cathode, significantly limits the commercial application of this technology. It should also be noted that, for commercial WE such asthe widely used alkaline/anion exchange membrane **(AEM}** and proton exchange membrane (PEM} WE, highly purified water is generally used as a reactant." Even tiny anions or cation impurities can result in serious performance decay. If WE technology is used to produce hydrogen in the future, it is important to keep in mind that freshwater **will** be used and consumed rapidly as the only reactant, leading to water shortages and crisesin normal domestic watersupplies.In contrast, seawater is more abundant than freshwater, with seawater accounting for 96.5% of the Earth's total water resources[22] (Figure 1). If seawater can be used as a reactant to replace freshwater in WE, it would be much more economical and sustainable than pure WE.

Using seawater as an alternative reactant offers many advantages. First, seawater is easy to obtain at no cost, as it is widely distributed throughout the world. By combining seawater with seawater electrolysis (SWE} and fuel cell technologies, it is possible not only to produce clean freshwater for arid regions but also to provide efficient technologiesfor energy storage and conversion. Second, seawater itself is a natural electrolyte without any additives, and its conductivity (5 S m^{-1}) is much higher than that of pure water ($5.5 \cdot 10^{-6}$ S m^{-1}).[3] With a salt content of ~3-5%, seawater is equivalent to a 0.5 M sodium chloride (NaCl} electrolyte[3] Its high conductivity makes it possible to perform direct electrolysis without the need for additional conductive electrolytes (such as KOH or NaOH for AEMWE and H_2SO_4 or $HClO_4$ for acid PEMWE} that are typically used in pure water.[24,25] Third, using seawater as the reactant can significantly reduce the chemical corrosion of electrocatalysts and electrolyzer devices, as it does not require the use of strong acid or alkaline electrolytes. Finally,the production of marine offshore hydrogen through the integration of SWE and marine renewableenergies,

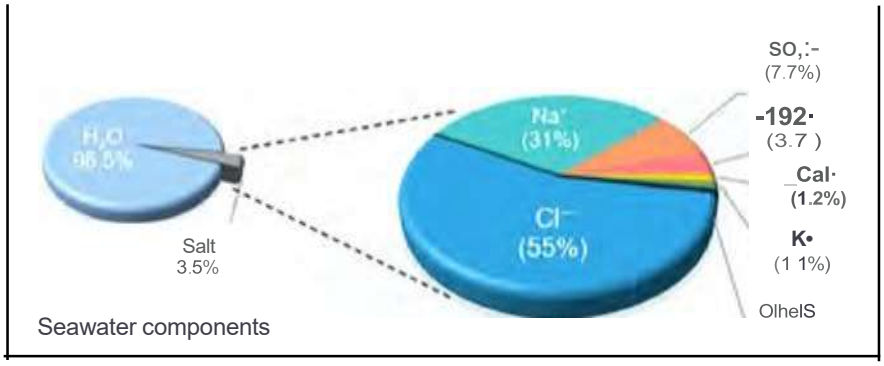

Figure 1 | *A chart showing the distribution of various elements in seawater. Reprinted with permissionfrom Ref. 22 Copyright 2020 Royal Society of Chemistry.*

DOI: 10.31635/renewables.023.202300034
Citation: *Renewab/es* **2023,** 1, 415-454
Link to VoR:https://doi.org/10.31635/renewables.023-202300034

such as wind and solar, presents a promising and sustainable solution to address the energy demands of developed nations such as the US in the future. As per the Wind Energy Technologies Office of the US Department of Energy, the coastal regions of the US, including state and federal waters along with the Great Lakes, have the potential to generate over 7200 terawatt-hours of energy annually.[3] Therefore, the cost-effective and efficient production of hydrogen from SWE presents a hopeful approach to storing offshore wind energy obtained from renewable sources.[6]

According to Driess et al.,[26] generating the entire world's electricity from hydrogen would result in a mere 0-4% usage of global freshwater. Hence, researchers hold the belief that current hydrogen production technology makes it viable and cost-effective to use freshwater in the process of water splitting. However, this approach is impractical for some countries/regions, where freshwater is scarce due to the uneven distribution of water resources. [27] In other words, the attainment of a complete hydrogen economy may result in an increase of ~10% in freshwater consumption. According to Kibria and colleagues,[27] the cost of a desalination system is~3% of the cost of a PEMWE, which is $460 **kw-•.** Thus, a desalination system should cost around $14 **kw-•.** The capital cost of an alkaline electrolyzer is $200 **kw-•,** and it can be further reduced with advances in electrolyzer design. This implies that the desalination system can be up to 7% of the cost of an alkaline electrolyzer, which cannot be ignored. Moreover, it should be noted that seawater desalination leaves behind some ions. Hence, developing seawater-tolerant electrocatalysts through surface/interface engineering and designing novel electrolyzers can be useful in improving long-term performance when using desalinated water for electrolysis. Therefore, generating hydrogen through direct SWE remains critical and urgent for replacing current WE technologies.

The process of pure WE consists of two half-reactions, namely the hydrogen evolution reaction (HER} occurring at the cathode and the oxygen evolution reaction (OER} taking place at the anode. To accelerate the sluggish reaction kinetics, both sides require high-efficiency catalysts. The same principle and related reactions apply to SWE; however, impurities such as Mg2+,Ca^{2}+, Na•, er-, Br-, $SO_4^{'-}$, bacteria, small particles, and microorganisms are more common in seawater (Figure 1). Consequently, SWE faces more challenges than WE. For instance, the biggest challenge is the competitive reaction between chloride oxidation/evolution reaction (CIOR/CIER} and OER onthe anode side due to their adjacent thermodynamic reaction potentials. Moreover, impurity ions, bacteria, and microorganisms can poison the catalyst and block the active sites of the catalyst and porous structure of the membrane, which can result in a significant decline in SWE performance. Additionally, direct SWE can lead to severe corrosion issues due to the decreased local pH value near the electrode, which is detrimental to both electrocatalysts and electrolyzer components. Hence, promoting the commercialization of SWE requires addressing the above critical issues.

In this review, we first introduce the mechanism of WE, followed by a discussion of the possible side reactions for SWE. We compare the thermodynamic and dynamic insights of WE and SWE to identify and screen potential selective electrocatalysts. Next, we summarize current strategies to engineer active sites, improve the activity and stability of the catalyst, and establish a structure-performance relationship. We also review innovative and smart designs of electrolytes and electrolyzers. Finally, we propose future challenges and opportunities for catalysts, electrodes, electrolytes, and electrolyzers, from fundamental research to applied electrolyzer applications. We believe that this review **will** create new avenues for tackling the challenges encountered in SWE.

Fundamental and Challenge Aspects of SWE

Reaction mechanism

The water-splitting reaction, which involves converting water (H_2O) into hydrogen (HJ and oxygen ($0_{2)}$, has a positive Gibbs free energy (G) value of +237.2 kJ mor-• for each mole of H_2 produced. This makes it a thermodynamically uphill process.[18] Therefore, external electrical energy, with a minimum voltage of 1.23 V, is required to facilitate the reaction.[19-31] The reaction can occur in both acidic and alkaline solutions, where Wand *OW* ions participate, respectively. The two half-reactions can be expressed differently depending on the reaction environment (SHE represents the standard hydrogen electrode}.[s,31]

In acid conditions:

Anode:

$$2H_2O \rightarrow 4H^+ + O_2 + 4e^- \quad E = 1.23 \text{ V vs SHE} \qquad (1)$$

Cathode:

$$2H^+ + 2e^- \rightarrow H_2 \quad E = 0 \text{ V vs SHE}$$

In alkaline conditions:

Anode:

$$4OH^- \rightarrow 2H_2O + O_2 + 4e^- \quad E = 0.4 \text{ V vs SHE} \qquad (3)$$

Cathode:

$$2H_2O + 2e\text{-} H_2 + 2OW \qquad E = -0.83 \text{ V vs SHE} \qquad (4)$$

From eqs 1-4, it isevident that the OER with a 4e pathway isa kinetically sluggish reaction compared to the HER, which only followsa 2e pathway.In acidic solutions, the HER ispreferred due to the high concentration of protons (W), while in alkaline solutions, the OER is more favorable because of the availability of hydroxide ions (OW}.

Compared to strong acidic and alkaline solutions, seawater is a neutral solution with a pH of around 8.o. Direct SWE without any additives is more challenging than electrolysis in acidic or alkaline solutions due to the absence of Wand *OW.* Generally, both HERand OER exhibit sluggish kinetics in SWE. Additionally, seawater contains a high concentration of impurity ions. The catalyst can be poisoned, and the membrane's pores can be blocked byvarious substances, including Ca^{2}+,Mg>+, er-, bacteria, microbes, and small particles coming from seawater, leading to a decline in performance over time. One of the major obstacles is

DOI: 10.31635/renewables.023.202300034
Citation: *Renewab/es* 2023,, 415-454
Link to VoR:https: /doi.org/10.3'1635/renewables.023-202300034

the elevated levels of cl- in seawater, which can trigger unwanted side reactions. For instance, in alkaline solutions, it may cause a CIER, while in acidic solutions, it may result in a CJOR. These side reactions can reduce electrolysis efficiency, and the production of chlorine (Cl,) or hypochlorite (clO-) can significantly alter the electrolyte's pH and corrode the electrode, the electrocatalysts, and the electrolyzer. Therefore, developing highly active, stable, and selective catalysts for SWE is an urgent priority. Furthermore, there is a pressing need for the development of efficient and robust electrolytes and electrolyzers.

Challenges of SWE on the anode side

As previously stated, the anodic OER reaction in WE proceeds sluggishly due to its four-electron transfer mechanism. Consequently, this lowers the overall energy conversion efficiency of the process. Additionally, due to the lower concentration of *OW* in seawater compared to alkaline solutions, additional procedures are necessary for the adsorption and dissociation of water to produce adsorbed oH· during SWE. As a result, achieving a current density of 10 mA cm-^{2} in neutral SWE typically requires an overpotential of more than 0.25 v_v.-[34] The high concentration of chloride ions in seawater creates competition between ClOR/CIER and OER at the anode. Strasser et al.[35] listed the potential redox reactions with the species (Figure 2) found In seawater. Based on the computed Pourbaix diagram, it is evident that the chlorochemistry in a 0.5 M chloride solution at ambient temperature is contingent upon the pH level.

In acid conditions:

$$2Cl^- \rightarrow Cl_2 + 2e^- \qquad E = 1.36\ \text{V vs SHE} \qquad (5)$$

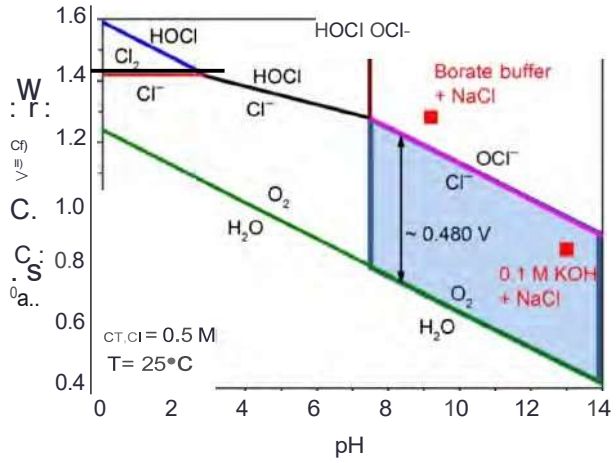

Figure 2 | *An artificial seawater model is shown on the Pourbaix diagramfor the chlorine system. In addition, the electrode potentialfor DER is provided, based on an oxygen partial pressure of 0.21 atm. Two red squares on the diagram display the operating potentials (vs SHE) that were obtainedfrom 1-h constant current electrolysis (10 mA cm-') using NiFe LOH catalyst. The suggested design criterion is emphasized in a light blue box. Reprinted with permission from Ref 35. Copyright 2016 Wiley.*

In alkaline conditions:

$$Cl^- + 2OH^- \rightarrow ClO^- + 2H_2O + 2e^- \qquad E = 0.89\ \text{V vs SHE} \qquad (6)$$

It can be seen from eqs 5 and 6 and the Pourbaix diagram (Figure 2) that Cl, is more likely to form in acidic conditions, while clO- is more likely to be generated in alkaline or neutral solutions. The most challenging anode reaction for SWE is asfollows: (1)The highcontent of impurity cl- ionsin seawater results in ClOR/CIER, which strongly competes with OER at a high potential. The ClOR/CIER has a much faster kinetic reaction rate since it isa 2e process (eqs 5 and 6), which is more kinetically favorable than the OER with a 4e process (eqs 1 and 3). On the contrary, OER is thermodynamically preferred over ClOR/CIER, especially in solutions with high alkalinity. The OER always has a 0-48 V standard potential lower than ClOR/CIER in alkaline seawater. While ClOR/CIER has much faster kinetics than OER with the decreased pH from neutral to acid solutions, most of the current studies focus on SWE in alkaline conditions to inhibit the competition from ClOR/CIER. (2) The presence of abundant impurities such as Ca^{2}· and Mg^{2+} ions, microorganisms, bacteria, and fine particles in seawater can impede the transmission of *OW* through the membrane channel and contaminate the cationic groups of the ionomer. Besides,the high concentration of ca>+and Mg^{2+} may further form hydroxide/carbonate precipitates, which willblock the pore structure of the membrane and catalysts, resulting in catalyst/membrane poisoning. These not only decrease the activity and stability of catalysts but also cause membrane degradation. (3) The dramatic local pH change near the electrode has been found.',., [36] Since seawater is natural, very low concentrations of free W/OH- are in it. Studies indicate that atthe anode OER sides, there could be a pH shift of 5 to 9 units near the electrode surface even with a low current density of 10 mA cm-•_ms The unstable electrolysis system caused by the significant pH alteration near the electrode surface leads to catalyst degradation.

Challenges of SWE on the cathode side

The HER is the main cathode reaction for both WE and SWE. Unlike the strong competition between ClOR/CIER and OER, there is no competing reaction with HER on the cathode side of SWE. However, during the reaction, impurity ions such as Ca,. and Mg,. in seawater combine with hydroxide and get deposited on the cathode side, leading to a decay in performance. More than half of the cathode's performance decay was found in neutral seawater due to hydroxide deposition.[24,,5] When using the traditional method, real devices experienced significant degradation in performance and electrocatalyst corrosion.These issues ultimately resulted in electrolysis failure within just one hour of operation and the appearance of milky-white tlocculent precipitates.[15] Therefore, developing advanced catalysts, electrolytes, and electrolyzer devices to mitigate or eliminate these issues is a big challenge. Strategies, such as surface/interface engineering, designing a unique 3D structure, and controlling the local microenvironment of electrode materials, have been developed, and some useful reviews have systematically summarized the HER side of seawater.3.2[8-44]

DOI: 10.31635/renewables.023.202300034
Citation: *Renewab/es* 2023, 1, **415-454**
Linkto VoR:https://doi.org/10.31635/renewables.023-202300034

Theoretical aspects of OER versus CER

Whether in acid or alkaline solutions, iridium (Ir)- and ruthenium (Ru)-based oxides are widely acknowledged as the most active monometallic materials for OER.'&-,BAs-[49] However, the conventional Ir0 $_2$ or Ru0 $_2$-based materials also show high activity for ClOR/ClER.[50,51] The strong competition between ClOR/ClER and OER makes them suboptimal choices for selective OER in seawater or simulated seawater {SSW).To comprehensively understand the selectivity of the electrocatalyst for OER and ClERI ClOR, it is crucial to conduct critical thermodynamic and kinetic assessments. Over's group[52] carried out extensive studies on conventional electrocatalysts such as RuO_2 for OER. They determined the free energies, transition states (TS}, and reaction intermediates (RI) during OER or ClER/ClOR in the alkaline or acidic medium on single-crystal models RuO_2(110). RuO_2(110) with a single crystalline surface consisting of uncoordinated Ru sites (Rucus) was capped with on-top oxygen (O.,J and bridging oxygen (Di,,}, partially saturated by hydrogen (denoted as OHb,}, depending on the overpotential {Figure 3a). The Pourbaix diagram (Figure 3a) indicates that the 0-capped RuO_2 surface is stable over a broad potential and pH range, in which both OER and ClER/ClOR may take place. For ClER/ClOR, the most stable phase involves the combination of (10br10Hbr + 20$_0$J on the RuO_2 surface.The Volmer-Heyrovsky mechanism was considered the most favored among the three mechanisms (i.e., Volmer-Tafel, Volmer-Heyrovsky, and Krishtalik mechanisms) that have been proposed to explain the ClER/ClOR reaction. The Volmer-Heyrovsky mechanism was considered the most favorable, involving the adsorption and discharge of chloride ions to form a RI of Ru-0$_0$tCl through the Volmer step (eq 7), followed by the recombination of adsorbed chlorine with free chloride in the Heyrovsky step (eq 8), leading to the release of Cl_2 as described below:

$$\text{Ru-0}_0\text{t+2Cl-RU-0}_0\text{tCl+e- +cl-} \quad \text{(Volmer step)} \quad (7)$$

$$\text{Ru-0}_0\text{tCl+c1-Ru-0}_0\text{t+C1}_2\text{+e-} \quad \text{(eyrovsky step)} \quad (8)$$

Over et al.[52] also analyzed the ClER/ClOR mechanism by altering the overpotential ('lrnJ > o V. They presented their findings in a Tafel plot acquired in acidic pH and a free energy diagram (Figure 3b}. The diagram indicated that when the

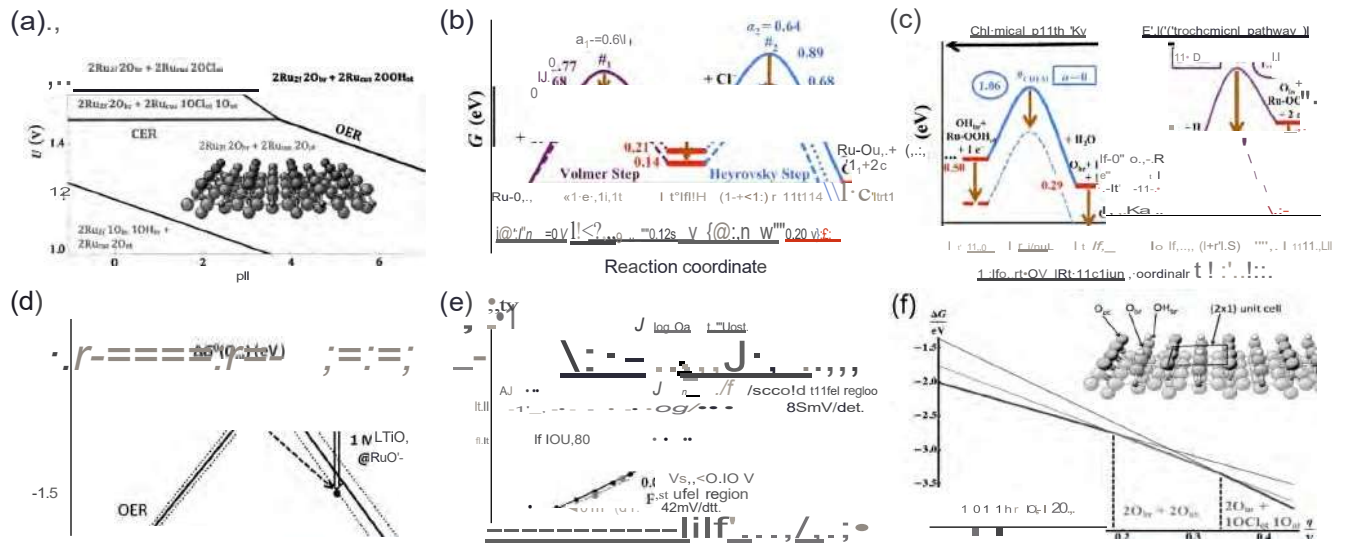

Figure 3 | *(a-d)The thermodynamics of RuO,(11o}for OER and CIER. (a) A Pourbaixdiagramisshown in equilibrium with H+,*C,, *and* H_2O *at T = 298 Kand a(c1-J = 1, indicating the various surface combinations of RuOi110). Reprinted with permissionfrom Ref 53. Copyright 2014 Wiley. (b and c) A free-energy diagramfor CIER (b) via Volmer-Heyrovsky mechanism at different overpotentials, and for OER (c) depicting two competing reactions, chemical and electrochemical, and their pathways at different overpotentials. Reprinted with permissionfrom Ref 52 Copyright 2014 Wiley. (d) A volcano diagram is presentedfor CIER (gray) and OER (black). Thegray cross denotes the catalytic activity (LIG1o,J for the CIER, and the black cross isfor the OER. The manipulation of the* LIG,.,,$_1$*values is demonstrated with TiO,(11o)@*RuO_2*(110) as an example, demonstrating selectivity among the OER and CIER. Reprinted with permission from Ref 53. Copyright 2014* ***Wiley.*** *(e) Thetheoretically calculated Tafel plot (black dots)for the CIER on RuO,(110) shows excellent agreement with the experimental Tafel plot (gray dots). In the first Tafel region, the applied overpotential strongly affects the surface coverage of chlorine* Be, *(inset), while in the second Tafel region, the chlorine coverage remains approximately constant. (f} Thestable surface terminations of the* RuO_2 *(110) model catalyst under different overpotentials, while in equilibrium with J-r, Cl-, and H,O. This was done at a temperature of T = 298.15 Kand pH o, with a(C/1 = 1. The surface structures were denoted using a (2 x 1) unit cell, which encompassed all surface species exceptfor the attached metal atom.The surface structure identified as (2Gb,+2Oot} consisted of two Ob, bridges linking two* Ru_{2f} *sites and two on-top oxygen atoms (*O_0J *attached to Rucu, sites. The structural depiction employed a stick and ball model, with theoxygen atoms represented by large black balls. Reprinted with permission from Ref 51. Copyright 2016 Wiley.*

DOI: 10.31635/renewables.023.202300034
Citation: ***Renewab/es*** **2023,** 1, **415-454**
Linkto VoR:https://doi.org/10.31635/renewables.023-202300034

overpotential value was high, the Heyrovsky step became the rate-determining step with a considerably high TS free energy value. However, the TS free energy could be reduced by increasing the overpotential, particularly in the Heyrovsky step where it's lowered more than in the Volmer step at 11cER > 0.20 V.

Compared to CIER/CIOR, OERproceeds through a four-electron transfer, resulting in a slower kinetic process. To study OER, the fully 0-capped $Ru0_2$(110} surface was utilized by coordinatively capping uncoordinated Rucus atoms with Oot as the top oxygen under acidic pH. The mechanism of OER was explained in four steps, as shown in eqs 9-12.si-[53]

$$20_0t+H_20\ Ru\text{-}10_0t100H_0t+H++e- \quad (9)$$

$$10_0t100H_0t\ 10\ t+H++e- \quad (10)$$

$$10\ t+H_20\ 10_0t10H_0t+H++e- \quad (11)$$

$$10ot10Hot\ 20ot+H++e- \quad (12)$$

According to Over's study? water split results in the adsorptionof OH* on the 0_0t site or *W* adsorption onto Ob,to form OHbr or the release of *W* into the electrolyte. In Figure 3c, the free energy diagram for OER displays two competing reaction pathways, one chemical and the other electrochemical, demonstrating the formation of corresponding RIs. The diagram showcases the alteration of pathways at variousoverpotential values, at the reversible electrode potential, l]oER = o V, and at l]oER > 0.3 V. At low overpotential values (lJoER < 0.3 V},the active {OHbr + $Ru\text{-}0_0$J surface combinationinitiates the OER mechanism, which follows the chemical pathway in the blue line (Figure 3c}. However, at l]oER > 0.3 V, the active site combination shifts to the (Ob, + $Ru\text{-}0_0$J surface combination, leading the reaction through the electrochemical pathways shown in the violet line in Figure 3c. Interestingly, at lJoER > 0.3 V, the TS for the electrochemical pathway {#EC} becomes lower than the chemical pathway's {#CHEM}. As a result, the electrochemical path becomes more favorable.

Expressing the activity for OER and CIER/CIOR with $aG_{10..}$, which represents the unfavorable Gibbs free energy change at the equilibrium potential, computational studies have found that thethermodynamic barrier for both reactions on the model $Ru0_2$(110} surface is not zero. Thus, suggesting an opportunity to manipulate the 0-capped $Ru0_2$ surface for selective catalytic reactions. The hypothesis was supported by a volcano diagram shown in Figure 3d, which represents the free oxygen adsorption energy. In the diagram, highervalues of aG^0{0ot}indicate limited cl- desorption, whereas smaller values lead to limited cl- adsorption for CIER/CIOR. In contrast, for OER, higher aG^0(0 J values indicate OOHot decomposition, whereas smaller values facilitate the restricted formation of OHot· It should be noted that both cases demonstrate maximum activity in the middle of the higher and smaller values. Although the volcano plot for CIER/CIOR is flat compared to OER, the slope's difference reflects the distinct number of RIs, i.e., 1 for CER and 3 for OER. The gap in aG,os, values at a specific aG^0{0 J defines the selectivity and can be measured by aG,e,- In this context, weakening the Ru-0 bond, i.e., lowering the OER catalytic activity or using a $Ti0_2$(110} monolayer on $Ru0_2$(110}, can provide substantial selectivity.

Based on the Tafel plot in Figure 3e, Over et al.[51]also found a theoretical representation of the relationship between overpotential and current density. The plot reveals two regions **with** Tafel slopes of 42 mV dee-• for 11 < 0.1Vand 85 mV dee-• for 11 > 0.15 V. The current density *j* is dependent on the rate-determining reaction step and the exchange current density *jo,*which is a function of the surface coverage $0c_1$of chlorine on the catalyst's surface.The study found that $0c_1$was strongly dependent on the applied overpotential. In the first Tafel region, $0c_1$ increases significantly by several orders of magnitude, whereas for higher overpotentials, the chlorine surface coverage varies much less dramatically.Therefore, the change in the Tafel slope was mainly ascribed to the variation of chlorine surface coverage, while the rate-determining reaction step remained unchanged. Besides, it is also found that the electrocatalytic activity of the (110) rutile surface is linked to the existence of two types of surface oxygen atoms under the reaction condltions.[51] The first type is found to form a bridge between two adjacent Ru atoms along the [001] direction, as depicted in Figure 3f; this type of oxygen is not believed to influence either OER or CIOR. The second type, denoted as coordination-unsaturated {Ocus}, is involved in only one Ru-0 bond.Thus,the selectivity of OER suppressing the CIOR was a challenging target with $Ru0_2$ and $Ir0_2$.

Rational design of OER and HER catalysts

Developing low-cost catalysts with high activity, selectivity, and stability is crucial, especially in seawater electrolytes.[54-58] Over the last few decades, numerous researchers have investigated new electrocatalysis for seawater splitting, including noble metal, nonnoble metal, and metal-free materials. Techniques such as elemental doping, protective layer construction, surface morphology modulation, and active-site regulation have been proposed to enhance the surface structure and electronic states of the materials. This increases the intrinsic activity of catalytic sites, protects the sites from corrosion/poisoning, and exposes more active areas. By adjusting the morphology and size of the catalysts, their activity and long-term stability can be improved. Further, bonding regulation and elemental doping can adjust the electronic states of individual sites to improve the intrinsic activity of the catalyst. Mutually bonding different metals can optimize the adsorption-free energy of the OER/HER intermediates {Figure 4a,b}, thereby reducing the energy barriers during seawater splltting.[59] Incorporating metals such as Fe can decrease the HER/OER energy barrier and enhance the catalytic activity of electrode materials[60] (Figure 4c-e}. Fe-doping was observed to enhance HER activity dueto the much lower limiting potential for HER (-0.28 V} compared to the undoped control samples (-o.6o V}, as surface Fe atoms were more favorable for H* adsorption than Ni atoms {Figure 4c}. Figure 4d shows the predicted free energy evolution of OER on $NiSe_2$ and Fe-$NiSe_2$. The limiting potential ofOER on Fe-$NiSe_2$ (1.71V} was much lower than $NiSe_2$ (1.82 V}. Additionally, the limiting potential of OER on

DOI:10.31635/renewables.023.202300034
Citation: *Renewab/es* 2023, ,, 415-454
Link to VoR:https: /doi.org/10.3'1635/renewables.023-202300034

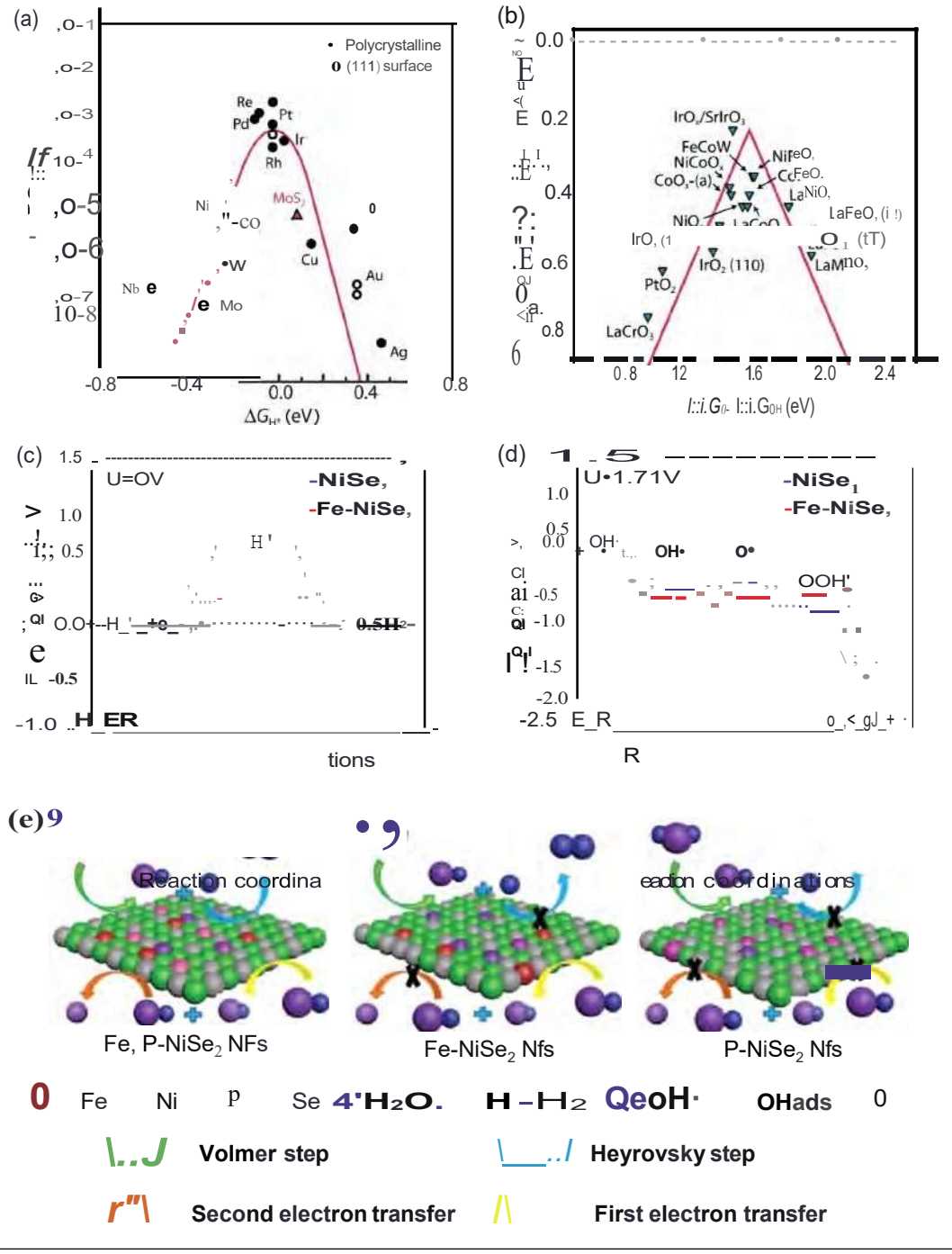

Figure 4 | *(a)HERand {b} OERvolcano plotsfor different metals and metal oxides. Reprinted with permissionfrom Ref 59.Copyright 2017 American Associationfor the Advancement of Sdence.The predictedfree-energy diagrams of HER (c) and OER {d) are presentedfor $NiSe_2$ and Fe-$NiSe_2$ under the electrode potential of U = o and 1-71 V, respectively. (e)An illustration is providedfor the HER and OER reaction pathways on different catalysts. Reprinted with permission from Ref 60. Copyright 2021 Wiley.*

the Ni site of the oxidized FeO-$NiSe_2$ surface is very close to that of the unoxidized Fe-$NiSe_2$, indicating a negligible effect of the oxidized surface on the OER activity of Fe-$NiSe_2$. These results suggest that incorporating Fe-dopants could reduce the over-potential of OER. The active site for OER on Fe-$NiSe_2$'s surface was predicted to be the Ni atom adjacent to Fe atoms, and the second electron-proton transfer step was identified as the rate-determining step of OER. Additionally, Yang et al.[60] also found that P-doping can increase the density of state on the Fermi level, which improved the electrical conductivity of the catalyst. Thus, the Fe and P dual-doping in the Fe,P-$NiSe_2$ NFs led to reduced adsorption energy and limiting potential, as well as increased electrical conductivity. This resulted in improved activ-ity, stability, and select.ivity for high-performance SWE.

Dot: 10.31635/renewables.023.202300034
Citation: *Renewables* 2023, 1, 415-454
Linkto VoR: https://doi.org/10.31635/renewables.023-202300034

Advanced OER Anode Catalyst for SWE

The scarcity and high price of PGMs largely limit their widespread use for commercial WE, let alone SWE. Furthermore, the stability of RuO_2 in acid conditions is very poor.[61] Significant efforts have been devoted to further increasing the activity, stability, and selectivity of Ir- and Rh-based catalysts for OER while suppressing ClOR in seawater or SSW. SWE is more challenging compared to WE because of the neutral conditions and abundant impurities, microorganisms, bacteria, and small particles that exist in the seawater. The challenge is much bigger on the anode OER side than the HERside because of the above-stated competition reaction with ClOR/ClER. Therefore, in this section, we will summarize the current advanced OER catalysts

Table 1 | *A Summary of Catalysts Reported for OER in Neutral, Alkaline, and SSW Conditions*

Catalysts	Electrolyte	*J* (mA cm^{-2})	Overpotential (mV)	O_2 selectivity (%)	Stability	Reference
$Pb_2Ru_2O_{7-}x$	o.6 M NaCl +0.1 M NaOH	50	~280		2 h@1o mA cm^{-2}	3
Cr,O$_3$-CoOx	Natural seawater	400	~770	~97	230 h@16o mA cm^{-2}	24
$Ru_{0.}aZn_{0.}$,O,	0.1 **M** $HClO_4$ + 0.15 M NaCl	6 μA cm^2	1.3 V versus Ag/AgCl	~100		65
Fe,P-$NiSe_2$ NFs	0.5 KOH + seawater	500	350	~100	24 h@400 mA cm^{-2}	
Co_3.xPdxO4	1 M PBS + 0.5 M NaCl	10	370		450 h@200 mA cm^{-2}	67
Ni-doped FeOOH	1 M KOH + seawater	200	~350		80 h@100 mA cm^{-2}	68
ptPd/Ti	Seawater	500	~2300		12 h@2.o V	75
(Mn-W)Ox/$Ir0_2$/Tl	0.5M NaClpH 8	100	~500	~100		85
$(Mn_{0-88}Mo_{0-12})O,_{-12}/IrO_2$	0.5M NaClpH 8	100		~100	1500 h@100 mA cm^{-2}	87
4.8 nm SiOxlpt	0.5 **M** $KHSO_4$ + o.6 **M** KCl	5	~175	~100	12 h@1.9 V	99
$(Na_2Co_{1.}xFexP_2O/C$	0.5 **M** NaCl + 0.1 M KOH	100	~37o	~100	100 h@50 mA cm^{-2}	100
S,P-(Ni,Mo,Fe)OOH/ NiMoP/wood aerogel	1 NaOH + seawater	500	297			101
GO @Ni-Co@NF GO@Fe@Ni-Co@NF	1 M KOH + 0.5 **M** NaCl	500	398303	~97	12 h@1000 mA cm^{-2}	103
NiFe/NiSx-Ni foam (Ni3)	1 M KOH + seawater	400	~56o		1000 h@400 mA cm^{-2}	102
NiFe LOH/C	0.5 **M** NaCl + 0.1 M KOH	25	~300			94
NiFeOxHy	1 M NaOH + 0.5 M NaCl	1000	650	~100		95
S-(Ni,Fe)OOH	1 M KOH + seawater	100	281		100 h@1oo mA cm^{-2}	71
Co-Fe LDH/GCEs	Seawater	25	~270	~100	8 h@10 mA cm^{-2}	97
CoP_1 and $Ni8_1$	SeawaterpH 9.2	~0.3 mA	1.2 V versus Ag/AgCl	>95	12 h@1.72 V	106
CoCH	0.5 M NaCl + 0.1 M NaOH	35°	47°	~100	12 h@50 mA cm^{-2}	107
Ni_2P-Fe_2P/NF	1 KOH + seawater	1000	431		48 h@100 mA cm^{-2}	57
Amorphous NiFeP	1.0 **M** KOH + 0.01 **M** $KHCO_3$ + 1 M NaCl	100	129		500 h@1oo mA cm^{-2}	108
Co-Fe_2P/NF	1 M KOH + 0.5 **M** NaCl	100	347	~100	24 h@1oo mA cm^{-2}	109
NiFe LOH	0.1 **M** KOH+o.5 M NaCl	10	~370	~100	2 h@10 mA cm^{-2}	35
NiFe-LDH nanoarrays/NF	1 NaOH + seawater +0.05 **M** Na_2SO_4	100	333		500 h@400 mA cm^{-2}	164
Co-Fe-O-B	1 M KOH + 0.5 **M** NaCl	10	294	100	20 h@1.65 V	166
HMIL-88@PPy-TA/NF	1 **M** KOH+ NaCl	500	309		48 h@100 mA cm^{-2}	167
NiCoP/NiCo-LDH	1 M KOH + 0.5 **M** NaCl	50	350		50 h@15 mA cm^{-2}	168
Ir2	0.1**M** $HClO_4$ + 5 wt% NaCl	50	250		2 h@1o mA cm^{-2}	169
NiCo-DEA	Seawater	400	~2300			76
NFAC-MELDHs	1 M KOH + 0.5 **M** NaCl	100	280		12 h@100 mA cm^{-2}	170
1 M KOH + seawater	1 M KOH + seawater	500	351		500 h@1oo mA cm-'	77
Echinops like Rh PNNSs	Seawater	10	79.5		50 h@1o mA cm^{-2}	135
Se NiFe+LOH	1 M KOH + 1 M NaCl	400	~670		600 h@1oo mA cm^{-2}	171
o.5Fe-$NiC0_2O_4$@CC	1 M KOH + seawater	120	~300		20 h@21.7 mA cm^{-2}	172
S-(Ni,Fe)OOH	1 M KOH + seawater	1000	462		100 h@1oo mA cm^{-2}	71

DOI: 10.31635/renewables.023.202300034
Citation: *Renewables* 2023, 1, 415-454
Link to VoR:https://doi.org/10.31635/renewables.02,3,202300034

based on the strategies that can be adopted to enhance the activity, especially the selectivity for OER. These strategies include elemental doping, alloy strategy, nonpreciousmetal oxides strategy, protective layer strategy, layered double hydroxide (LDH) strategy, surface engineering, and so on. Table 1 provides a summary of the representative catalysts and the effectiveness of the OER electrocatalysts that have been recently reported in either seawater or SSW.

Design of efficient OER catalyst by elemental doping

Koper's group[62] studied the OER and ClORselectivity on Ir-based double perovskites (A_2BIr0_6) in acidic media. The simultaneous occurrence of these two reactions was due to the coupling between the key binding intermediates. The discovery of a strong linear correlation between ClOR and OER activity and selectivity highlights the challenge of designing effective OER catalysts with excellent selectivity due to the resulting scaling relationship between the two. In addition, the high ClORactivity also results in the quick dissolution of the noble metal component. They conclude that selectively promoting one reaction over the other through kinetic considerations alone is extremely challenging. Instead, it is more feasible to manipulate pH changes or the mass transport of chloride to the active catalyst to improve selectivity. Hegner et al.[63] studied the catalytic selectivity of cobalt hexacyanoferrate (CoFe-PB) toward OER in neutral SWE. They found that more than 30% of the faradic efficiencies(FEs) for ClORwere observed on CoFe-PB in untreated SWE. They also emphasized the difficulty in achieving truly selective SWE, especially under working conditions.

Elemental doping with transition metalsis a necessary step to regulate the electronic structure of the catalyst.This process can optimize the free energy of adsorption of OER intermediates.[64] Recently, Petrykin et al.[65] studied the effect of Zn-doped RuO_2 deposited on TI mesh on the selective OER over ClOR in a 0.1 **M** $HClO_4$ with 0.15 M NaCl solution. $Ru_{1-x}ZnxO_2$ (where x = 0.0-0.3) was synthesized employing a spray freezing-freeze drying approach, and its selectivity for OER and ClORwas verified through voltammetry and differential electrochemical mass spectroscopy (DEMS). The results showed that the pristine RuO_2 mainly

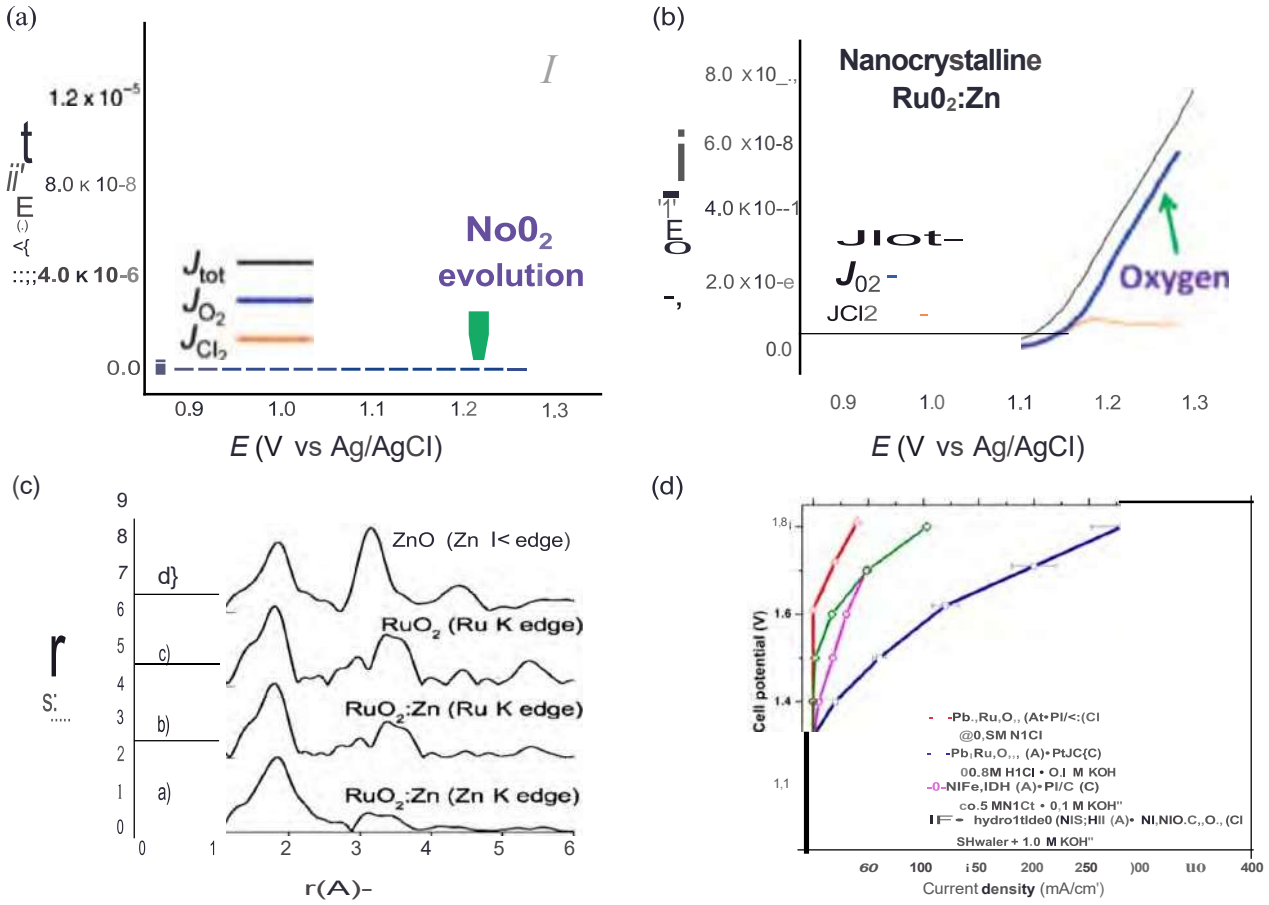

Figure 5 | *Measured current density on (a) $Ru0_2$ and {b} $Ru_{0\_8}Zn_{0\_2}0_2$ electrodes in a 0.1M $HCl0_4$ with 0.15M NaCl solution.The black line represents the measured current density, while the red and blue lines correspond to the components of chlorine and oxygen evolution respectively. (c) The normalized EXAFSfunctions of the $Ru_{0\_8}Zn_{0\_2}02$, ZnO, and $Ru0_2$ materials at Zn Kand Ru K edges. Reprinted with permissionfrom Ref 65. Copyright 2010 Wiley. {d} The performance of electrolyzers in neutral and alkaline SSW using $Pb_2Ru_20_{7\_x}$, Pt/C, and Fumapem-FAA-3-50 as the anode, cathode, and separator, respectively. The variables A and C represent the anode and cathode, respectively. Reprinted with permission from Ref. 66. Copyright 2020 American Chemical Sodety.*

DOI: 10.31635/renewables.023.202300034
Citation: *Renewables* 2023, 1, 415-454
Linkto VoR:https://doi.org/10.31635/renewables.023-202300034

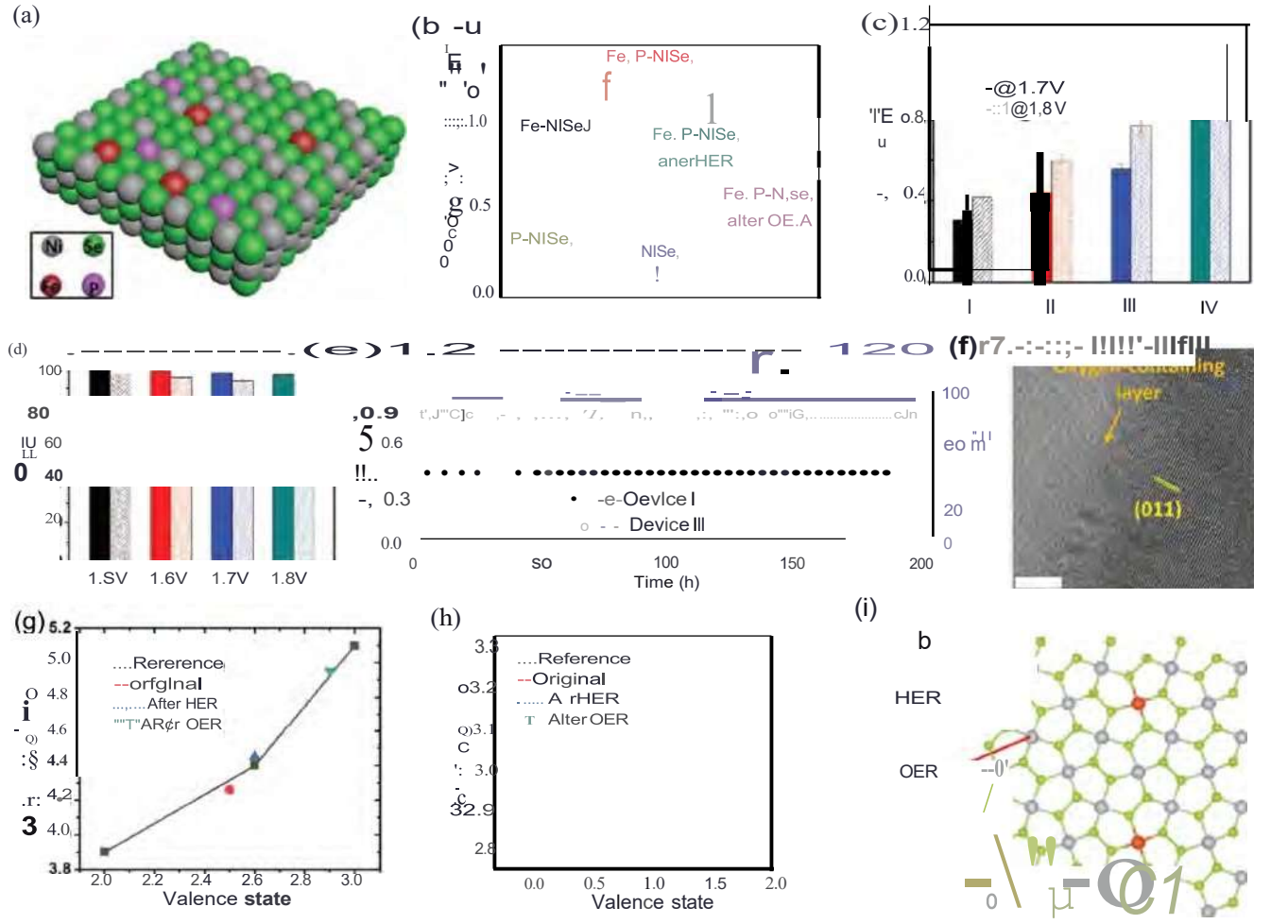

Figure 6 | *(a) Fe,P-NiSe$_2$NFs with a dual-doped structure. {b)Comparison of the electric conductivity between Fe,P-NiSe nanofibers and control samples. (c) AEM electrolyze,current density at Ece1,1.7 and 1.8 V with different seawaterfeeding modes. {d} 0$_2$ FE using natural seawaterfeedstock solution at varied Ece1P•(e) Long-term operation test and 0$_2$FE on seawater electrolyzers operating at 1.8 V.(f) High-resolution TEM image of Fe,P-NiSe$_2$NFs after DER test, scale bar:5 nm.(g)Calibration curvefor FeL_IL$_2$white-line intensity ratioversus Fe oxidation state. (h} Calibration curvefor Ni L_IL$_2$ white-line intensity ratio versus Ni oxidation state. {i} Atomic structures of Fe,P-NiSe$_2$ surfaces and real activesitesfor OER and HER, where Ni, Fe, and Se atoms were expressed by gray, orange, and green balls, respectively. Reprinted with permission from Ref* 60. *Copyright* 2021 *Willy.*

catalyzed CIOR without OER (Figure 5a). However, the $Ru_{0\_8}Zn_{0\_2}0_2$ catalyst showed the highest selectivity for electro-catalytic OER while suppressing CIOR under the same electrolyte conditions(Figure 5b).The increased selectivity towards OER was attributed to the insertion of Zn in $Ru0_2$, which prevents the formation of peroxo-bridged intermediates due to the realign-ment of the $Ru0_2$ crystal structure. The doping of Zn into $Ru0_2$ disrupted the perfect arrangement of Ru atoms in the [001] direction, causing neighboring metal atoms to rearrange in the [m] direction. This resulted in the production of more oxygen vacancies near Zn ions (Figure 5c), which boosted OER while restraining CIOR. Ramani et al.[66] reported on a lead-doped ruthenium oxide pyrochlore ($Pb_2Ru_20_{7.x}$) catalyst that exhibited higher OERactivity and selectivity in SSW. It was found that Pb doping induced a high oxidation state of Ru(V) on the surface and created a large number of oxygen vacancies, which were responsible for the better selectivity for OER than CIOR. The catalyst achieved a current density of 275 mA cm-• at a cell voltage of 1.8 V in a real electrolyzer in simulated alkaline seawater (Figure 5d). Furthermore, it exhibited only a 10 mV voltage loss at 200 mA cm-• afters h of operation, demonstrat-ing the potential of the elemental doping strategy for practical applications. However, the operation was still too short for commercial use.

Yang's group developed a dual-doping strategy for highly efficient SWE, using iron (Fe) and phosphorus (P) to dope nickel selenide nanoporous films (Fe,P-$NiSe_2$ NFs), as shown in Figure 6a. They found that the electronic conductivity of Fe,P-$NiSe_2$ NFs increased due to the doping of P and Fe cations (Figure 6b). A current density of 1.2 A cm-• was achieved in a real seawater electrolyzer (Figure 6c), and the OER FE was about 92% on the anode side (Figure 6d). The catalyst achieved a

DOI: 10.31635/renewables.023.202300034
Citation: *Renewables* 2023, 1, 415-454
Linkto VoR:https://doi.org/10.31635/renewables.023-202300034

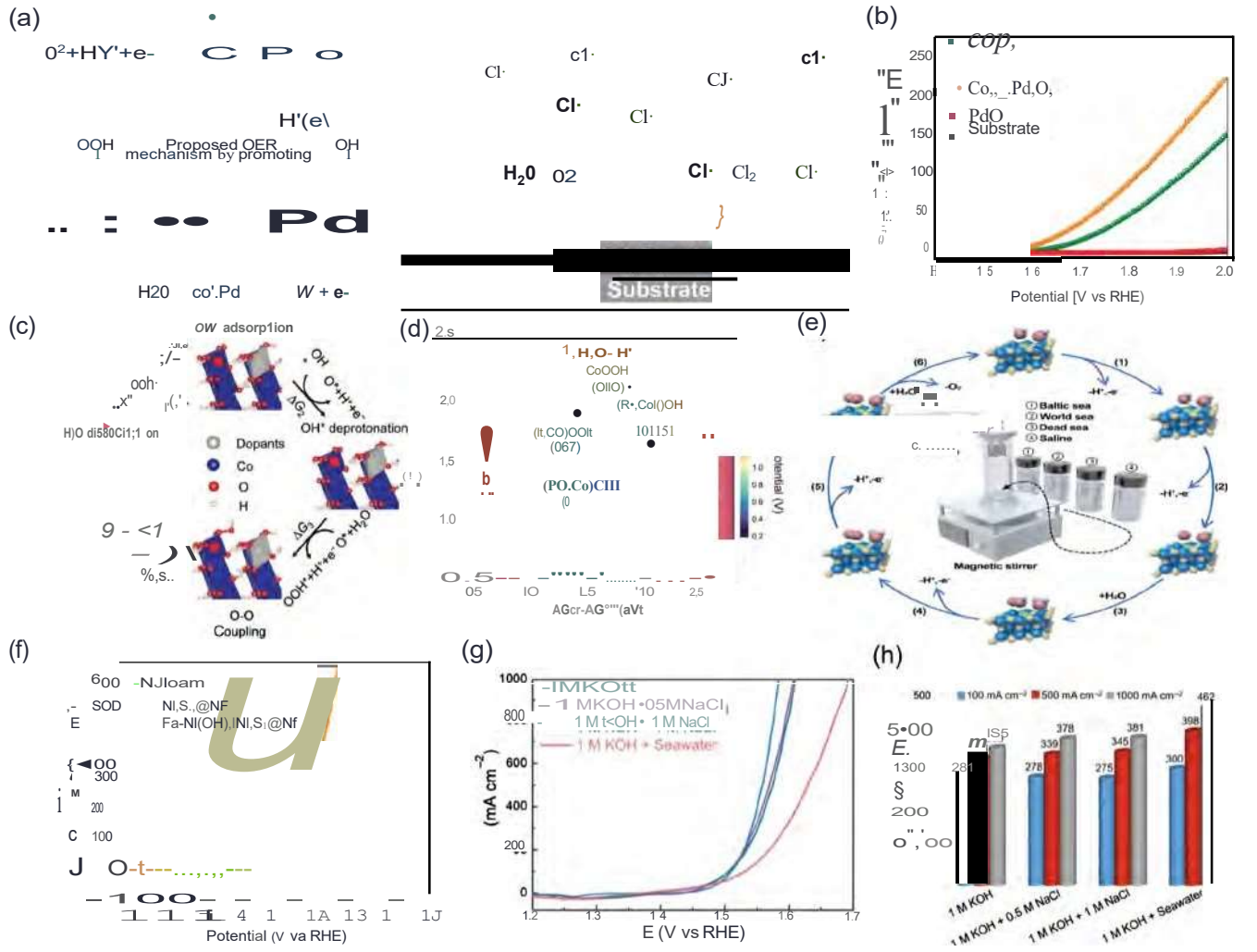

Figure 71 *(a) Proposed OER mechanism of Co_3.xf'dx0_4 and proton-adsorption-promoting strategy for pH-neutral seawater oxidation reaction. {b}OER catalytic performance of Co_3.x$PdxO_4$ and controls on carbon paper substrates in pH-neutral SSW (1M PBS+ o.sM NaCl} at a scan rate of 1 mV s-'. (c) Proposed DER cycle of {Pd,Co}OOH by promoting water dissociation assisted by adsorbed H" (cobalt-blue, palladium-grey,oxygen-red, hydrogen-pink). {d)20 DER activity map of theoretical overpotentials regarding different dopants in CoOOH {Pd, Ir, pt, and Re} constructed by assuming a scaling relation J.1$E_{00}w$ = J.1E_0w + 3.2 ell.G denotes Gibbsfree energy and• denotes either a vacant site or adsorbed RI. Reprinted with permissionfrom Ref 67- Copyright 2023 Willy.(e)Neutral/alkalinewater oxidation mechanism of CNC-MS(outside} and schematic illustration of the eledrolyzerfor a long-range test {inside}. Reprinted with permissionfrom Ref 69. Copyright 2021 Elsevier Ltd. (f) The CV curves of Fe-Ni{OH}$_2$/Ni_2@NF, Ni_3S_2@NF, and Nifoam at a scan rate of 5 mV-,' in 1 M KOH/0.5 NaCl. Reprinted with permission from Ref. 70. Copyright 2020 Springer-Verlag GmbH Germany. (g) Polarization curves and {h} comparison of the required voltages at current densities of 100, 500, and 1000 mA cm-, for the $NiMoN_8S$-{Ni,Fe}OOH electrolyze, in different electrolytes. Reprinted with permission from Ref 71. Copyright 2020 The Royal Society of Chemistry.*

current density of o.8 A cm-^{2} at ,.8 V in natural SWE in a real device with high OER selectivity, and it remained stable for over 200 h (Figure 6e), demonstrating its great potential for practical and commercial applications. The author found that a P-O species surface passivation layer formed during the SWE process (Figure 6f}, which prevented the dissolution of $NiSe_2$ under high overpotential and alkaline conditions. The electron energy loss spectroscopy results indicate that the Fe and Ni L/½ white-line intensity ratios (Figure 6g,h) were increased from +2.6 and +0.76 *to* +3 and +1.25 after the OER test. Density functional theory (DFT) calculations (Figures 4c-e and 61) indicate the Fe-doping stimulated the adjacent Ni atoms as active centers for OER.This work highlights the dual-doping strategy *to* boost SWE performance by tuning the electronic structure and adsorption energy of intermediate products.

In a recent study by the group of Sargent.6[7] a strategy was reported utilizing proton-adsorption promotion *to* enhance the rate of OER, leadingto an improvement in the stability of neutral seawater splitting. Strong-proton-adsorption {SPA) materials, such as palladium-doped cobalt oxide (Co_3.xPdxO.J catalysts (Figure 7a), are deemed the most efficient catalysts for the purpose. They can produce an OER overpotential of 370 mV at

DOI: 10.31635/renewables.023.202300034
Citation: *Renewables* 2023, 1, 415-454
Linkto VoR:https://doi.org/10.31635/renewables.02,3,202300034

10 mA cm-^{2} in simulated pH-neutral seawater (Figure 7b), surpassing Cop_4 by 70 mV. The Co_3.xPdxO_4 catalysts can sustain consistent catalytic activity for 450 hat 200 mA cm-' and 20 hat 1 A cm-^{2} in neutral seawater. According to both theoretical calculations and experimental studies(Figure 7c,d), the presence of SPA cations is believed to enhance the speed of the rate-limiting water dissociation step in the neutral OER pathway. A study by Choi and colleagues[68] describes the development of a high-efficiency anode for AEM alkaline SWE. The anode, which is Ni-doped FeOOH, demonstrated remarkable OER activity and stability when tested in a half cell containing 1.0 M KOH+ seawater.The super hydrophilicity of the Ni-doped FeOOH was found to effectively remove the generated oxygen gas and minimize mass transfer resistance. In addition, the AEM electrolyzer catalyzed by this anode exhibited high performance and cell efficiency in 1.0 M KOH + seawater.

Wang and colleagues[69] discussed the use of Co/Ni-doped defect-rich Cu-based oxides (CNC-MO) nanoarrays to split alkaline seawater. The nanoarrays facilitate water dissociation by bonding with OH*. Additionally,they utilize Ni/Co-doped defect-rich Cu-based sulfide (CNC-MS) nanorods to modify the adsorption state of OH*, and effectively absorb and isolate H* to enhance the kinetics of the OER (Figure 7e). With asymmetric electrodes,they achieved alkaline SWE at 100 mA cm-' and1.61V. The electrodes demonstrated high efficiency, selectivity, and corrosion resistance that remained stable for 1200 h in a saline-alkali medium but gradually declined due to site blocking and deep corrosion. From a thermodynamic perspective, the effects of water on breaking chemical bonds are well-researched. By focusing on attraction mechanisms and conversion paths, saline electrolysis can be accelerated through metal doping, defect construction, and surface texturing.The catalyst's exceptional activity not only allows for high selectivity in an alkaline medium but also contributes to an extended service life. To ensure longevity, it is crucial to prevent impurities from adsorbing on the anode's self-corrosion. These findings can guide the production of cost-effective electrocatalysts applicable in demanding environments and promote the efficient use of low-grade natural resources in the future.

Cui and colleagues[70] presented a Ni_3S_2 nanoarray heterostructure with additional Fe-Ni$(OH)_2$ lamellar edges, which expose a multitude of active sites for seawater oxidation.Theresulting Fe-Ni$(OH)_2$/Ni_3S_2 nanoarray serves as a freestanding anodic electrode in alkaline artificial seawater. Withonly an overpotential of 269 mV, a current density ofio mA-cm-' is achieved (Figure Jf). and the Tafel slope is notably low at 46 mV-dec'. Despite operating for 27 h at a high current density of 100 mA-cm-^{2} during the chronopotentiometry experiment, there is almost no deterioration, indicating the Fe-Ni$(OH)_2$/Ni_3S_2 electrode's exceptional stability. The catalyst exhibits decent selectivity in saline water, with a faradic efficiencyfor oxygen evolution of up to ~95%. The excellent catalytic performance observed in this work can be attributed to the incorporation of a Fe activator and the heterostructure, resulting in numerous active and selective sites. The large exposed area of the lamellar edges and the intimate contact between Fe-Ni$(OH)_2$ and Ni_3S_2 promote electron/mass transfer and gas release from the surface. DFT calculationsindicate that the highly active and selective sites for OER in artificial seawater are located at the Fe species in the lamellar edges, rather than Ni.Thisstudy provides a direction for the rational design of effective and economical electrocatalysts in practical SWE.

In addition to metal doping, nonmetal doping is also an important strategy for enhancing OER performance in SWE. For instance, Ren's group[71] reported highly porous self-supported S-doped Ni/Fe (oxy)hydroxide catalysts (S-(Ni,Fe)OOH) on Ni foam using a one-step surface engineering method. This ultrafast technique effectively modifies the surface of Ni foam into a hydrophilic S-doped Ni/Fe (oxy)hydroxide layer with multiple levels of porosity, alarge surface area,and numerous active sites. The unique feature of this catalyst ensures a strong and durable connection that promotes rapid electron transfer and enhances stability. Furthermore, during the reaction process, S was introduced both on the surface and within the lattice of the Ni/Fe (oxy)hydroxide, which might adjust the valence state of Ni/Fe and optimize the absorption energy of OER intermediates, leading to improved OER performance. As a result, this S-(Ni, Fe)OOH exhibits excellent OER performance, regardless of whether it is in an alkaline solution, such as KOH, SSW (1M KOH+ 0.5M NaCl), or1M KOH+ seawater (Figure7g). Specifically, it requires only overpotentials of 300, 398, and 462 mV to achieve a current density of 100, 500, and 1000 mA cm-' in 1M KOH + seawater (Figure 7h). A proof-of-concept application was performed using S-(Ni,Fe)OOH and **NiMoN** nanowire arrays supported on **Ni** foam as anode and cathode in a two-electrode electrolyzer for overall seawater splitting. In 1MKOH + seawater, potentials of 1.661, 1.837, and 1.951 V were required to achieve current densities of 100, 500, and 1000 mA cm-'. Moreover, it demonstrated outstanding stability in different solutions, even at high current densities of 100 or 500 mA cm-'. Thus, the reported S-(Ni,Fe)OOH is an excellent candidate OER catalyst for real SWE.

Design efficient OER catalyst with alloy strategy

Although RuO_2 and IrO_2 show the most catalytic activity for OER, Ir/Ru-based catalysts still require an overpotential of 340 mV in acid[7 8 48 9] or alkaline solutions[5 47] and more than 46o mV in neutral[67] solutions to reach a current density of 10 mA cm-'. Moreover,Ir /Ru-based materialstypically exhibit catalytic activity for both OER and CIER/CIOR in natural seawater,[10.s] which results in relatively low selectivity of Ir/Ru-based catalysts for OER under seawater conditions. Additionally, cl- containing species and products accumulate on the electrode surface, corroding the electrode and causing stability issues for Ir/Ru-based catalysts.[25] While pt is more robust in neutral seawater and displays better stability than Ir/Ru-based catalysts, it exhibits only moderate catalytic activity for OER due to strong bonding with oxygen intermediates.[7'] Moreover, pt readily oxidizes to soluble high-valence pt'>+ derivatives (where 6 = 4 and 6) when the anode potential exceeds 1-4 VRHE in an excessively oxidative environment, leading to the dissolution of pt species

DOI: 10.31635/renewables.023.202300034
Citation: *Renewab/es* 2023,,, 415-454
Link to VoR: https:/ /doi.org/10.3"1635/renewables.023-202300034

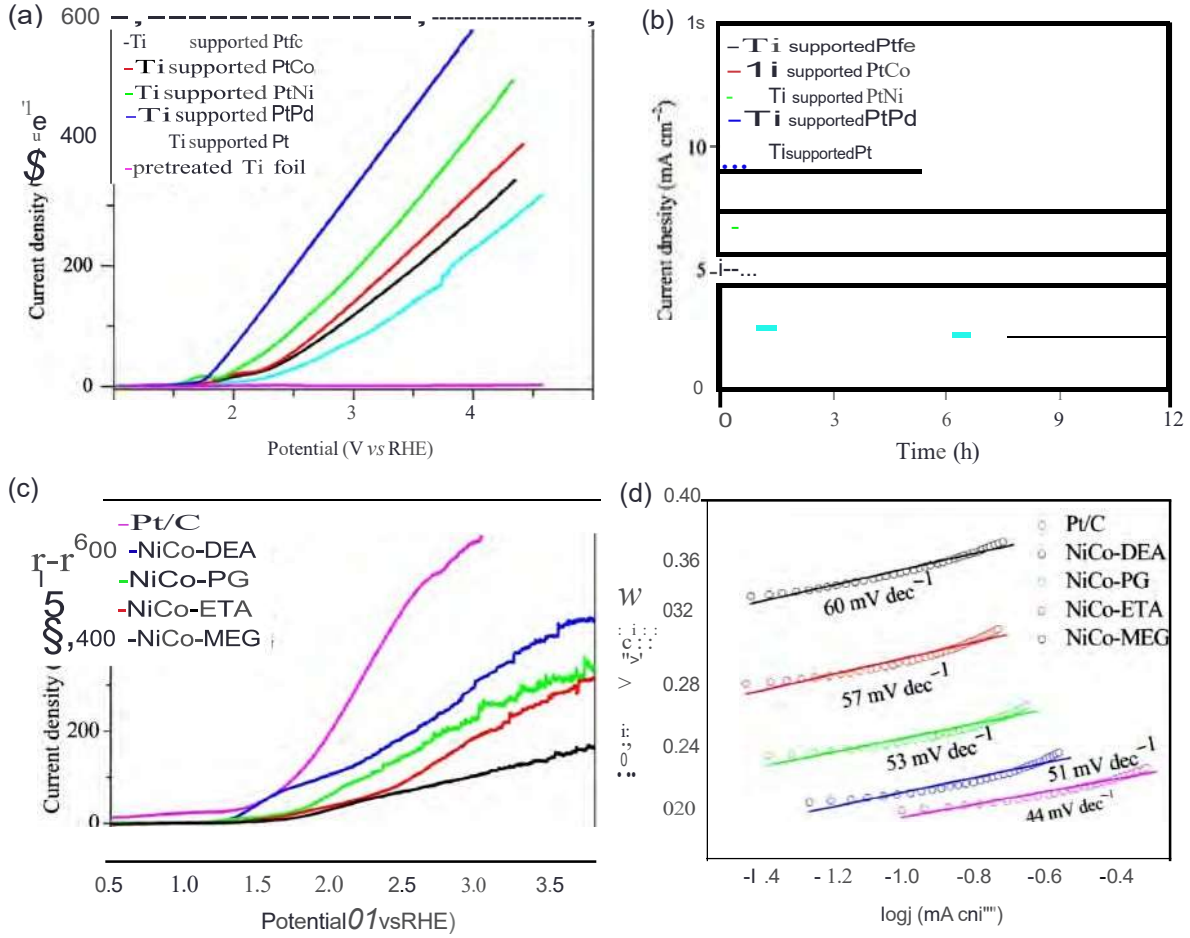

Figure 8 | *(a) Polarization curves of Ti-supported ptM alloy recorded in seawater at a scan rate of 50 m y" ; {b) The long-term stabilities of DER recorded at an overpotential of 2.0 V(vs RHE}. Reprinted with permission from Ref 75. Copyright 2017 Elsevier.(c) The LSV plots and {d) Tafel curves of various NiCo all(!Y electrodes in seawater a scan rate of 1 ', . Reprinted with permission from Ref 76. Copyright 2017 Elsevier.*

and a sharp performance decay.[73] Therefore, it is necessary to design pt-based catalysts that areboth highly active and stable, with a dissolution-resistant structure that manipulates the electronic and local coordination environment of pt_[74]

Recently, Zheng[75] reported on a series of pt-based binary alloy electrodes for 0ER in seawater splitting. ptM alloys (where **M** = Fe, Co, **Ni,** or Pd} were prepared by electrodeposition of metal chloride onto Ti substrates. The alloying of Mand pt was discovered to cause charge transfer from **M** to pt_ This generates an electronic effect that decreases the binding energy of pt, thereby boosting the catalytic activity of the **ptM** alloy. Through the alloying effect between pt and Pd, ptPd/Ti produces a moderate metal-oxygen bond strength and oxygen-binding energy, resulting in the best 0ERperformance in neutral seawater compared to other ptM/Ti catalysts examined. To achieve a current density of 100 mA cm-^{2} (Figure Ba}, ptpd/Ti necessitates an overpotential of just 0.87 V, and it operates reliably for over 12 h at an overpotential of 2.0 V (Figure Sb).

Apart from PGM-based alloys, non-PGM electrodes have also been investigated as anode materials for SWE. To illustrate, Zheng[76] reported on the pt-free NiCo electrocatalysts for 0ER by seawater splitting. The NiCo alloy electrocatalyst was synthesized through a one-step hydrothermal method, with reducing solvents, such as diethanolamine (DEA}, propanediol (PG}, ethanolamine (ETA), or monoethylene glycol (MEG), carefully studied. NiCo-DEA was found to exhibit the best 0ER activity in seawater electrolytes, displaying an onset potential of 1.31 V and a Tafel slope of 51 mV dee', which was better than other control samples (Figure 8c,d}. However, it should be noted that thebest NiCo-DEA still exhibited inferior performance compared to pt/C nad thus needs to be further modified, such as through N-doping.

Feng et al.n recently reported thatNixFeyN@C microsheet alloy arrays on Ni foam (Figure 9a} can be used as efficient electrode materials for 0ER in SWE. The porous architecture and superhydrophilic/superaerophobic surface of NixFeyN@C ensure adequate exposure of active sites and mass transfer, while the synergetic coupling between the carbon coating and NixFeyN facilitates electron transport. This electrocatalyst's superior corrosion-resistance and electron conductivity result in exceptional

DOI: 10.31635/renewables.023.202300034
Citation: *Renewab/es* 2023, 1, 415-454
Link to VoR:https://doi.org/10.31635/renewables.023-202300034

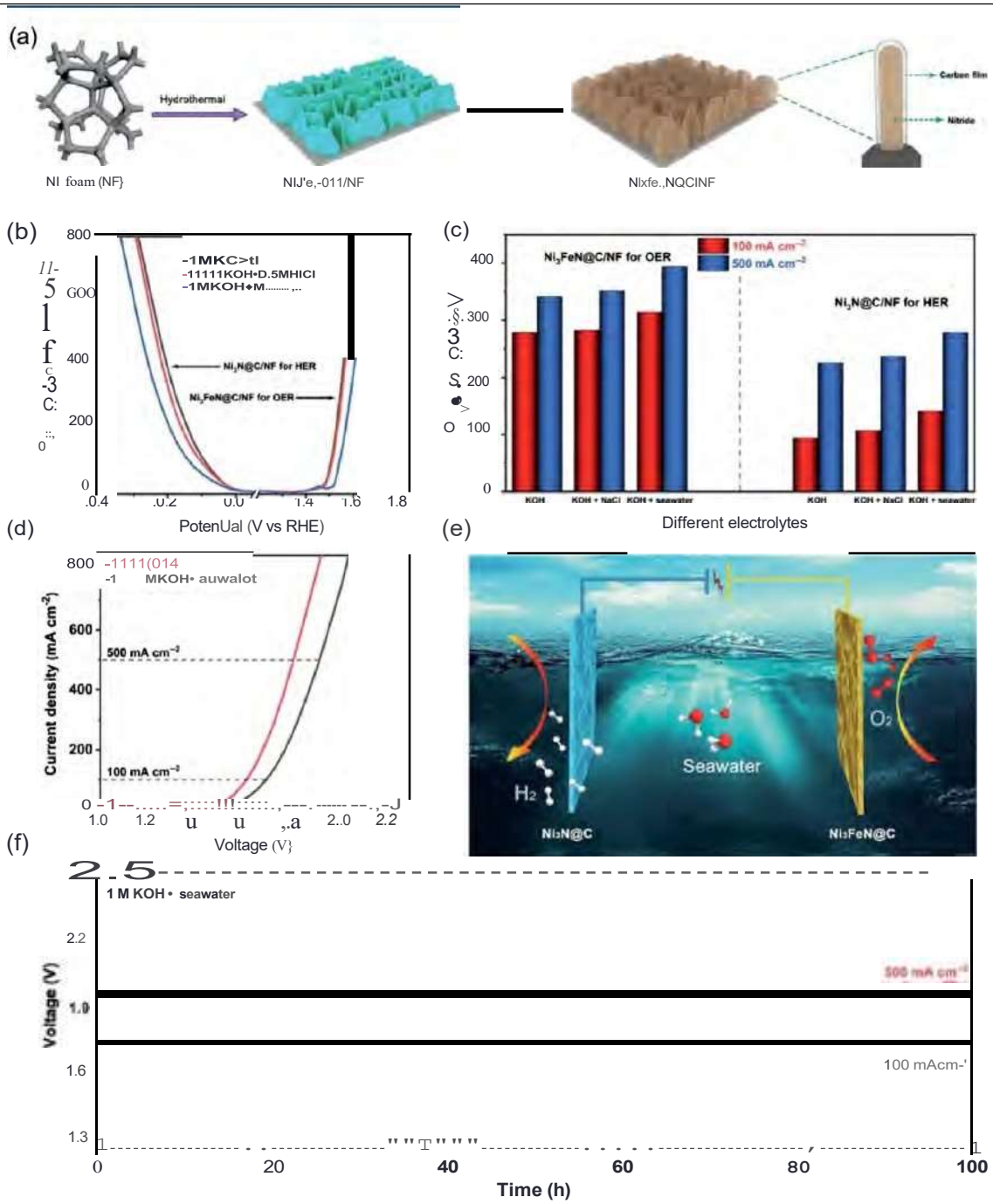

Figure 9 | *(a) Polarization curves in different electrolytes; {b) comparison of required overpotentials at current densities of 100 and 500 mA cm-,for OER with Ni_3FeN@C/NF and HER with Ni_3N@C/NF in different electrolytes; (c) polarization curves of the electrolyzer when tested in 1 M KOH and alkaline seawater (1 M KOH+ seawater) electrolytes; {d)a schematic illustration of the electrolyzerfeaturing Ni_3FeN@C/NF as the anode and Ni3N@CINF as the cathode; (e) durability tests of the electrolyzer at current densities of 100 and 500 mA* cm-^{2}. *Reprinted with permission from Ref 77. Copyright 2021 The Royal Society of Chemistry.*

OER performance, with NixFe_IJ@C/NF requiring overpotentials of 283 (314) and 351(394) mV to achieve current densities *of* 100 and 500 mA cm-^{2}in alkaline-SSW (1M KOH+0.5M NaCl} and alkaline seawater (1 M KOH + seawater} electrolytes, respectively (Figure 9b,c). It also exhibits excellent two-electrode electrolyzer performance, achieving current densities *of* 100 and 500 mA cm-^{2} at cell voltages of 1.69 and 1.91 V, respectively, in the alkaline-seawater electrolyte (Figure 9d,e), and can maintain stability for at least 100 h (Figure 9f}. This study emphasizes the significance of constructing a porous structure and achieving desirable surface superaerophobicity and superhydrophilicity to ensure adequate exposure of active sites and efficient mass transfer.

DOI: 10.31635/renewables.023.202300034
Citation: *Renewab/es* **2023,** 1, 415-454
Linkto VoR:https://doi.org/10.31635/renewables.02,3,202300034

Design of efficient OER catalyst with nonprecious metal oxides

Due to the low abundance and high cost of PGMs, it is crucial to develop nonprecious catalysts for OER. While transition metals are not stable in acid solutionsbecause of their susceptibility to chemical corrosion, most of the transition metal catalysts have been studied in alkaline and neutral solutions. Due to transition metals' ability to exchange d-orbital electrons with the electrolyte {OH-), materials based on these metals exhibit a moderate metal-oxygen bond strength and binding energy for OER intermediates.72Among all nonprecious metals, transition metal oxides based onMn, Fe, Co, and Ni arethe most studied catalysts due to their variable valences and tunable electron states for OER.7s--s,

As the number of electrons in the metal antibonding orbitals rises, the metal-ligand bond order falls.[82] This makes the MnOx almost the earliest studied material for OER in SWE due to the internally stable character of MnOx than other transition metal oxides. As early as 1980, Bennett8Jpointed out that the electrodes can be coated by manganese dioxide (MnO_2), which results in theevolution of oxygen from seawater with a FE of 99%, and even a 95% efficiency from saturated sodium chloride brine.The MoO_2 coating on the electrode results in the CIOR/CIER mass transfer being limited more quickly. In this way, the limiting current density of CIORdecreased 2-3 orders of magnitude, thus making the OER the dominant anodic reaction during the electrolysis in ci--containing electrolyte. In addition to their research on MnO_2 as OER catalysts under basic conditions, Nakamura's team[84] investigated these catalysts in neutral conditions, discovering that Mn^{3+} exhibits high OER activity. Mn>+is promoted by electrostatic interactions to spontaneously form Mn3+,resulting in theexcellent stability of Mn-based catalysts. It is worth noting that while MnOx displays better selectivity for OER over CIOR, its OER activity is typically low.Thus, the activity of MnOx should be further promoted by doping or combining it with other materials.

Hashimoto et al.[8 86] reported that Mn-WOx electrodes, in which Mn^{4+} and w&+ ions are homogeneously distributed in the catalysts (Figure 10a), show improved OER activity compared to pure MnO_2. This is due to the electronic interaction between Mn^{4+} and w&+, resulting in the charge transfer between Wand Mn and a reduction in the binding energy of **w&+**{Figure 1ob,c). Furthermore, the incorporation of **W** atoms into (Mn-W)Ox reduces its lattice constant and increases Its surface roughness, leading to a further improvement in Its activity. A current density of 100 mA cm-^{2} can be achieved with only an overpotential of 0.29 V. Further, they also reported a series of Mn-based OER catalysts for SWE with a similar mechanism, such as {Mn-Mo) Ox,Bi,ssMn-Mo-Fe,[89]Mn-Mo-Sn oxide.[90] According to Fujimura et al.'sresearch,[87,88] Mo-doping enhanced the OER stability of MnO_2. The (Mn-Mo)Ox material exhibited significantly less surface corrosion than pure MnO_2 after a 1500-h test, suggesting that Mo-doping can improve the stability of MnO_2 in seawater. The authors also observed that when sufficiently thick oxides are grown on IrO_2-coated Ti substrates, the OER efficiency can reach almost 100% at a current density of 1000 A m^{-2} in 0.5M NaCl solution at pH12.However, during electrolysis,the OER efficiency

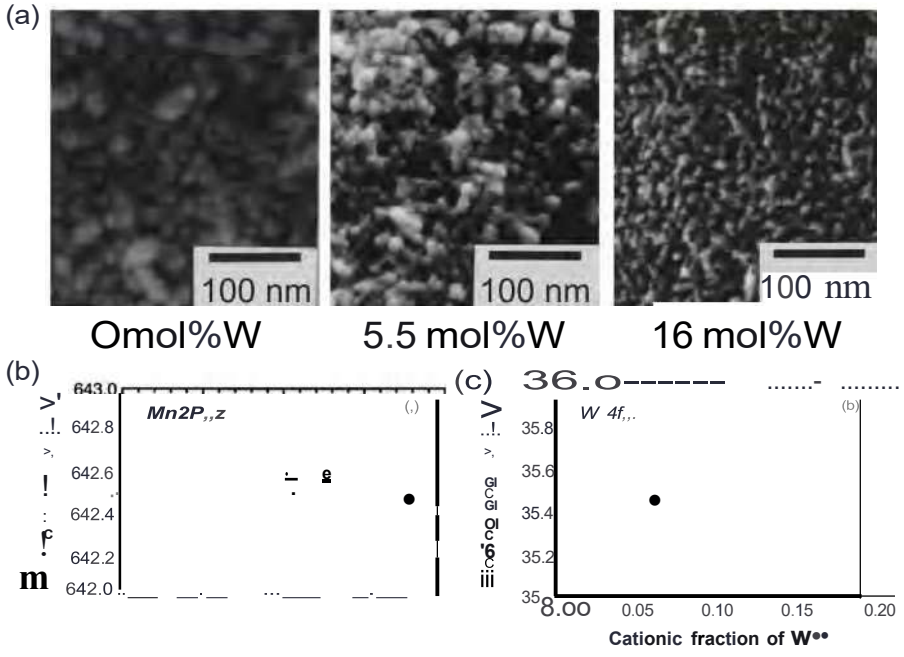

Figure 10 | *(a) SEM images of (Mny-W}OxllrO,ITi electrodes with varying cationicfractions of hexavalent tungsten. From left to right, the images correspond toy=o,5.5, and16 mo/% w, respectively.The binding energies of (b}Mn 2p$_{312}$and (c) W 4!$_{712}$electrons areplotted in {b) and (c), respectively, as a function of the cationicfraction of hexavalent tungsten present in the manganes tungsten oxides. Reprinted with permission from Ref 85. Copyright 1998 Elsevier.*

DOI: 10.31635/renewables.023.202300034
Citation: *Renewab/es* 2023, 1, 415-454
Link to VoR: https://doi.org/10.31635/renewables.023-202300034

gradually decreased due to the exfoliation ofoxides, which were largely mitigated by using Ir0_2-coated expanded Ti substrates. Transition-metal sites like Fe, Co, and Ni have e_g orbitals that are involved in bonding with surface adsorbates, resulting in a higher OER activity in metal-based oxides compared to Mn-based materials.[91] Because the electron occupation of group VIII metals in thee_g orbital is closer to the volcano apex thanMn, the adsorption energy difference between OH* and HOO* is reduced.[92] Bimetallic or multimetallic oxides, which offer the possibility of synergistic effects between different metals, have attracted more attention than pure metal oxides.[93]

Design of efficient OER catalyst with layered double hydroxide

Strasser et al.[94] studied the fundamental understanding of the interaction between the catalyst and electrolyte, which is difficult to investigate under operating conditions. The study presents an operando structure-reactivity analysis of NiFe LOH as an electrocatalyst for the OER in both alkaline and alkalinized NaCl electrolytes. This was achieved by combining operando wide-angle X-ray scattering and electrochemical characterization. LOH is recognized as one of the most active electrocatalysts for both the alkaline OER and selective seawater oxidation of OER.[71,94,95] The research carried out by Strasser et al.[94] presents an analysis of the structure-reactivity of NiFe LOH, an electrocatalyst for OER in both alkalinized NaCl electrolytes and alkaline environments. The findings from the operando experiment indicate that an increase in pH level leads to a higher proportion of the OER active y-NiFe LOH in the catalyst layer composition, as well as larger Ni redox peaks and enhanced OERactivity. When the KOH concentration is reduced, the presence of 0.5M NaCl stabilize the residual a-phase and improved the OER activity. Furthermore, the inclusion of0.5M NaCl in moderate alkaline electrolytes (0.1-0.5 M KOH} resulted in larger Ni redox features and higher activity (Figure11a,b). However, it seemed to limit the percentage of y-NiFe LOH during the OER compared to electrolytes without NaCl. Interestingly, a higher KOH concentration (1.0 M KOH, pH 14) can offset this structural effect by aligning the proportion of OER-active y-NiFe LOH in both NaCl-free and NaCl-containing electrolytes (Figure 11c). Upon further examination of the scan rate, a significant link between the electrochemical availability of NiFe LOH and its past, scan rate, and introduction of NaCl was discovered (Figure 11d-f). The research suggests that the introduction of NaCl leads to a faster and more effective break-in process, resulting in improved activity at lower pH levels despite a lower percentage of the y-phase. Overall, this study provides valuable information on the catalytic performance of NiFe LOH in various electrolytes, allowing for the development of effective electrocatalysts for the OER.

Jiang's group[95] reported that NiFe LOH displays a high efficiency in catalyzing OER, with an onset potential of 1.51 V at 100 mA cm^{-2} in simulated saline water consisting of 0.5 M NaCl + 1 M NaOH. The Ni-Fe oxyhydroxide catalyst was electrochemically activated, leading to the structural reconstruction of amorphous Ni (oxy)hydroxide and modulation of electronic structure through Fe intercalation. Characterizations using ex situ X-ray radiation and in situ Raman spectroscopy revealed these changes during the electrochemical activation process.The activated NiFeOxHy showed a FE of ~100% in the evolution of 0_2. The use of NiFe LOH as an anode catalyst in the AEM electrolyzer resulted in a voltage decay of only 350 mV after 100 h of continuous electrolysis at 500 mA cm^{-2}. This is attributed to the synergy effect of the alkaline microenvironment, the surface-enriched Fe^{13+o}>+ooH component, and the tunable Ni chemical state, which enhances OER selectivity and suppresses CIER side reactions. With the ample reserves of low-grade saline water and the availability of renewable marine and wind energy, this study may lead to the development of clean electricity-to-chemical energy conversion technologies.

According to Strasser et al.,[96] an effective alkaline electrolyzer was discussed previously, which can selectively split artificial alkaline seawater into oxygen and hydrogen. The performance of the electrolyzer, measured by current density, shows an increase with higher concentrations of KOH, but a decrease in relative stability. When 0.5M NaCl was introduced into the electrolyte, the current density was lower due to the decreased OW conductivity of the AEM, as a result of the presence of cl-ions. The study was successful in conducting 100-h measurements and found that only the NaCl-free 0.1 M KOH measurement exhibited stable performance after an activation time of 12 h, while the current density decreased over time for all other electrolyte conditions. Scanning electron microscopy {SEM) images and impedance investigations suggest a loss of stability induced by the membrane, but the study also revealed a recovery effect that can be utilized in a day-night cycle. According to the study, utilizing the natural day-night patterns can serve as a natural rejuvenation process when employing sustainable energy sources, such as photovoltaics or wind power, to operate the electrolyzer. Additionally, the findings demonstrate that the membrane is obstructed by chloride ions, impeding the transfer of OH- across the membrane and resulting in a significant loss of activity. Finally, the study evaluated selectivity to establish FE, revealing degrees of efficiency as high as 88% and cell efficiencies reaching 64% at high current densities.

Besides Ni Fe LOH, CoFe LOH was also found to be a high active anode electrode for SWE. According to Yang and colleagues,[97] Co-Fe LDH nanoparticles can act as electrocatalysts for oxidizing seawater at a near-neutral pH without any additional buffered electrolytes. The Co-Fe LOH electrocatalyst demonstrated high selectivity and electrocatalytic activity for OER at pH 8 in seawater and showed acceptable stability over a diurnal cycle under the given operating conditions. The study suggested that the Co-Fe LDH catalyst's electrocatalytic properties were due to the synergistic effect of the multiple ions present in seawater, making it an encouraging electrocatalyst for practical, direct, and efficient seawater oxidation applications.

Overall, it has been found that the high catalytic activity and selectivity of LOH-based anode materials for SWE is mainly due to the synergistic effect between the two cation ions in LOH, as well as the unique layered structure and presence of active metal sites. The metal cations in the LOH structure can present in

DOI: 10.31635/renewables.023.202300034
Citation: *Renewab/es* 2023,,, 415-454
Link to VoR: https://doi.org/10.3'1635/renewables.023-202300034

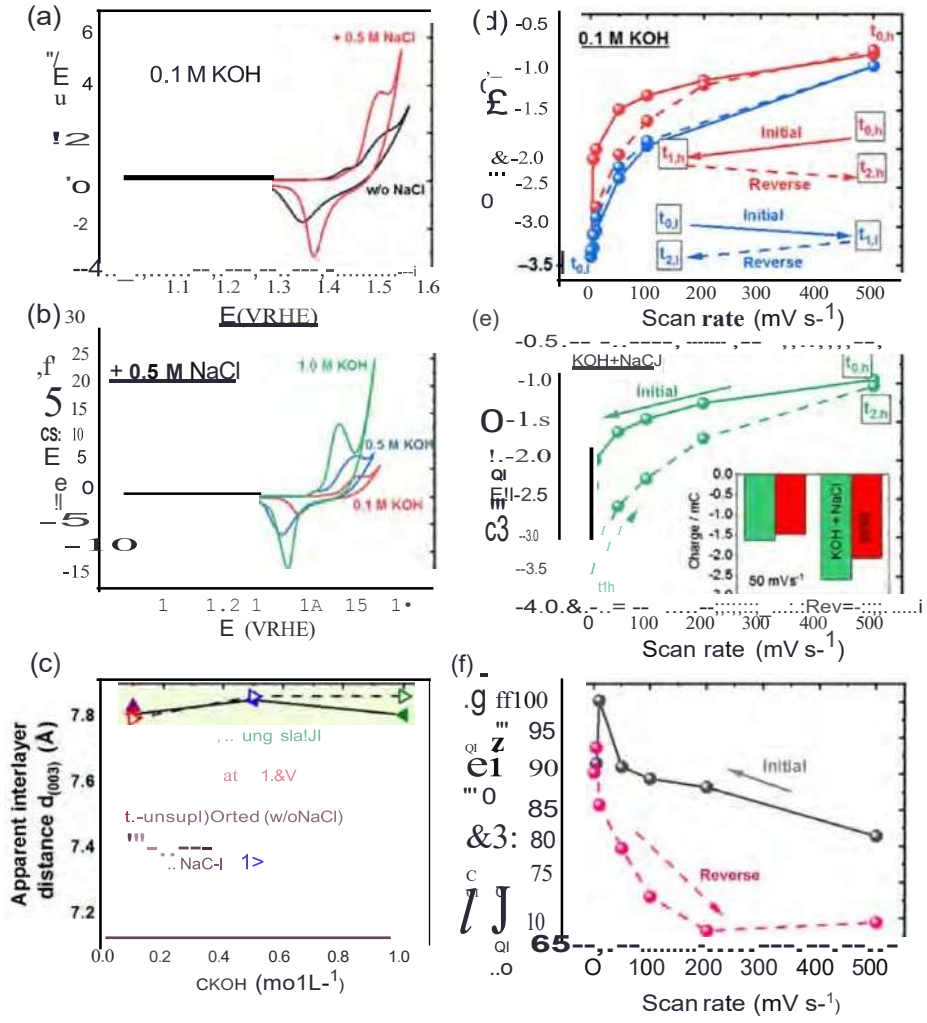

Figure 11| *(a and b} Various electrolyte solutions were used to conduct cyclic voltammetry on supported NiFe LOH in a grazing incident diffraction cell. (c) A plot illustrating the estimated interlayer distance d{oo3) based on reflection maxima was created to provide an overview of all three effects. (d and e) The Ni redox charge that was accessible was measured with the scan rate. The charge was associated with theNi reduction peak at different electrode potential scan rates and was also monitored as afunction of test history in different electrolytes. (f) The percentage ratio of the charge displayed in the red and green curves in panels {d} and (e}, respectively, was analyzed as a function of the scan rates. Reprinted with permission from Ref. 94. Copyright 2021 American Chemical Society.*

different oxidation states, which facilitates the OER process. Additionally, the layered structure of LDHs provides a large surface area and abundant active sites for the OER to occur. Furthermore, the hydroxide ionsin LDHs can act as nucleophiles, participating in the OER processby attacking water moleculesto form oxygen gas.Further in-depth studies, such as investigating the mechanism and stability, are necessary for the commercialization of LOH in SWE applications.

Design efficient OER catalysts with protective layers

Dueto the instability of manytransition metal catalyst electrode materials, it is crucial to cover them with a thin protective layer on the surface to improve their electrocatalytic stability. Koper's group[98] recently reported that deposition of MnOx on IrOx electrodes can decrease ClORselectivity (Figure12a). Ina solution containing 0.5 MH,SO_4 and 30mM c1-,theselectivity for ClORof *MnOxllrOx* decreased to <7%, whereas IrOx alone exhibited a ClOR selectivity of 86%. When athin MnOxfilm is deposited onto IrOx, it decreases the catalytic activity but increases selectivity from Cl_2 to 0_2. Thus, theMnOxfilm does not act as a promoter or active site and is catalytically inactive. Instead, it acts as a diffusion barrier that prevents c1- from reacting on the IrOx catalyst underneath. Despite this, the MnOx film still facilitates the transport of water, protons, and 0_2 between IrO_2 and the electrolyte, essential for OER activity. Therefore, the protective layer is widely used as an effective strategy to improve OER catalyst selectivity, which will be discussed further in the following.

A team led by Qiao"' has recently presented an effective technique for splitting water molecules and catching hydroxyl

DOI: 10.31635/renewables.023.202300034
Citation: *Renewables* 2023, 1, 415-454
Link to VoR:https://doi.org/10.31635/renewables.023-202300034

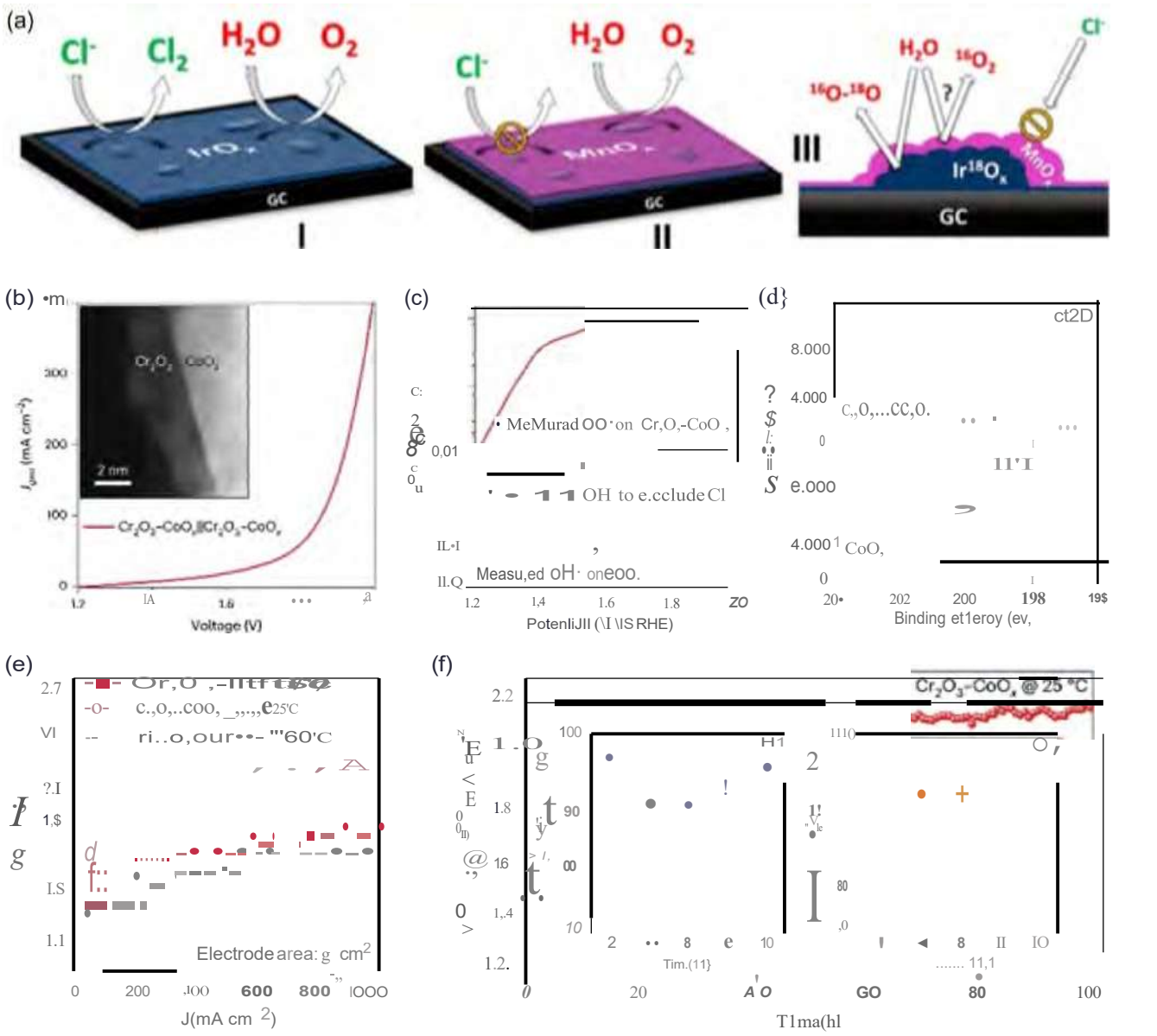

Figure 12 | *(a) Illustrationfor the DER and CIOR reaction pathways on (I} IrOxIGC and {II} MnOxIIrOxIGC {III} shows the side view of the Isotopic labeling Experiment on MnOxIIrOxIGC. Reprinted with permission from Ref 98. Copyright 2018 American Chemical Society. {b) The performance of Cr20$_3$-Co0xfor splitting seawater. The inset of {b) shows the high-angle annular dark-field-scanning transition electron microscopy {HAADF-STEM) image of Cr20$_3$-Co0x. (c) The concentration of OH- measured and the excess* 01, *concentration required to resist CJ·. (d) The XPS spectra of Cl* 2p *for the Cr20$_3$-Co0x and CoOx anode ofter continuous operationfor* 12 *hat* 2.0 *VrmE• (e) Polarization curvesfor the Crp$_3$-Co0x seawater and Pt/C Ru0$_2$ pure water electrolyzers at different temperatures. (f) Thestability of the Cr20$_3$-CoOx seawater eledrolyzer, with the FEs of H$_2$ and 0$_2$ shown in the insets of (f). Reprinted with permission from Ref 24. Copyright 2023 Springer Nature.*

anions. This involves applying a Lewis acid layer, like Cr_2O_3, onto transition metal oxide catalysts, such as *CoOx* (Figure 12b,c). The local alkalinity produced through this approach promotes OER kinetics and prevents chloride attack and electrolyte precipitation on the electrodes (Figure 12d). Figure 12e shows that by modifying the electrodes with Lewis's acid {Cr_2O_3-CoOx), a flow-type natural seawater electrolyzer is capable of achieving an industrial current density of 1.0 A cm^{-2} at 1.87 V and 6o •C. The research indicates that introducing a hardLewis acid layer on the catalysts created an alkalized microenvironment. Furthermore, the study demonstrated that the Lewis acid layer on Cr_2O_3-CoOx produced a substantial amount of *OW,* which primarily participated in OER. Some excess *OW* also reacted with the positive charge on the anode surface to create a secure electrical double layer. By preferentially accumulating excess *OW,* the amount of c1- in seawater is reduced, which is important for direct SWE. Even when the anode potential was as high as 1.90 VRHE, the concentration of surface *OW* on Cr_2O_3-CoOx was still higher than

DOI: 10.31635/renewables.023.202300034
Citation: *Renewables* 2023, 1, 415-454
Link to VoR:https://doi.org/10.31635/renewables.023-202300034

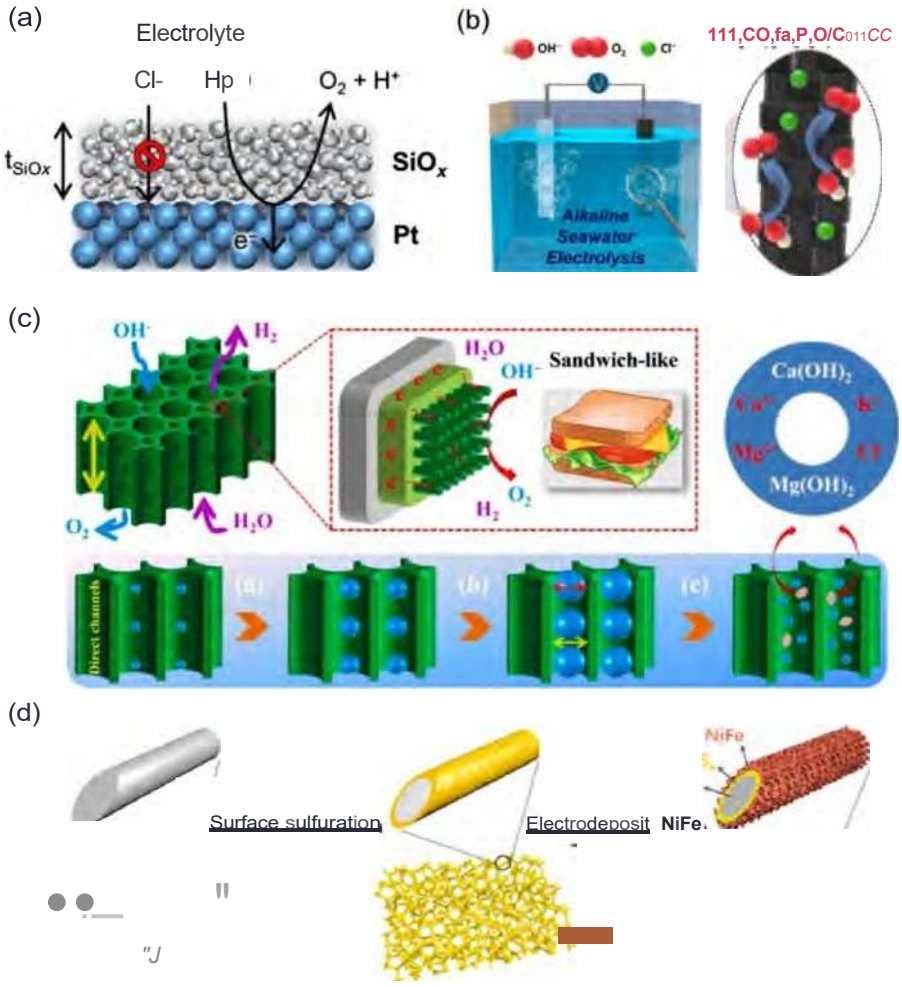

Figure 13l *(a)Aschematicfigure to illustrate the design of a Pt thinfilm electrode protected by SiOx encapsulation.The catalytic interface beneath the encapsulation layerfacilitates the desired OER, whereas the undesired CIER is effectively inhibited f¥ the electrode's selective suppression. Reprinted with permissionfrom Ref 99. Copyright 2021 American Chemical Society. (b)Schematic illustrationfor the alkaline SWE using NCFPOIC@CC as anode catalyst. Reprinted with permission from Ref 100. Copyright 2019 American Chemical Society. (c) A schematic diagram shows that the wood aerogel electrode coated with S,P-(Ni, Mo, Fe}OOH/NiMoP layers demonstrates effective catalysis of OER in alkaline seawater.Thanks to the porous and interconnected structure of the wood aerogel, the electrodefeatures open channels thatfacilitate electrolyte penetration and rapid bubble liberation. Reprinted with permission from Ref 101. Copyright 2021 Elsevier. (d) The process of producing a dual-layer anode {Nil} made of NiFe/NISx-Ni foam for seawater splitting. Reprinted with permission from Ref 102 Copyright 2019 National Academy of Sciences.*

the necessary amount, indicating that the surface-generated *OW* effectively prevented the migration of cl- t0V11ard the electrode surface. This experimental finding demonstrates that the Cr_20_3-Co0x anode can achieve excellent OER selectivity (~98%} and long-term stability (over 200 h at 1.80 VRHE} by avoiding harmful cl- chemistry during direct SWE, as sh0V11n in Figure 12f.

Esposito and colleagues[99] conducted an experiment that showed ultrathin silicon oxide (SiOx} overlayers on platinum anodes (shown in Figure 13a} to be highly effective in reducing CIER, even in the presence of o.6 M ci- in both acidic and pH-neutral electrolytes.Thisisdue to the obstructive effectthatSi*Ox* overlayers have on the transport of cl- to the catalytically active buried interface while enabling the desired OER to proceed. The cl- permeability of SiOx overlayers was three orders of magnitude lower than that of cl- in a conventional salt-selective membrane used in reverse osmosis desalination. Additionally, the overlayers proved to be highly stable over 12 h in chronoamperometry tests conducted at moderate overpotentials. Hence, SiOx overlayers hold great potential in achieving highly selective and stable SWE while avoiding the need to tweak the electrolyte's pH.

Kim et al.[100] reported that carbon-coated sodium cobalt-iron pyrophosphate ($Na_2Co_1\_xFexP_20_7$} nanoparticles enabled electrocatalytic, selective OER during alkaline SWE (Figure 13b}. To fabricate OER electrocatalysts for alkaline SWE, $Na_2Co_1\_xFexP$, /C (where o ***x*** 1) were utilized and loaded onto a carbon cloth to create NCFPO/C@CC. By controlling the Co/Fe ratio, the electrocatalytic OER performance of the NCFPO/C NPs was

DOI: 10.31635/renewables.023.202300034
Citation: *Renewables* 2023, 1, 415-454
Link to VoR:https://doi.org/10.31635/renewables.023-202300034

optimized. NCFPO/C@CC is a highly effective OER catalyst when used in an alkaline saline solution without causing electrode corrosion or generating reactive chloride species. It also demonstrates long-term stability and durability in continuous oxygen generation. NCFPO/C@CC shows electrocatalytic OER activity in alkaline seawater, indicating that it is a promising candidate for OER electrocatalysts in realistic alkaline SWE. During the OER process, the (oxy}hydroxides formed on the NCFPO/C NP surfaces function as oxygen generation sites. NCFPO/C@CC exhibited a low overpotential of <480 mV at a current density of 100 mA cm-' in the alkaline saline solution, where only OER is thermodynamicallyallowed. Selective OER was confirmed by the absence of reactive chlorine species in the solution after the OER test. Moreover, cyclic voltammetry (CV} and long-term chronopotentiometric tests over 100 h confirmed that NCFPO/C@CC is highly stable and durable.The electrocatalytic OER performance of NCFPO/C@CC in alkaline seawater demonstrates its potential as a cost-effective OER electrocatalyst for alkaline SWE.

Yang et al.[°'] created a highly efficient and stable electrocatalyst for OER in seawater, as depicted in Figure 13c.The catalyst, which had a sandwich-like structure composed of S,P-(Ni,Mo,Fe} OOH/NiMoP/wood aerogel, required minimal overpotentials of 297 mV to generate a current density of 500 mA cm-' in alkaline seawater. This remarkable electrocatalytic performance was primarily attributed to the unique interfacial micro/nanostructure and hydrophilic features of the wood aerogel. Additionally, the authors demonstrated the catalyst's practicality for industrial applications, achieving a current density of 500 mA cm-' at 1.861 V with excellent cycling performance. This study has contributed to the advancement of clean and renewable energy systems by utilizing heteroatom-doped multimetal oxyhydroxideselectrocatalysts supported on wood-derived 30 aerogels for overall SWE.

Dai's group[°'] reported a multilayer anode for solar-driven SWE consisting of a nickel-iron hydroxide electrocatalyst layer uniformly coated on a nickel sulfide layer formed on porous nickel foam (NiFe/NiSx-Ni}, as illustrated in Figure 13d. This anode displayed excellent catalytic activity and corrosion resistance at current densities necessary for industrial applications (0.4 to 1 A cm-'). The NiFe electrocatalyst layer, which drives anodic currents toward water oxidation, along with the in situ formation of sulfate and carbonate-rich passivating layers, contributes to chloride repellence and corrosion resistance in the salty-water-splitting anode. The findings suggest that the NiFe/NiSx/Ni anode is both active and stable for SWE. This anode produces a uniform electrodeposited NiFe that acts as a highly selective OER catalyst for alkaline seawater splitting. The NiSx layer situated below serves as a conductive interlayer and a source of sulfur for generating a cation-selective polyatomic anion-rich anode, which exhibits stability against chloride etching/corrosion. Significantly, the electrolyzer exhibited unrivaled durability, with no substantial activity loss detected, even after 1000 h of stability testing.

Jadhav et al.[°3] have developed a dual-purpose catalyst, GO@Fe@Ni-Co@NF, for alkaline seawater splitting.This catalyst comprises interfacial FeOOH NP and Ni-Co hydroxide 20 sheets that reduce the overpotential for OER catalysis. The GO and oxidized carbon layer enhance chloride corrosion resistance while the -Ni-Co LDH's lower interlayer distance decreases the catalyst's charge transfer resistance. The team constructed an alkaline seawater electrolyzer that showed exceptional durability for seawater splitting at an industrial current density of 1 A cm-'. Even after up to 378 h of stability testing, no noticeable activity drop was observed. This study promises a practical and cost-effective approach to producing hydrogen by utilizing vast seawater splitting.

In summary, the protective layer strategy can effectively suppress CIER/CIOR by inhibiting the diffusion of chloride ions. However, it remains highly controversial whether the protective layer can enhance the activity of OER at the same time. We encourage more experiments and theoretical simulations to study the real effect of the protective layer and confirm whether it can improve the activity and selectivity of OER while suppressing CIER/CIOR.

Design of efficient OER catalyst with surface reconstruction engineering

The phenomenon of surface reconstruction is commonly observed in the majority of OER catalysts due to the high current density/voltage during operation.[°4.°5] An exemplary case is presented by Ren et al.[°5] where they developed a sturdy oxygen-evolving electrocatalyst that consists of ferrous metaphosphate on a self-supported conductive nickel foam, which is available in large quantities. The catalyst possesses in situ generated nickel-iron oxide/hydroxide and iron oxyhydroxide catalysts on the surface (Figure 14a-f}, and can achieve a current density of 10 mA cm-' at an overpotential of 177 mV, 500 mA cm-' at 265 mV, and 1705 mA cm-' at 300 mV, with remarkable durability in an alkaline electrolyte of 1M KOH, even after 10,000 cycles. Compared to the state-of-the-art $Ir0_2$ catalyst, the $Fe(P0_{3}\}_2$ catalyst supported on commercial Ni foam shows a 49-fold improvement in water oxidation activity at 300 mV. It is highly effective for water oxidation in electrocatalytic water splitting, requiring only an overpotential of 265 mV to generate a current density of 500 mA cm-' in 1 M KOH. The catalyst'sexcellent electrochemical durability during OER testing for 10,000 cycles and ability to operate at 500 mA cm-' for over 20 h is noteworthy. Additionally, the fabrication process of this outstanding electrocatalyst is in line with industrial standards and is economically feasible for large-scale production. This research is a significant milestone towards cost-effective hydrogen production by water splitting, which will contribute to the reduction of fossil fuel consumption.

Other catalyst materials and strategies

other types of catalysts, including oxide,[°06] carbonate hydroxide,[°07] phosphide,[57,08-°9] selenide,[°] sulfides,n, and others, have also been investigated as catalysts for the OER in seawater splitting. Keane and Nocera,[°6] for instance, reported on self-healing oxygen evolution catalysts made of cobalt or nickel that

DOI: 10.31635/renewables.023.202300034
Citation: *Renewab/es* 2023,,, 415-454
Link to VoR:https:/ /doi.org/10.3'1635/renewables.023-202300034

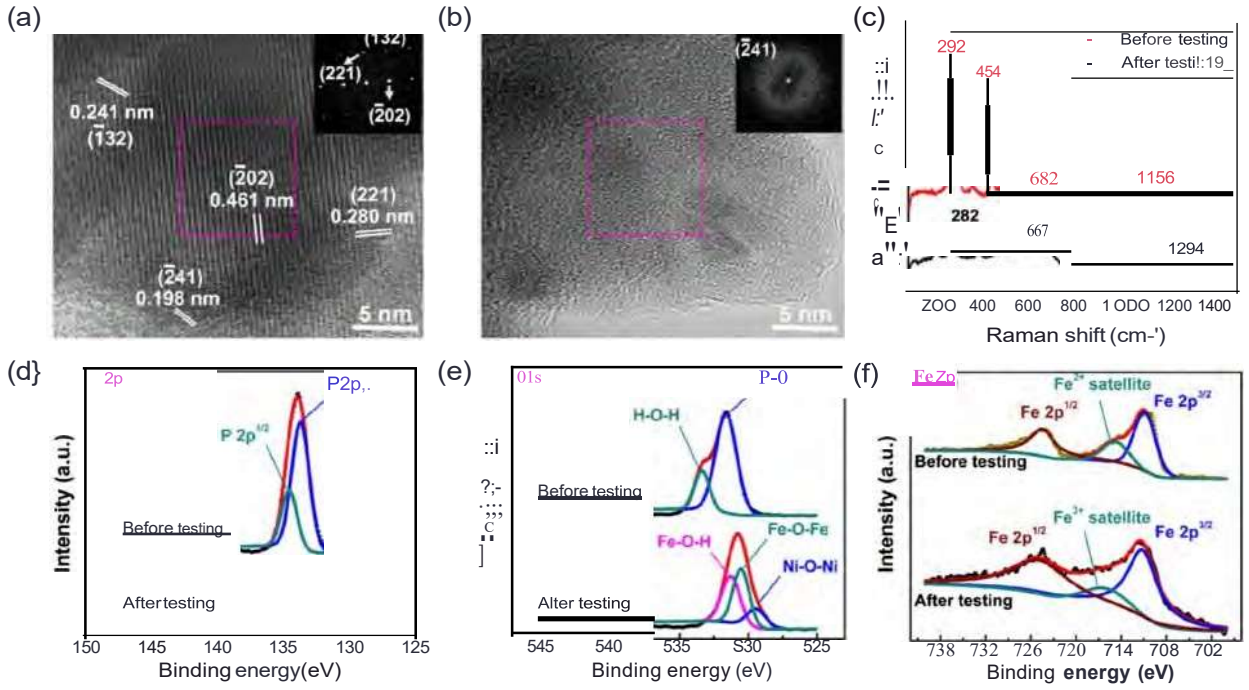

Figure 14 | *Thecatalyst's high-resolution TEM images andfast Fourier transform patterns (insets) depict (a) its initial good crystallization state and (b) its post-OER state in an amorphous state. (c)Raman spectra of the as-prepared and post-OER catalyst. XPSspectra of (d} P 2p, (e) 0 1s, and (f) Fe2p binding energies before and after OER tests. Reprinted with permissionfrom Ref 105. Copyright 2017 National Academy of Sciences.*

could produce oxygen selectively from both 0.5 M NaCl solutions and seawater. DEMS analysis revealed no presence of halogens in the product stream, and chemical analysis showed only small amounts of hypohalous acid were produced. DEMS results demonstrated that CoPi and **NiBi** catalysts could achieve high selectivity in generating 0_2 from seawater by inhibiting the oxidation *of* cl- and Br-.The reactivity of the substrate's edges dictated the kinetics of oxidation by these catalysts.The activity of these catalysts in promoting oxidation is determined by the reactivity of the substrate at the edges. The hindered ability of halides to displace water molecules from the edge sites on the cluster plays a significant role in the selective production of oxygen. These discoveries hold potential value for practical applications aimed at producing oxygen from seawater.

Advanced HER Cathode Catalyst for SWE

Different from the OER anode for SWE with its strong competition with CIOR/CIER, there is no gas-evolving reaction at the cathode competing with HER. However, there are still some challenges for HER cathode electrode catalyst for SWE (Figure 15a), such as reduced stability due to deposition of impurities such as metal ions (Ca,. and **Mg,.)** and hydroxides, and corrosion of the catalyst. The active site can be blocked by these impurities. Besides, the ca>+and Mg,. may be deposited at the cathode as hydroxides under reductive conditions, and current density losses of >50% have been reported due to salt deposition after short periods of operation.[2s.n2,n3] There are several ways to enhance cathode stability (Figure 15b-d),2uo,43,,14-1,[6] such as utilizing membranes in an engineering approach (e.g., PEM electrolyzers) to prevent impurities from reaching the cathode, creating catalysts with HER-selective surface sites and resistance to side reactions or deactivation, and depositing overlayers on the catalyst to obstruct impurities while still enabling the transfer of reagentsand products. In this section, we will mainly focus on the cathode electrode materials for SWE, and the electrode materials can be divided into two categories: noble metals and nonnoblemetals.Table 2 providesa summary of the representative catalystsand the effectiveness of the HER electrocatalysts that have been recently reported in either seawater or SSW.

Noble metal catalysts

The Sabatier principle suggests that Pt group metals have the best HER catalytic performance (Figure 16a)/r'[19] but their high cost limits their commercial applications.[10.,160.1 20-1 21] Transition metals like Ni, Co, and Fe can be used as an alternative. Alloying Pt with a transition metal can produce a low-cost, highly active electrocatalyst. The atomic orbital interaction between the transition metal and **Pt** can contribute to the formation of chemical adsorption bonds between hydrogen and the metal, enhancing the adsorption of H atoms on catalysts and accelerating hydrogen evolution in seawater. Synthesizing **PtM** alloys can enhance the HER performanceby adjusting the species, composition, and stoichiometric ratio of the transition metal **M** to Pt.[128] For

Dot: 10.31635/renewables.023.202300034
Citation: *Renewables* **2023,** 1, 415-454
Linkto VoR:https://doi.org/10.31635/renewables.023-202300034

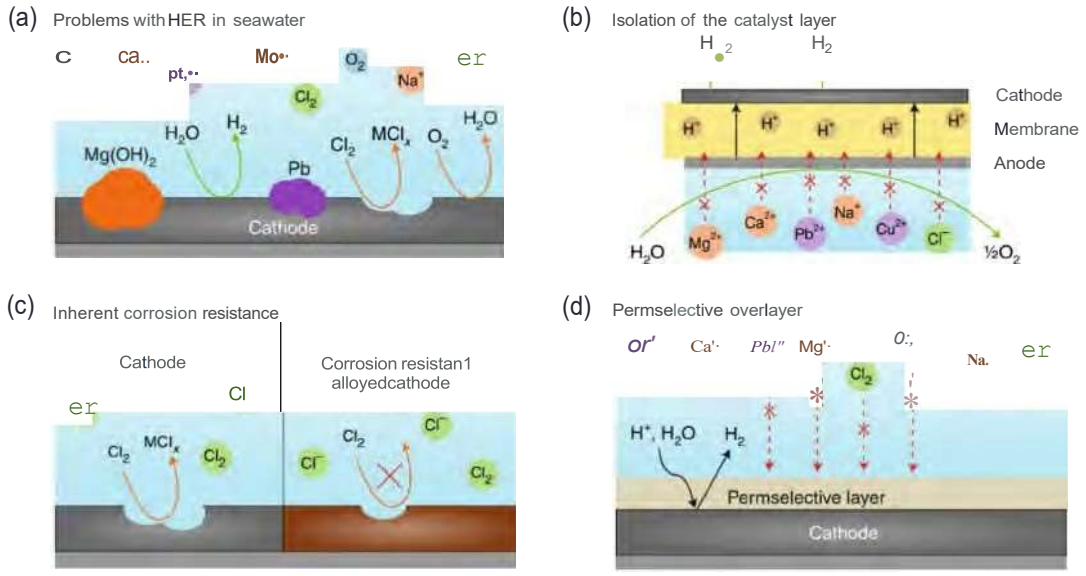

Figure 15 | *To improve the long-term stability of HER in SWE, (a) challenges must be addressed, and (b-d} potential solutions can be considered. Reprinted with permission from Ref 21. Copyright 2020 Springer Nature.*

Table 2 | *A summary of Catalysts Reported for HER in Neutral, Alkaline, and SSW Conditions*

Catalysts	Electrolyte	*J* (mA cm-')	Overpotential (mV)	Stability	Reference
Ni_2P-CoOOH	Seawater	1000	530		173
Ni_2P-Fe_2P	1.0 M KOH + seawater	1000	**389**	40 h@500 mA *cm-'*	57
NiMoN@NiFeN	1.0 M KOH + seawater	1000	**218**	100 h@500 mA *cm-'*	174
NiCoP Holey Nanoarrys	Seawater	10	287	12 h@10 mA cm-'	151
Mos, QD	Seawater	100	690		175
Mo_5N6	Natural seawater	10	26o	100 h@20 mA cm-'	152
o.5Rh-GS1000	SeawaterpH 8.32	10	19	10 h@15 mA cm-'	136
Fe,P-NiSe, NFS	0.5 **M** KOH + seawater	500	186		60
CoxM0$_2$.xCIMXene/NC	Natural seawater	40	440	225 h@4 mA cm-'	54
Ni-SN@C	1 M KOH + seawater	100	180	40 h@12 mA cm-'	55
Ni-SA/NC	1 M KOH + seawater	10	139		56
pt@mh-3D MXene	Natural seawater	30	360	250 h@io mA cm-'	129
S,P-(Ni,Mo,Fe)OOH/ NiMoP/wood aerogel	1 M KOH + seawater	500	255		101
Co-Fe_2P	1 M KOH +0.5 NaCl	300	300	24 h@100 mA cm-'	109
$ptNi_3$	Seawater	100	1100	12 h@Jo mA cm-'	176
RuCo	Seawater	100	850	12 h@100 mA cm-^{2}	133
Mn-NiO-Ni/Ni-F	Seawater	40	435	14 h@7 mA cm-,	112
CoMoP@C	Seawater	6o	410	10 h@20 mA cm-,	146
GDY/$Mo0_3$	Seawater	150	660	120 h@10 mA cm-,	156
ptRuMo	Seawater	50	600	180 h@ioo mA cm-^{2}	134
Fe-Co_2P BNRs	Seawater	350	780	100 h@40 mA cm-'	147
U-CNT-900	Seawater	20	820	7 h@10 mA cm-^{2}	148
Fe-Mos, NSA	Buffered seawater	100	200	30 h@100 mA cm-^{2}	149
Rh/GDY	1.0 **M** KOH+0.5 M NaCl	1000	65		137
Cr_20_3-Co0x	Natural seawater	2 mA cm-, (ECSA)	210		24
ptMoo.1	Seawater	160	800	180 h@150 mA cm-,	128

DOI: 10.31635/renewables.023.202300034
Citation: *Renewab/es* 2023, 1, 415-454
Linkto VoR:https://doi.org/10.31635/renewables.023-202300034

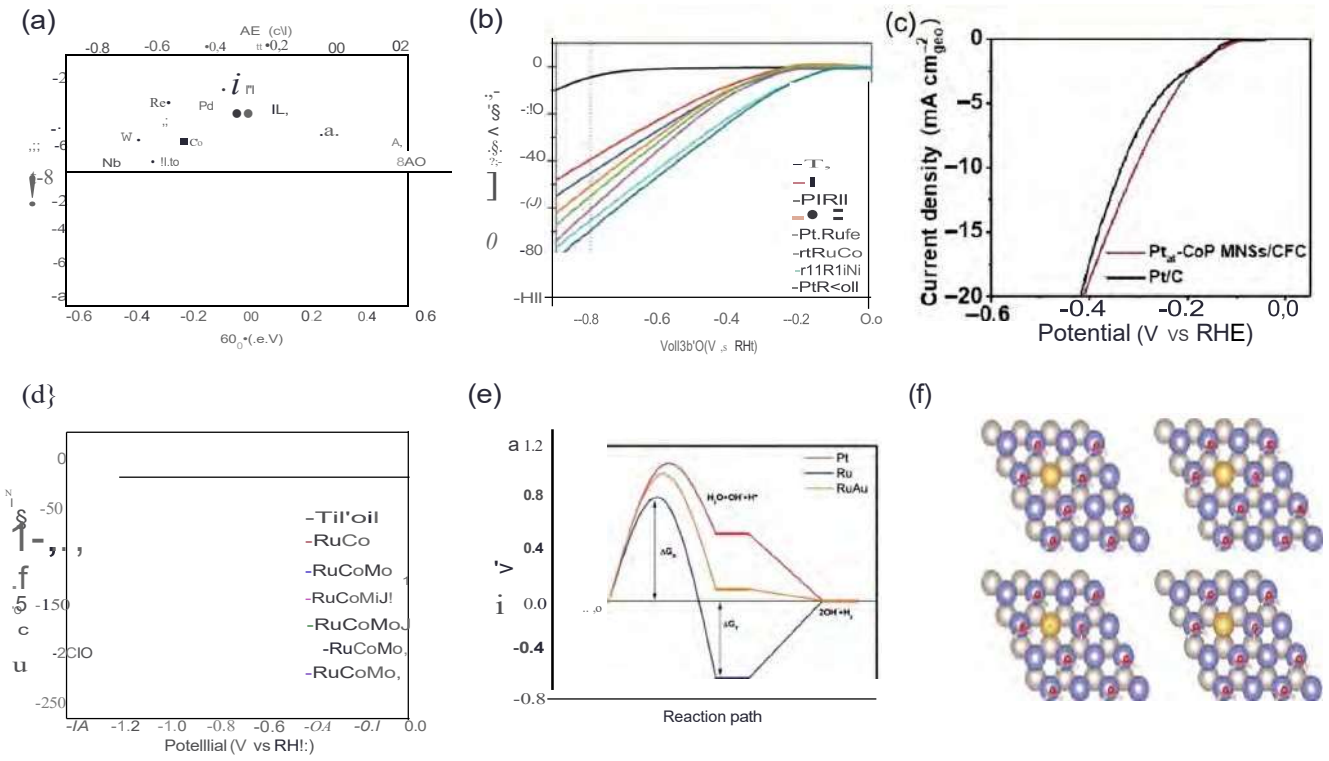

Figure 16 | *(a) Exchange current density and log(iJ of HER at different transition metals. Reprinted with permission from Ref. 75. Copyright 2017 Elsevier. (b) HER curves of different PtRu-based ternary alloys recorded in seawater. Reprinted with permission from Ref 134. Copyright 2017 The Royal Society of Chemistry. (c) HER LSVcurves of Ptat-CoP MNSs/CFC in seawater. Reprinted with permission from Ref 130. Copyright 2020 The Royal Society of Chemistry. (d} HER performance of Tifoil supported RuCo and RuCoMox electrodes in seawater. Reprinted with permissionfrom Ref 133. Copyright 2016 Elsevier.(e) Gibbsfree energy profile of the HER on Pt(m), Ru(oo1), and RuAu(oo1) surfaces.Where .1Gr represents the energy barrier for the Heyrovsky reaction. .1G$_8$ represents the activation energy of water dissociation. (f)A schematic representation of hydrogen evolution on RuAu.Where the blue and gray balls represent the top and bottom layers of Ru, respectively, the yellow and red balls represent Au and O atoms, and the white andgreen balls represent hydrogen atoms. Reprinted with permission from Ref 131. Copyright 2019 Wiley.*

example, Li et al."[8] synthesized ptM alloys (**M** = Cr, Fe, Co,Ni,Mo} and evaluated their HER performance in neutral seawater. ptM0$_{0.1}$ showed an overpotential of 650 mV at 100 mA cm-^{2}. Additionally, the transition metal **M** can react with Cl_2 gas generated at the anode, thereby delaying the dissolution of pt_ As a result, the catalyst can operate for over 173 h at a potential of o.8 V versus RHE in neutral seawater splitting. Therefore, adjusting the species, composition, and stoichiometric ratio of the transition metal **M** to pt can enhance the HER performance. Yang et al.'[34] reported a series of pt-Ru-M (M = Cr, Fe, Co, Ni, Mo} alloy for HER in SWE (Figure 16b}. It is found that the pt-Ru-M electrodes have significantly enhanced catalytic activity for the HER compared to pt or pt-Ru electrodes. This is due to the alloying effects between the transition metals and the pt species.

The size effect,the low coordination environment of the metal center, and the metal-support interaction make single pt[129,130] and Ru•n•[32] catalysts attractive alternatives to metallic pt and Ru for HERin SWE.These catalystsexhibit extraordinary catalytic performance in heterogeneous reactions. For instance, Liu's group'[30] developed a single atom pt on CoP mesoporous nanosheets (MNSs} that grew on carbon fiber cloth (CFC} catalyst, ptat-CoP MNSs/CFC, with an ultralow pt loading of 0.7 wt% relatives to CoP. The high dispersion of ptat sites and strong interaction between ptat and CoP leads to spontaneous water dissociation, resulting in a low HER kinetic barrier and outstanding HER performance in seawater (Figure 16c}. The high utilization rate of pt and the modulation of the electronic states of pt by the CoP matrix are responsible for the enhanced HER performance of ptat•CoP MNSs/CFC

Besides pt, Ru is another alternative electrode materials for HER in SWE because of their much lower price than pt, However, due to the lackluster HER capabilities of Ru in seawater, its coordination environment and surface structure have been optimized in order to enhance its performance.•[32-34] As an example, Yang and coUeagues'[33] developed a RuCoMox catalyst that shows overpotentials of 550 mV at 10 mA cm-^{2} (Figure 16d} in natural seawater. The surface of this catalyst is marked by numerous defects that serve as active sites for absorbing water molecules and constructing metal-hydrogen bonds. Results indicate that ternary alloys with more shared *d* electrons possess an unconventional electronic configuration that facilitates the

DOI: 10.31635/renewables.023.202300034
Citation: *Renewables* **2023**, 1, 415-454
Link to VoR:https://doi.org/10.31635/renewables.023,202300034

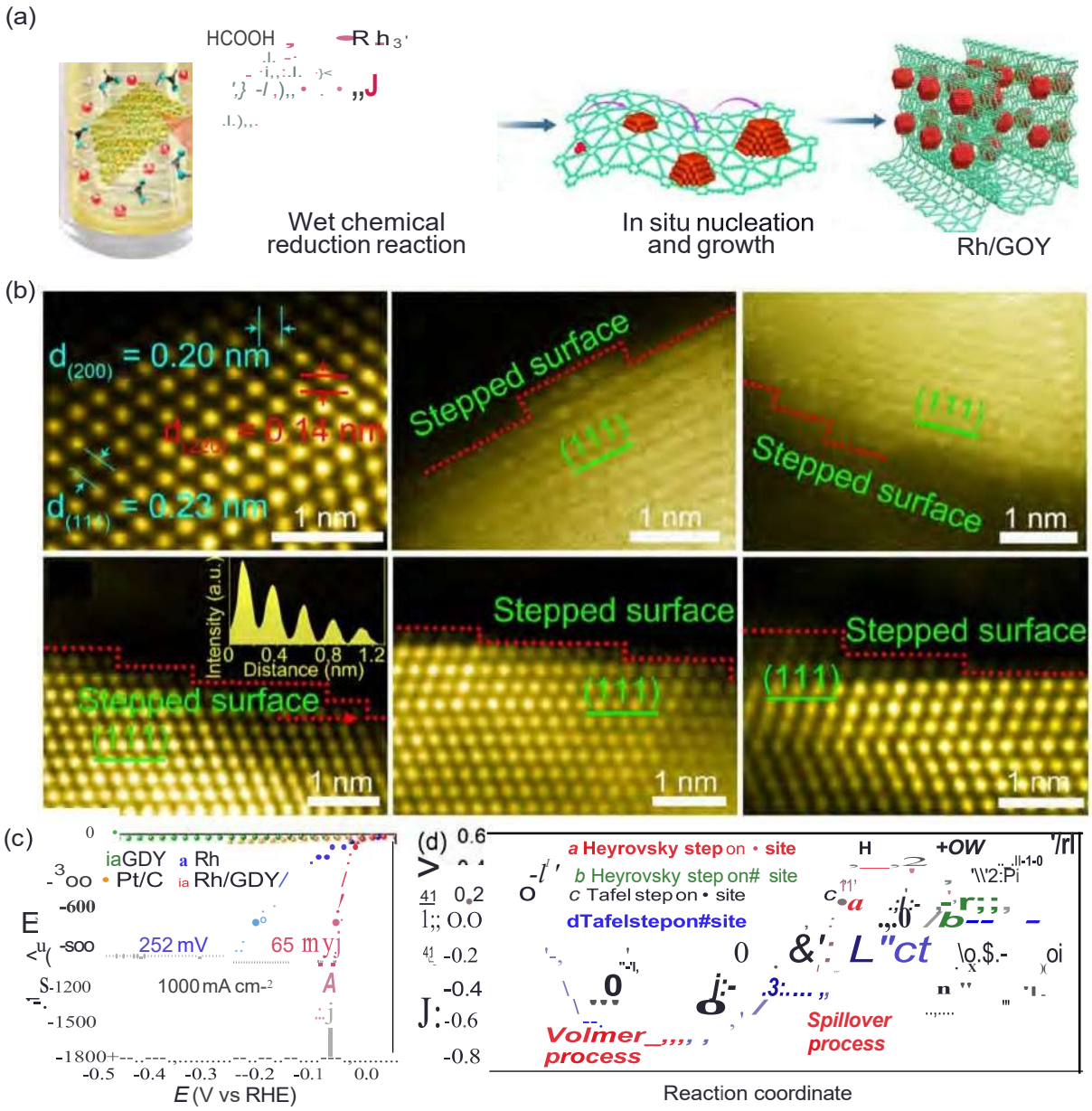

Figure 17 | *(a)Synthesis routes of porous Rh/GOY electrodes. {b} HAAOF-STEM image of Rh/GOY, where the intensity profile along the red dotted line indicates a stepped surface along the edge. (c) HER polarization curves of the as-synthesized catalysts in H_2-saturated1.0 **M** KOH+ 0.5 M NaCl electrolyte. (d} An energy diagram of the Volmer-Tafel pathway for HER on the Rh/GOY. Reprinted with permission from Ref 137- Copyright 2022 Springer Nature.*

provision of electronsfor taking partin the HER.Additionally, the Ru-3(1 core energy level peaks of $Ru0_2$ do not alter during the HER process of seawater, preventing the Ru from chemical dissolution or corrosion. In addition to pt and Ru single-atom catalysts, incorporating Au atoms into Ru-based catalysts can transfer electrons from Ru to Au atoms, resulting in positively charged Ru atoms and negatively charged Au atoms.[131] This configuration improves the adsorption of water molecules and hydrogen atoms, respectively, leading to an accelerated HER process (Figure 16e). The material also exhibits relay catalysis, where Ru atoms serve as the first active sites for capturing and splitting water molecules, while Au atoms act as the second active site for proton absorption and H_2 desorption (Figure 16f). This balance between the adsorption of water molecules and protons and gas release in a neutral medium results in a perfect HER performance. Therefore, single-atom catalysts may play a crucial role in seawater HER.

Other precious metals, such as rhodium (Rh), have also been widely used as electrode materials for HER in SWE.[111-137] For example, Li et al.[137] reported that formic acid as the reducing agent and porous graphdiyne (GDY) as the stabilizing elementto supported Rh nanocrystals (Rh/GDY, Figure 17a). Transmission electron microscopy {TEM) results revealed that high-density atomic steps on the faces of hexahedral Rh nanocrystals

DOI: 10.31635/renewables.023.202300034
Citation: *Renewables* 2023, 1, 415-454
Linkto VoR:https://doi.org/10.31635/renewa bles.023-202300034

(Figure 17b). It was found that the exposed high active stepped surfaces and various metal atomic sites affect the electronic structure of the catalyst, resulting in reduced overpotential and large-current hydrogen production from saline water. In ,.o **M** KOH + 0.5 **MNaCl** saline-alkaline electrolyte, the Rh/GOY just need an overpotential of 28, 48, and 65 mV to reach a current density of 100, 500, and 1000 mA cm-2, respectively. From OFT calculations, It was found that HER on stepped Rh/GOY determined the most preferred pathways (Figure 17c,d). The Volmer-Tafel process was found to be the most favorable pathway, one H_20 molecule tends to stably adsorb on the corner site of the catalyst surface and is easily dissociated into (H-OH), generating abundant hydroxyl (OH°) and hydrogen (H*) sources. Thus, rational control of the catalyst surface, structure with exposed crystal plane should be an efficient way to boost the HER performance. Xie et al.[136] reported Rh nanoparticles modified by N/5-doped carbon nanosheets as a highly effective electrocatalyst for HER in seawater. The use of mesoporous graphene-like nanosheets allowed for a highly dispersed Rh nanoparticle catalyst and unexpected electronic asymmetry depending on the intensity of Rh-support interaction. The introduction of S in the graphene-like nanosheets enhanced the interaction between Rh nanoparticles and carbon supports, resulting in superior HER activity in seawater. It is believed that the active site for the HER comes from the electron-rich interface between Rh and the support.

Nonnoble metal catalysts

Even though the noble metal-based catalysts show a lot of high activity for HER in SWE, however, the scarcity and high cost of pt-based materials have limited their large-scale commercial use.[126,138–142] As a result, researchers have shifted their focus to transition metal-based materials. The electrocatalytic performance for HER and the adsorbed hydrogen energy relationship can be represented by volcano plots, as shown in Figure 16a. Transition metals such as **Ni,**[55,57,101] Co,[5,109,146,148] and Mo,[5,6,101,143,146,149] are located near the precious metals on the plots, indicating moderate adsorption/desorption energy for **H".** This makes them a promising candidate for HER, as they can potentially replace pt-based catalysts.[150]

Ni-based nonnob/e metal catalysts

Ni-based catalysts are widely employed as electrode materials for HER. However, the catalytic activity and stability of pure metallic Ni still need to be improved. Qiao et al.[55] reported an unsaturated nickel surface nitride (Ni-SN@C)catalyst for HER in

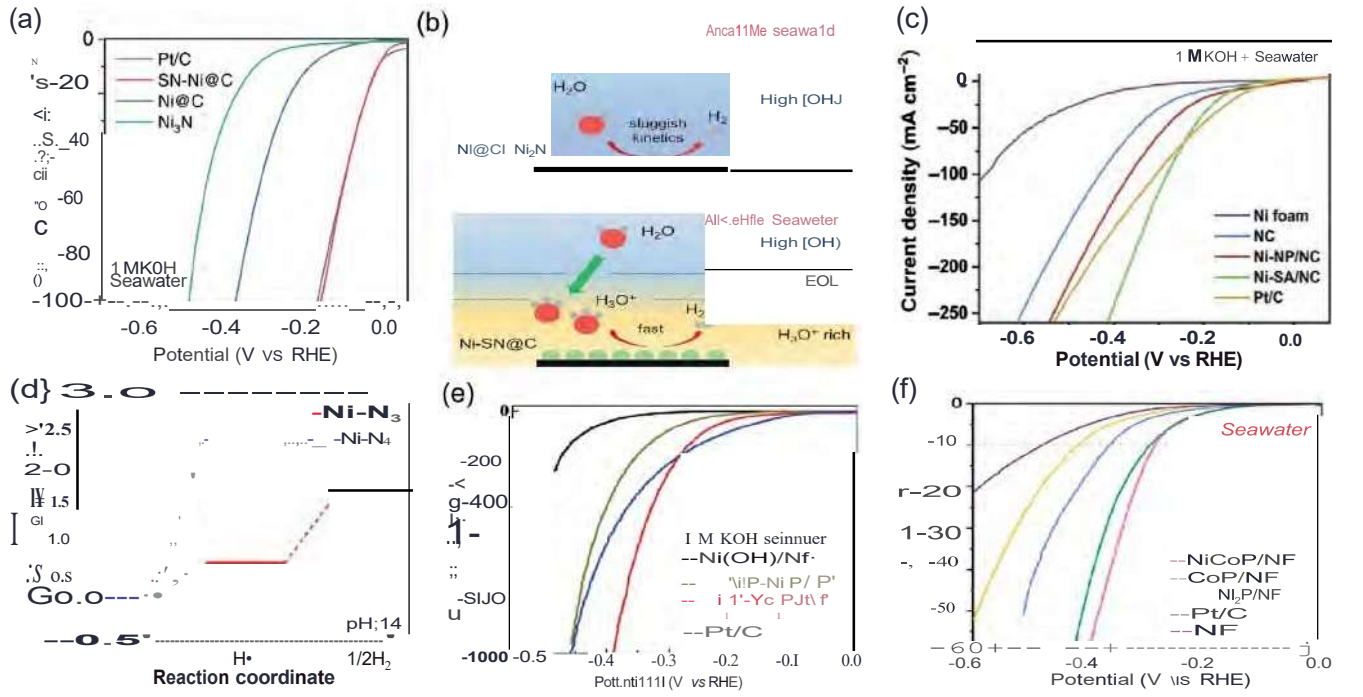

Figure 18 | *(a) LSV curves of different catalysts in 1 M KOH seawater. (b} Illustration of the hydronium ion generation mechanism on Ni-SN@C EDL: electric double layer. Reprinted with permission from Ref 55. Copyright 2021 Wiley. (c) HER performance of Ni-SA/NC in realistic alkaline seawater. (d} The Gibbsfree energy diagram of HER on the* ***Ni-N3*** *and* ***Ni-N4*** *structures at pH 14, whereW denotes one hydrogen atom adsorbed on an adsorption site('}, and1/2H2 refers to one gas-phase hydrogen molecule. Reprinted with permissionfrom Ref 56. Copyright 2021 Wiley. (e) HER LSV curves of Ni2P-Fe2P/NF and other control samples in 1 M KOH seawater electrolyte. Reprinted with permission from Ref 57- Copyright 2022 Wiley. (f} Polarization curves of NICoPINF and different electrocatalystsfor HER at a scan rate of 1 mVs-• in real seawater. Reprinted with permission from Ref 151. Copyright 2019 American Chemical Society.*

DOI: 10.31635/renewables.023.202300034
Citation: *Renewables* 2023, 1, 415-454
Link to VoR:https://doi.org/10.31635/renewables.02,3,202300034

alkaline seawater. The catalyst exhibits exceptional activity and stability, with a low overpotential of 23 mVat a current density of 10 mA cm-^{2} in alkaline seawater electrolyte, outperforming pt/C (Figure 18a). Unlike traditional transition metal nitrides or metal/metal nitride heterostructures, Ni-SN@C does not have any bulk nickel nitride phase. Instead, it features unsaturated **Ni-N** bonding on the surface. Further in situ Raman spectral analysis demonstrates that Ni-SN@C functions similarly to pt in generating hydronium ions in a high-pH electrolyte, which creates a localized acid environment during the alkaline HER process (Figure 18b). This behavior is not observed on metallic nickel and nickel nitride catalysts. This work presents a surface modification of earth-abundanttransition metalsas a promising strategy for low-cost and clean hydrogen production.

Recently, Pennycook et al.5[6] developed a new type of **Ni** single-atom electrocatalyst (Ni-SA/NC). The Ni-SA/NC was created using a surfactant-assisted method and consists of Ni with either Ni-N_3-0_2 or Ni-N_4 coordination. It was discovered that Ni atoms dispersed atomically with triple nitrogen coordination (Ni-NJ showed superior HER performance, with overpotentials as low as 139 mVat10 mA cm-^{2} in alkaline seawater electrolytes (Figure18c). OFTcalculations confirmed that the **Ni-N_3** coordination having a lower coordination number than **Ni-N_4**, promotes water dissociation and hydrogen adsorption (Figure 18d), thereby improving the HER activity. In addition, the operational stability of **Ni-SA/NC** is impressive, with no observable decline in activity even after 5000 cycles and continuous electrolysis for 14 h.This highlightsthe significance of microcoordination control in electrocatalysts.

Metallic phosphide is another efficient electrode material for HER due to its platinoid properties. Ren's group[57] reported a self-supported Ni_2P-Fe_2P electrocatalyst with high intrinsic activity, abundant active sites, and superior transfer coefficient, enabling it to display remarkablecatalytic activity toward HER in1M KOH seawater electrolyte due to its improved corrosion resistance and hydrophilic surface. It only requires low voltages of 252 and 389 mV to achieve current densities of 100 and 1000 mA cm-^{2}, respectively (Figure 18e). Dong et al.'[51] reported porous feather-like NiCoPnanoarrays on nickel foam (PF NiCoP/NF) for HER in seawater. The 30 morphology, holey structure, and conductive substrate are advantageous for the enhanced HER activity, which can increasethe electrode's specific surface area, facilitate efficient electron and mass transfer, expose more active sites, and aid the release of generated H_2.As a result, the PF NiCoP/NF just needs an overpotential of 287 mV to reach a current density of 10 mA cm-^{2} in real seawater (Figure 18f). This work demonstrates the importance of the development of novel electrode structure, which will not only maxize the specific surface area and inhibitthe occupation and blockage of catalytic active sites, but it will also be conduciveto the removal of hydrogen bubbles during SWE.

Co- and Mo-based nonnob/e metal catalysts

Researchers have taken a keen interest in Co- and Mo-based catalysts owing to their abundance and high electrocatalytic activity for HER. For example, OFTcalculationshave revealed that the d-band structure of Mo can be broadened by hybridizing it with N, S, P, or C. This allows it to attain a d-band structure similar to that of pt, resulting in excellent HER catalytic activity. Therefore, doping or hybridizing Co and Mo compounds with heteroanions can be advantageous in enhancing their HER activity.For example, Li's group'[46] demonstrated that a few-layer N-doped carbon-coated cobalt molybdenum phosphide nano-crystal (CoMoP@C)is an outstanding alternative HER in seawa-ter.The CoMoP@C catalyst was synthesized via pyrolysis using a molecular platform of polyoxometalate on a large scale in a single step (Figure 19a). In real seawater, CoMoP@C displays an overpotential of 590 mV at a current density of 50 mA cm-^{2} (Figure 19b) and demonstrates stable HER performance with a high FE of 92.5%. The catalyst's superb electrochemical perfor-mance was mainly owing to the synergistic effect of CoMoP and the interaction betweenthe CoMoP nanocrystallinecore and the N-doped graphite carbon shell, which optimizes the free energy for H adsorption (Figure 19c). Furthermore, the N-doped carbon shell works to protect the Mo-Co-based active sites from corro-sion, agglomeration, and poisoning by ions in the neutral seawater electrolyte, thereby enhancing the material's long-term stability.

Qiao et al.'[52] created single-crystal nitrogen-rich 20 **Mo_5N_6** nanosheets through a synthesis process induced by Ni, where the addition of **Ni** induced the formation of **Mo_5N_6** rather than MoN.They combined a 20 horizontal growth method with this transition metal phase state to fabricate ultrathin Mo_5N_6 nanosheets at the atomic level.The Mo_5N_6 nanosheets showed exceptional HER catalytic properties and durability in seawater. It was found that the addition of extra nitrogen atoms led to a higher molybdenum valence and a platinum-like electronic structure, significantly enhancing itsintrinsicactivity.TheMo_5N_6 nanosheets synthesized with Ni-induced salt templates demon-strated better HER activity than non-Ni-induced Mo, only requir-ing an overpotential of 257 mV to produce 10 mA cm-^{2} in natural seawater (Figure 19d). It was found that the enrichment of N made the center position of the d-band for Mo closer to that of pt, improving the valence state of Mo and optimizing the decomposition kinetics of water.

The support also plays an important role in electrocatalytic reactions, For example, MXene has been widely reported to be used as an efficient support[54.'29.'53-,ss] due to its high conductivity, rich terminal groups (-0,-OH,and-F),and synergistic properties with metal. Qiu et al.[54] proposed a methodology for creating a multifunctional collaborative catalytic interface to formulate multifunctional CoxM0_2.xCIMXene/NCwith the cooperative cat-alytic interface (Figure 19e), which enhances HER in natural seawater. With the interfaces of CoxM0_2.xC, MXene, and nitro-gen-doped carbon, CoxMo$_2$.xC/MXene/NC showed greatly im-proved electrical conductivity, water dissociation kinetics, and W/water adsorption for SWE (Figure 19f). Notably, the catalyst demonstrated an overpotential of 312 mV to achieve10 mA cm-^{2} in natural seawater. Recently, Guo et al.'[56] presented a novel self-supporting 30 GOY/molybdenum oxide (Mo0_3) material that is highly efficient for HER in seawater due to a well-planned

DOI: 10.31635/renewables.023.202300034
Citation: *Renewab/es* 2023,,, 415-454
Linkto VoR:https:/ /doi.org/10.3'1635/renewables.023-202300034

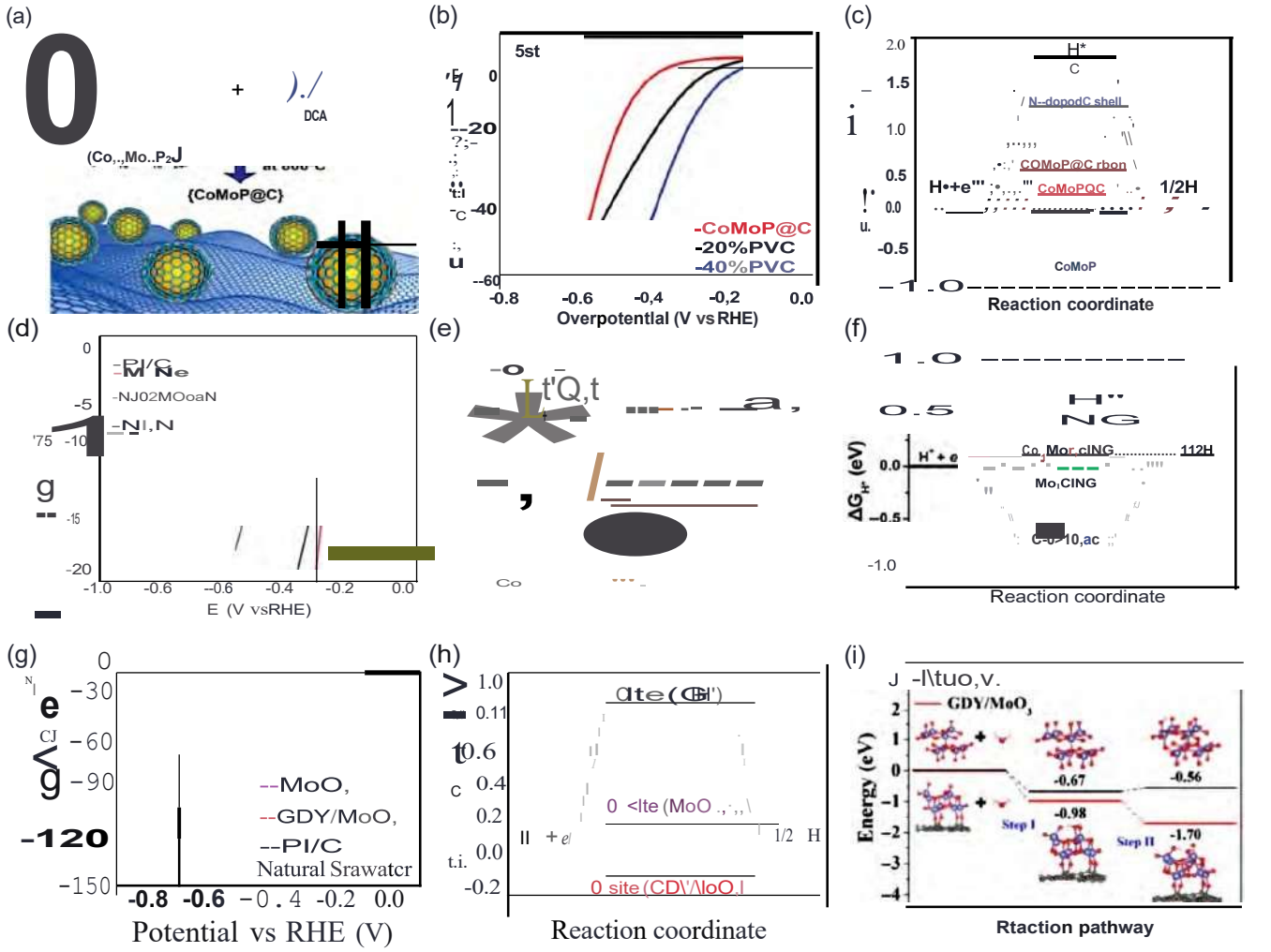

Figure 19 | *(a) Illustration of the preparation of the CoMoP@C catalyst, {b} HER polarization curves of CoMoP@C, and 20% and 40% Pt/C in SSW at a scan rate of 5 mVs1 in the sth tests. (c) The calculated free-energy diagram of the HER on various catalysts. Reprinted with permission from Ref 146. Copyright 2017 The Royal Society of Chemistry. {d) LSV curves of different catalysts measured in Ar-saturated natural seawater. Reprinted with permission from Ref 152. Copyright 2018 American Chemical Society. (e) Schematic illustration of the synthetic strategy of the CoxMo$_2$.xCIMXene/NCcatalyst by annealing of the polymerized chelate of Mop$_{246}$-, co», anddopamine in the presence ofTi_3C_2 MXene and the merits of collaborative interfacefor HER under multi-pH conditions. {f} Free energy diagramsfor HER on the NG, Mo_2C, Co..MonC, Mo_2CING, and Co..Mon CING at zero potential. Reprinted with permission from Ref. 54. Copyright Wiley. (g) HER polarization curves of the samples obtained in natural seawater; {h}free energy of hydrogen adsorption {t.Gw} on GOY,MoO_3-Vo, and GDY/MoO_3; {i} calculated energy diagram of H_2O adsorption and H_2O dissociation {inset: corresponding atomic structures of initial state, H_2O adsorption, and water dissociation on MoO_3-Vo and GDY/MoO}. Reprinted with permission from Ref. 156. Copyright 2021 American Chemical Society.*

"sp C-0-Mo hybridization" at the interface. This hybridization creates new intrinsic catalytic active sites (nonoxygen vacancy sites} and amplifiesthe number of active sites (eight times more than pure Mo0$_3$}. The GDY/Mo0$_3$ just needs an overpotential *of* 660 mV to reach a current density of 150 mA cm-', which is comparable to commercial pt/C in natural seawater (Figure19g}. From the DFTcalculations (Figure19h,i}, it was found that the "sp C-0-Mo hybridization" at the interface plays a critical role in facilitating electron transfer from GDY to Mo0$_3$, resulting in significantly enhanced electron injection during HER (25 times higher thanMo0JThishybridization also reducestheformation energy of oxygen vacancies and provides more active sites. Additionally. hydrophilic properties and a 3D self-supporting substrate are essential components for achieving high performance and excellent stability.

Electrolyte

The pH level of seawater plays a crucial role in SWE, as local changes in pH occur at the electrodes during 0ER. When catalyzing, the anode and cathode experience a steady decrease and increase in pH during the evolution of oxygen and hydrogen.[157]

DOI: 10.31635/renewables.023.202300034
Citation: *Renewab/es* 2023, 1, **415-454**
Link to VoR:https://doi.org/10.31635/renewables.023-202300034

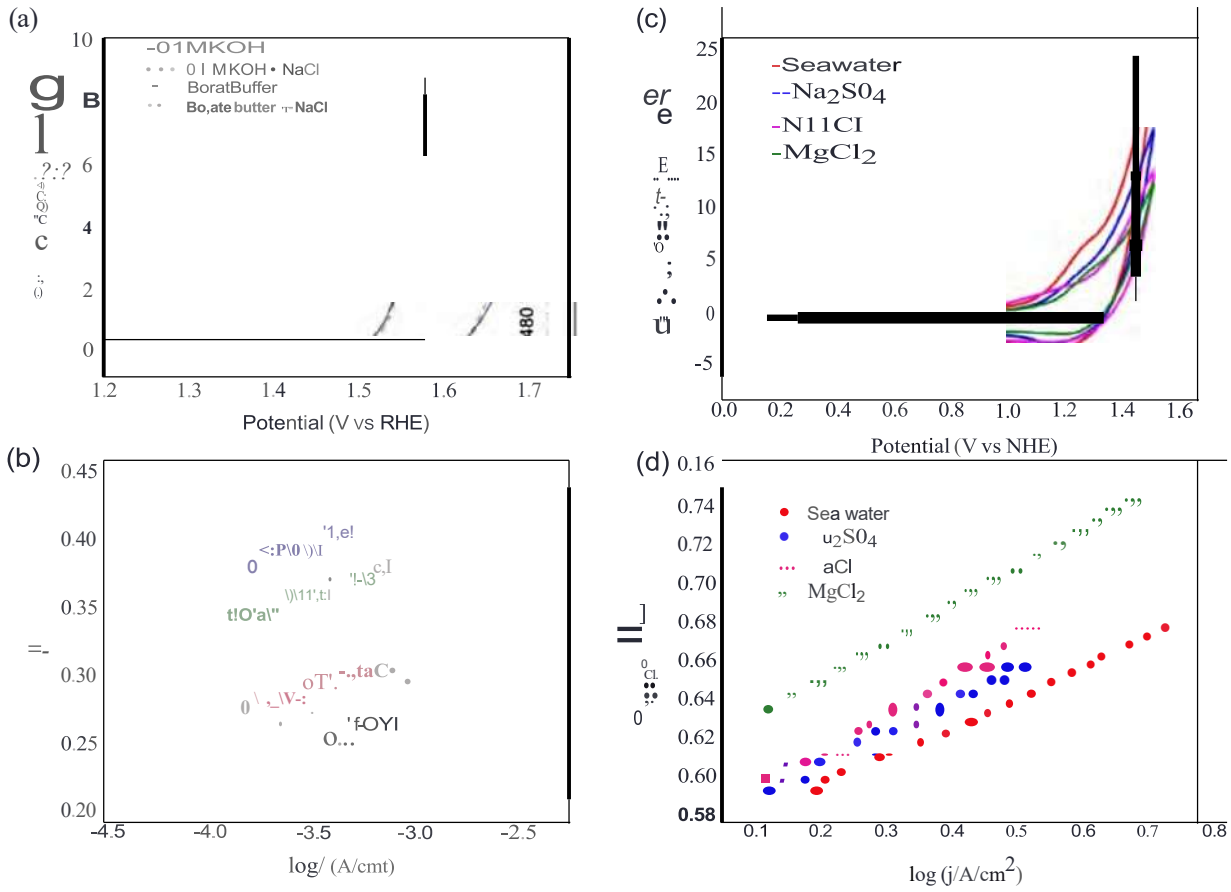

Figure 20 | *(a) Ameasurement of the electrocatalytic OER activities of carbon-supported NiFeWH nanoplates was conducted usingfour different electrolytes. A dashed vertical line denotes a voltage of ~0.480 V, which corresponds to the limit of design criteria. {b} The Tafel plot exhibited low current density. Reprinted with permissionfrom Ref 35. Copyright 2016 Wiley.The{c) CVs with a scan rateof 100 mvs-' and (d} the Tafel plot scanned at 1 mVs·' of Co-Fe LDHIGCEs in seawater and aqueous solutions containing electrolytes such as MgCI:,, NaCl, or Na_250_4. Reprinted with permission from Ref 97- Copyright 2017 Elsevier.*

which can be damaging to the electrocatalysts.This damage can occur" even at low current densities of less than 10 mA cm^{-2}. Continual pH fluctuation at the anode (cathode) results in the electrolyte turning acidic at the anode (cathode) electrode surface, thereby causing severe corrosion. Refer to the Pourbaix diagram (Figure 2), which indicatesthat a dropin local pHmakes OER unfavorable while enhancing the formation of chlorate. Meanwhile, hypochlorlte production seems to remain unchanged within the pH range of 6.5-10.5, relying instead on the convective diffusion of ions.'[58] To avoid CIER/CIOR, it is essential to maintain the pH level of the medium above J.5, as illustrated in Figure 2 of the Pourbaix diagram, by strict control.[5] The pH level at the electrode surface can only be regulated by buffer solutions, which are capable of consuming protons generated during OER. Therefore, It Is highly recommended to add buffer solutions. Previous studies by various researchers[3,59] have explored using borate buffer (pH 9.2), carbonate buffer (pH 8.6), and phosphate buffer (pH 7). Although studies on electrocatalytlc performances typically utilize 1 M KOH and 0.5 M NaCl as SSW, the presence of trace amounts of borate and carbonate is not sufficient to significantly change the situation.

Strasser and his team[35] reported a significant difference in OER overpotential values at a particular current density when comparing the use of borate buffer solution and not using it, while utilizing NiFe LDH nanoplates supported on carbon as the electrocatalyst. This observation was confirmed by a shift of 487 mVRHE overpotential per pH at a current density of 1 mA cm-', as illustrated in Figure 2oa,b. The addition of NaCl to the electrolyte improved the current density In the linear sweep voltammetry (LSV) plot for the borate buffer electrolyte at pH 9.2 in Figure 20a, mainly by decreasing the solution resistance. However, in electrolyzers containing a membrane, cl-Interference had a detrimental effect on performance when NaCl-containing electrolyte was used. By not exceeding an overpotential value of 480 mV, chlorine evolution can be avoided, although substantial localized pH changes may occur.The quadrupole mass spectrometer ion currents for 0_2 and Cl, were measured during chronopotentiometric experiments with an electrolyte made up of borate buffer and NaCl of pH 9.2 to confirm this phenomenon. The results showed no spikes for Cl, evolution, as depicted in Figure 20b.This confirms the effectiveness of borate buffer in proton consumption at the electrode

DOI: 10.31635/renewables.023.202300034
Citation: *Renewables* **2023**, 1, 415-454
Link to VoR:https://doi.org/10.31635/renewables.023-202300034

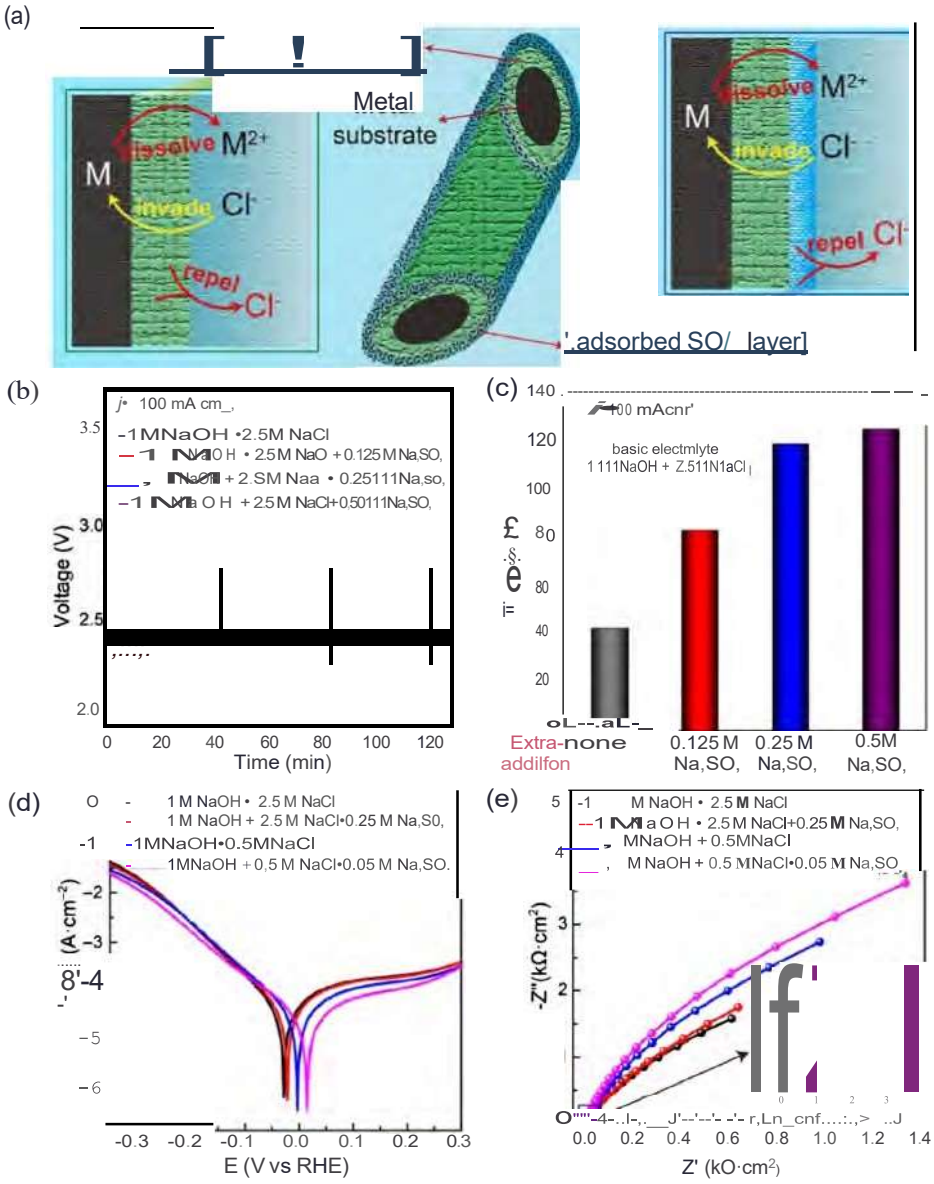

Figure 21 | *(a) In order to prevent the corrosion of the metal substrate caused by ct·, it is necessary to optimize the catalysts and electrolytes. {b} The stability of pure nickelfoam {NF} at a constant current of 100 mA cm-• in electrolytes containing different ratios of Na O4. (c) The durability of NF in various electrolytes. (d} Tafel plots and (e) Nyquist impedance plotsfor NF in the different electrolytes. Reprinted with permission from Ref 164. Copyright 2021 Wiley.*

surface, making OER preferable. Esswein et al.[160] demonstrated that the Co-borate compound is an effective OER catalyst, exhibiting 550 mV overpotential at a low current density of 1 mA cm-• in borate buffer electrolyte with pH 9.2. The metal-based catalyst maintained its catalytic activity when used in near-neutral pH-buffered seawater electrolytes by reducing the formation of passive oxide layers of metals.

Research has also been conducted on the use of phosphate buffer with a nearly neutral pH. Overall, it has been discovered that the overpotential for OER is greater when compared to highly acidic or alkaline media. Several works[97.160.161] have demonstrated this trend. Nocera and his team[16, 163] went further by investigating the use of cobalt-based phosphate/borate compounds as OER catalysts.These compounds, including Co-Pi, Co-MePi, and Co-Bi, werecreated through electrodeposition and were found to be remarkably effective for OER in seawater, even in the presence of chloride ions. The catalysts exhibited proton-accepting properties in phosphate electrolytes, with phosphate serving as a proton carrier and ensuring a steady local pH. According to the above research, this distinctive occurrence is accountable for producing a high density of current, achieving an oxygen FE of 100%. Moreover, the CoFe-LDH catalyst supported on a Ti mesh was utilized to study the OER of a SSW solution without the addition of a buffer solution at a nearly neutral pH level of 8 (Figure 20c), resulting in an overpotential of 530 mV at 10 mA cm-'. It is speculated that the presence of

DOI: 10.31635/renewables.023.202300034
Citation: *Renewab/es* 2023, 1, 415-454
Link to VoR: https://doi.org/10.31635/renewables.023-202300034

numerous ions in real seawater may impact the process by mediating proton transfer reactions, thus accelerating kinetics. This impact is evident by the smaller Tafel slope value of 140 mV dee',compared to electrolytes based on NaCl, Na_2S0_4, or $MgCl_2$, while maintaining a pH value of 8.o across all cases (demonstrated in Figure 20d).

Ma et al.'[64] recently reported that the addition of sulfate to both synthetic and authentic seawater electrolytes is an effective method to slow down chloride ion corrosion to the anode (as depicted in Figure 21a-e). Nickel foam was used as an example, and it was observed that the addition of sulfate significantly enhanced corrosion resistance and resulted in longer operational stability. The researchers discovered that sulfate anions could be selectively adsorbed onto the anode surface, creating a negatively charged layer that repels chloride ions away from the anode through electrostatic repulsion. This repulsive effect of adsorbed sulfate also applies to highly active catalysts, such as nickel-iron LOH, on nickel foam. For instance, only 268, 274, and 333 mV overpotentials were required to generate a current density of 100 mA cm-• in pure 1 M NaOH, 1 M NaOH + 0.5 **M** NaCl, and 1 M NaOH + seawater, respectively.

The addition of buffer solutions is a powerful method to control and stabilize the pH of the electrode surface, slowing down chloride ion corrosion to the anode by creating a negatively charged layer that repels chloride ions away from the anode through electrostatic repulsion.This increases the activity and, especially, the stability and selectivity of the electrolysis system. However, this is an indirect method, and our final target is to realize direct SWE technology.There is still a long way to go, and many challenges need to be addressed to implement real SWE without any additives.

Electrolyzer Devices

As shown in Table 3, developing a device for SWE is both an important and challenging task. Recently, Xie and colleagues2[5] reported a direct seawater splitting strategy that is scalable, free of side-reactions and corrosion, enabling in situ self-driven water purification and electrolysis within a single system. The strategy combines SWE with an in situ water purification process that uses a self-driven phase transition mechanism (see Figure 22a). This is achieved through a gas-path interface constructed with a hydrophobic porous polytetrafluoroethylene (PTFE)-based waterproof breathable membrane and a self-dampening electrolyte (SOE), consisting of concentrated KOH solution (Figure 22b). The membrane is designed to allow for the diffusion of water vapor and preventthe passage of liquid seawater and impurity ions. As the water vapor pressure differs,the seawater evaporates on the seawater side, and water vapor diffuses through the membrane to the SOE side for reliquefaction during operation.This method generates pure water on site, with 100% efficiency in blocking ions, which can be used for electrolysis. Through a "liquid-gas-liquid" mechanism, as shown in Figure 22a,b, a continuous and stable water migration provides fresh water for electrolysis when the water migration rate is equal to the electrolysis rate, establishing a new thermodynamic equilibrium. The water purification process has a unique mechanism that guarantees 100% efficiency in blocking ions. A scaled-up system for

Table | *Summar"t_ o[Eledrol"t_sis Devices Oe_eratin9. in Seawater*

Catalysts	Electrolyte	Performance (Current Oensity@Voltage)		Stability (h)	Reference
$Cr,0_3$-CoOx	Natural seawater	1000 mA cm-•	~2.3 V	100	24
CoFe-PB	Seawater, pH 8	o.8 mA cm-•	2.7 V	40	63
$Pb_2Ru_20_7$_x	o.6 M NaCl + 0.1 M NaOH	275 mA cm-•	1.8 V	5	66
Fe,P-$NiSe_2$ NFs	0.5 KOH + seawater	1200 mA cm-•	1.8 V	200	
Co_3.xPdx0_4	1 M PBS + 0.5 M NaCl	200 mA cm-2iooo mA cm-•	1.8 V2.65 V	450	67
MnMoSn oxide	0.5 M NaCl	100 mA cm-•	1. 60 V	1500	go
NiFeOxHy	1 M NaOH + 0.5 M NaCl	600 mA cm-•	2.7 V	100	95
S-(Ni,Fe)OOH	1 M KOH + seawater	1000 mA cm-•	1.951V	100	71
NiFe-LDH	0.5 M KOH + 0.5 M NaCl	300 mA cm-•	1.7V	12	165
Amorphous NiFeP	1.0 M KOH + 0.01 M $KHC0_3$ + 1 **M** NaCl	100 mA cm-•	1. 57 V	500	108
Co-Fe_2P/NF	1 M KOH + 0.5 M NaCl	100 mA cm-•	1. 6g V		109
Co-Se	Seawater +phosphate buffer solution pH 7.4	50 mA cm-•	2.0 V		110
NiCoS/NF	1 M KOH + seawater	1000 mA cm-'	2.04 V	100	111
$Mn_{0.929}$Moo.o6_7Sno.oo_4 O,.o6/Iro.$s_4Sn_{0\_}$,60_2/Ti	0.5m NaCl	100 mA cm-•	2.5 V	500	177
Ni-doped FeOOH	1 M KOH + seawater	800 mA cm-'	1.72 V		178
NiNS	seawater	48.3 mA cm-'	1.8 V		145
NiMoN@NiFeN	1 M KOH + seawater	100 mA cm-•	1.581 V	100	179
Ru-CoOx/NF	1 M KOH + seawaterSeawater	1000 mA cm-•	2.2 V2.62 V	100	132
S-(Ni,Fe)OOH	1 M KOH + seawater	1000 mA cm-'	1.951V	100	71

DOI: 10.31635/renewables.023.202300034
Citation: *Renewab/es* 2023,,, 415-454
Link to VoR: https: / /doi.org/10.3"1635/renewables.023-202300034

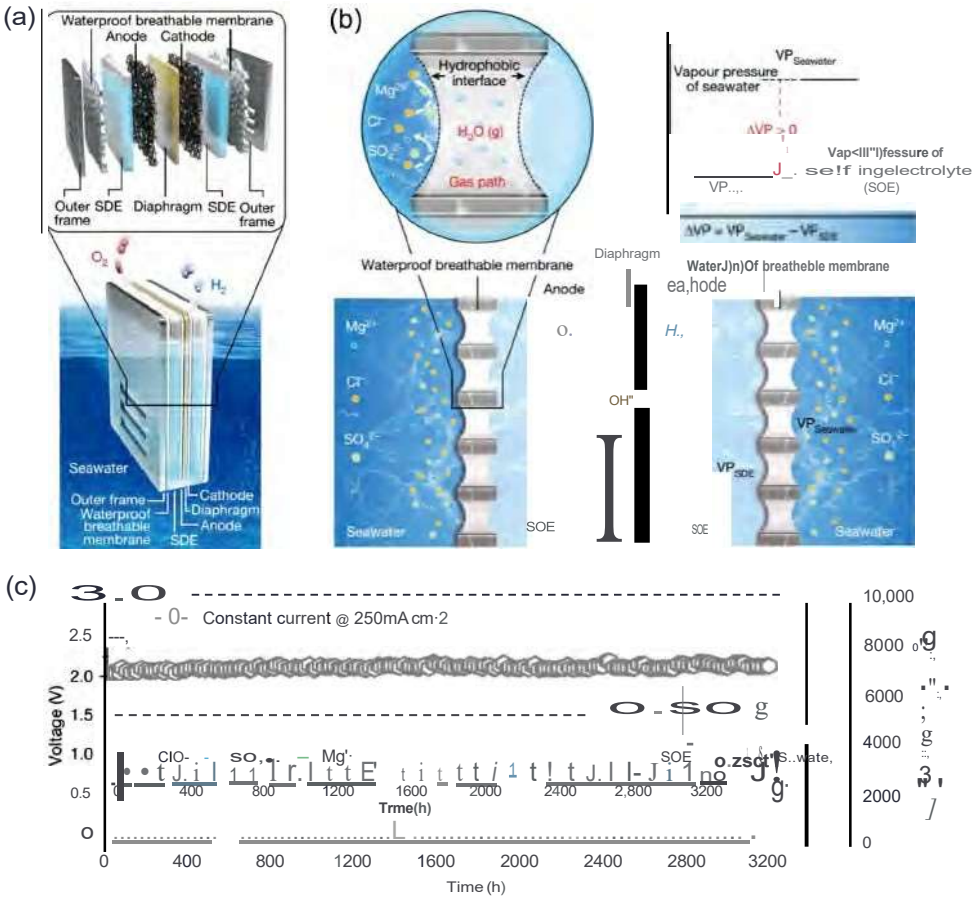

Figure 22 | *(a) Thediagram displays the structure of a typical SWE system. {b} The process of water purification and migration is powered by a mechanism based on liquid-gas-liquid phase transition and migration, as well as the drivingforce behind it. (c) The durability test for the upscaled SES was conducted through electrolysis at a consistent current density of 250 mA cm·², and the inset shows the average ion concentration. Reprinted with permission from Ref 25. Copyright 2022 Springer Nature.*

electrolyzing seawater hasbeen successfully maintained for over 3200 h at a stable rate of 386 L of H_2 per hour and a current density of 250 mA cm·² without experiencing electrocatalyst corrosion or membrane wetting, as shown in Figure 22c. This approach can beused in energy•intensive industries, wastewater treatment, and resource recovery processes that involve simul• taneous H_2 production.

An efficient direct SWE method utilizing asymmetric electro· lyte feeds was presented by Strasser's group.'[65] As illustrated in Figure 23a-f, this technique enables the direct introduction of neutral seawater to the cathode in a single pass while circulating pure KOH electrolyte at the anode. When employed in a cl-containing alkaline electrolyte, NiFe•LDH displayed superior cat• alytic activity and OER selectivity compared to Ir•based bench-mark catalysts, even at cell voltages up to 4.0 Vcell· Despite trace amounts of ci- crossing the membrane to the anode compart· ment, the NiFe•LDH anode catalyst remained fully selective for OER, avoiding any oxidation of er-, which renders it ideal for continuous high-power direct SWE at high cell voltages and current densities. However, the catalytic mechanism underlying the suppression of CIER by the use of NiFe•LDH remains ambig• uous and demands further investigation in future research. Furthermore, this asymmetric electrolyte feed saves only half of the water because the anode still requires pure KOH electro-lyte. We encourage more researchers to be dedicated to the development of advanced electrolyzers since it is one of the most important components in SWE.

Conclusion and Outlook

Hydrogen is a major resource that can be found and obtained in/ from seawater. However, the presence of impurities such as er- makes SWE more challenging than freshwater electrolysis.Thisis because er-interfereswith the anodicreactions, competing with OH-. To tackle this challenge, it is essential to develop an electrocatalyst that can selectively perform OER to minimize CIER/CIOR. Some electrocatalysts have the ability not only to choose OER over CIER/CIOR but also to maintain stability during prolonged electrolysis. According to the Pourbaix diagram for the oxygen and chlorine system in seawater, a successful OER must have a selectivity criterion of an overpotential lower than 480 mV, as the anodic chlorine reaction necessitates at least 1.73 V in an alkaline environment. Even though slightly alkaline

DOI: 10.31635/renewables.023.202300034
Citation: *Renewables* **2023,** 1, 415-454
Link to VoR: https://doi.org/10.31635/renewables.023-202300034

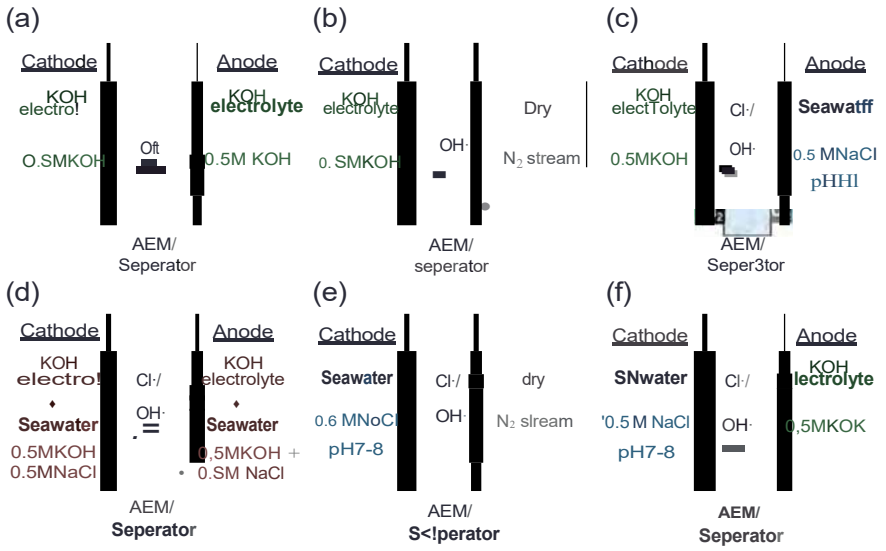

Figure 23 | *Several different approaches were proposed for AEM eledrolyzers. These methods utilized independent electrolytefeeds of varying composition, including (a)standard symmetricfeeds of 0.5 M KOH, {b) a single cathodefeed of KOH, (c)an asymmetricfeed with 0.5 M NaCl at the anode, and 0.5 M KOH at the cathode, {d} symmetric alkalinized feed of0.5 M NaCl, (e) a singlefeed of NoCl at the cathode, and (fJ an asymmetricfeed with 0.5 M KOH at the anode and 0.5 M NaCl at the cathode. Reprinted with permission from Ref 165. Copyright 2020 Royal Society of Chemistry.*

seawater with apHof 8.2 is conducive to OER, fluctuations in pH near the electrode surface demand the use of buffer solutions for consistent performance.

In practical SWE, numerous challenges must be addressed. For example, most SWE is currently performed under alkaline conditions. However, the development of SWE in acidic and neutral environments is significant for several reasons. First, acidic environments can offer improved selectivity and efficiency for certain electrochemical reactions. For example, in acidic conditions, the HER can occur with higher efficiency and selectivity, leading to increased hydrogen production rates. Second, neutral environments can offer improved stability for some electrode materials. For instance, some electrode materials may be more stable in neutral environments compared to other environments, which can lead to longer device lifetimes and improved durability. Third, developing SWE in acidic and neutral environments can expand the range of applications for the technology. For example, some industrial processes may require acidic or neutral environments, and being able to perform SWE in these environments can enable the integration of SWE into these processes. Overall, developing SWE in acidic and neutral environments can offer improved efficiency and stability and expand the range of applications for the technology.

One such challenge is the low catalytic activity and stability of anode and cathode materials. Additionally, competition reactions between OER and CIOR/CIER on the anode side and the formation of precipitates on the cathode side are also issues that require attention. Moreover, the electrolyte, pH, and potential corrosion problems must be prioritized and considered. For instance, different types of electrolysis cells, such as acid, alkaline, and neutral, require different catalyst characteristics. Addressing these issues is critical and requires significant attention and effort to solve. Further, efficient gas removal iscrucial to prevent gas bubbles from attaching to the electrode surface, blocking active sites, and causing short circuits. Various factors can affect gas removal, including current density, electrode material, electrolyte composition, electrolysis cell design, and gas evolution rate. Higher current densities generally lead to increased gas evolution, which make it more difficult to remove gas bubbles. The surface of the electrode can also influence gas removal, with rougher surfaces tending to trap gas bubbles and smoother surfaces allowing for easier gas removal. The type and concentration of electrolytes used also affect gas removal, with certain additives reducing gas bubble formation. Meanwhile, the design of the electrolysis cell plays a role, with flow-through cells or gas removal mechanisms that improve efficiency. Finally, the gas evolution rate also affects gas removal, with slower rates being easier to manage than faster ones. These factors, therefore, must be taken seriously when conducting SWE to ensure efficient gas removal and prevent the disruption of active sites.

Efficient SWE requires an ideal 30 structure and suitable hydrophilicity of the electrode materials. For the anode, a porous or nanostructured material with a high surface area can promote the electrochemical reactions involved in the OER. The anode should also be wettable by the electrolyte to enhance the transfer of charges and reactants across the interface. For the cathode, it is important to develop advanced materials with novel 30 structures that can addressimpurity deposition, such as $Ca(OH)_2$ and $Mg(OH)_2$. Impurity deposition can block active sites and pore channels of catalysts, poison and inactivate the catalysts, increase mass transfer resistance, and ultimately reduce device lifetime and cell efficiency.

DOI: 10.31635/renewables.023.202300034
Citation: *Renewables* **2023,** 1, 415-454
Link to VoR: https://doi.org/10.31635/renewables.023-202300034

Moreover, the surface hydrophilia/hydrophobicity of the catalyst electrode and gas diffusion layer {GDL) is crucial in avoiding water flooding and ensuring well-controlled hydrogen/oxygen gas diffusion during SWE. A hydrophobic electrode/GDL is necessary to prevent water flooding and maintain controlled hydrogen/oxygen diffusion. Conversely, a hydrophilic electrode/GDL is required to enlarge the three-phase reaction interface and ensure intimate contact between the electrolyte and electrode. Achieving a well-balanced hydrophobic/hydrophilic property of electrode/GDL is essential. Therefore, the rational design of electrode materials with optimal hydrophobic/hydrophilic properties and a friendly interface structure/architecture is critical to the success of SWE.

The commercial implementation of SWE has been hindered by various challenges compared to freshwater electrolysis. However, as hydrogen-based fuel technology becomes increasingly important, these challenges need to be addressed to take advantage of the significant hydrogen source available and meet future energy demands. Removing unwanted ionic species from seawater through filtration or other methods may not be practical due to the cost of implementing and maintaining expensive, unsustainable membranes and the additional energy required, which increases the cost of producing hydrogen from seawater. Therefore, simply developing new electrocatalysts with selective active sites for OER will not be enough to overcome these challenges. Researchers must also explore the design of novel electrolyzers. SWE differs significantly from conventional alkaline WE. The reactor and membrane {either PEM or AEM) must be carefully designed to protect the membrane as much as possible. Nonetheless, it should perform as well as freshwater electrolysis in alkaline WE. Recent research suggests that asymmetric reactor design is a promising technique. This technique uses a single electrolyte feeder, seawater, for the cathode chamber and alkaline water for the anode chamber. The design employed effectively hinders the migration of c1- ions towards the anode and consequently safeguards the electrocatalyst, resulting in a superb and enduring performance. Nonetheless, this approach hasits limitations since it solely employs a mixture of 50% seawater and 50% alkaline freshwater, and cannot be considered a definitive solution.

Despite significant efforts aimed at SWE, the mass production of hydrogen through this process still faces significant obstacles to commercialization. A market survey focused on sustainable industrial hydrogen production from seawater has indicated that the electrolyzer must achieve an efficiency target of 70-80%. Given that seawater covers 97% of the earth's surface and can potentially serve asa source of hydrogen, extensive research in this field is necessary. The purpose of this review is to provide fundamental theories on seawater splitting and to discuss the design of electrocatalysts for selective anodic reactions, cathodic reactions, electrolytes, and recent developments in rational electrolyzer design. We anticipate that future research on seawater splitting catalysts will prioritize the following areas of focus:

(1) Improving the intrinsic activity, especially the selectivity and stability of catalysts.

Despite considerable advancements in creating OER catalysts that are highly active in alkaline seawater, there is still a need to enhance the activity of OER electrocatalysts that operate in neutral seawater. Furthermore, certain catalysts exhibit a trade-off between activity and selectivity, where an increasein activityis accompanied by a corresponding reduction in selectivity and stability. In certain cases, even though selectivity has significantly improved, activity has decreased. Therefore, the development of highly effective catalysts with improved intrinsic activity, selectivity, and stability for the OER in SWE reactions is desirable.

(2) Strengthening mechanism research by integrating theoretical computation with experimental methods organically.

The current research methods for catalysts still mainly focus on the trial-and-error approach. This classical process is time-consuming and labor-intensive, and it is not conducive to screening and optimizing catalysts. Combining mechanism research and theoretical calculations helpsto effectively clarify the intermediate products of OER and CIER/CIOR as well as the adsorption energy on different material surfaces, which can effectively guide the design and preparation of the optimal catalysts. The rapid development of DFT calculations and in situ characterization techniques is expected to accelerate the progress of catalyst development. These techniques include in situ X-ray diffraction, X-ray photoelectron spectroscopy {XPS), Fourier transform infrared Raman spectroscopy, and in situ synchrotron radiation spectroscopy, which can offer direct observations of the catalyst's structural modifications and the adsorption of molecules such as H_20 and OH° during the OER/CIORin seawater. By using DFT calculations, it is possible to gain a comprehensive understanding of the adsorption of OER/CIORintermediates on active sites.This advantage has great importance for identifying the rate-determining step of the reaction and improving reaction pathways for OER. In situ characterization techniques can analyze the deterioration of catalysts during seawater splitting. DFT calculations and high-throughput screening methods can effectively screen materials for structural stability issues. A comprehensive approach that involves theoretical calculations, thorough reaction kinetics analysis, and operando characterization can assist in creating cost-effective and efficient catalysts for direct SWE.

(3) Developing efficient nonprecious metal catalysts.

Currently, the most effective catalysts for oxygen evolution still heavily rely on expensive iridium and ruthenium oxides, which is economically unfavorable for SWE hydrogen production. Moreover, iridium and ruthenium oxides are often plagued by side reactions such aschlorine gas evolution, making it crucial to develop alternative nonnoble metal catalysts.

(4) Increasing the number of catalytically active sites.

Enhancing the catalytic activity efficiency of a material can be achieved by increasing the number of active sites. One effective method is to customize the morphology of the catalyst to generate a large number of active sites, such as by creating a porous or ultrathin 2D or 3D structure. This approach to design enhances the material's catalytic performance. Alternatively, it is also possible to create single atomic catalysts, which utilize each atom to the maximum and increase the number of active sites.

DOI: 10.31635/renewables.023.202300034
Citation: *Renewab/es* 2023,,, 415-454
Link to VoR:https:/ /doi.org/10.3"1635/renewables.023-202300034

Moreover, by increasing the active site count, it is possible to limit catalyst decay caused by impurity of ion deposition in seawater, especially on the cathode side, which leads to an extended catalyst lifespan.

(5) Designing efficient electrolytes for SWE.

In comparison to the pure freshwater utilized in traditional WE, as well as the SSW that employs chloride solutions, real seawater boasts a more intricate composition. Therefore, conducting a mechanistic study of reactions in natural seawater becomes necessary. During direct SWE, the pH change near the electrode surface is dramatic, which can cause corrosion to the catalyst and electrolyzer. Therefore, it is advisable to add an additive or buffer solution, such as carbonate, sulfate, phosphate, and others.

(6) Optimizing the triple-phase interface and developing novel electrolytic cells/electrolyzer.

To carry out effective industrial-scale SWE, it is important to take into account the mass transport occurring at the triple-phase interface in the electrolyzers' membrane-electrode assembly. The thickness of the catalyst layer, membrane, and operational conditions must be optimized to maximize hydrogen/oxygen production efficiency. In addition, adjustments to the hydrophilicity of the electrode are also critical. WE catalysts are usually designed to be hydrophilic to facilitate electrolyte transport and the diffusion of hydrophobic 0_2 and H_2 produced during the OER and HER. Additionally, a comprehensive understanding of catalyst uniformity and stability is indispensable for practical catalyst applications at both micro and macro levels. Moreover, the development of innovative electrolyzers presents a daunting yet essential task.With the electrolyte pHfluctuation and the corrosive nature of chloride ionsin SWE, electrolyzers are confronted with significant hurdles. As such, researchers must strive to create efficient and cost-effective electrolyzers that possess increased resistance to acid and alkali corrosion.

(7) Pay more attention to electrode materials and supporting matrices.

To ensure the efficient and effective operation of the electrolysis cell, electrode materials and matrices require more attention. Electrode materials must meet several requirements. First, they must be conductive to allow for the transfer of electrons between the electrode and the electrolyte. This is essential for the electrochemical reactions to occur at the electrode surface. Second, the electrode material must be stable under the conditions of the electrolysis cell, including resistance to corrosion, oxidation, and reduction reactions that may occur during the electrochemical reactions. Third, the electrode material must have a high surface area to maximize the number of active sites available for the electrochemical reactionsto occur.This can be achieved through the use of porous or nanostructured materials. Fourth, the electrode material must be cost-effective to reduce the overall price of SWE. Finally,the electrode material must be compatible with the electrolyte used in the electrolysis cell, including factors such as pH, ionic strength, and potential for impurity deposition.

Currently, metal-based nickel, iron,titanium, copper, stainless foam, foil, plate, mat, carbon paper, carbon cloth, carbon fiber paper, glassy carbon, and so on are widely used as electrodes/matrices to support the catalysts. It is suggested to consider the above-mentioned factors, especially the friendly interface between the electrode and catalyst when selecting an electrode.

(8) Using real seawater instead of simulative seawater.

Currently, many researchers still use SSW to investigate the performance of SWE. We encourage researchers located near the ocean to use real seawater instead. This is because the composition of real seawater is complex and varies worldwide compared to SSW. Therefore, it is crucial to use a standardized electrolyte composition to benchmark new catalyst materials. Similarly, for buffered saline water, a similar standard should be employed, along with a clearly defined nature and concentration of the buffer species. other relevant parameters that require standardization include long-term stability assessment (>100 h) at a standard current density of10 mA cm^{-2} in batch systems and 200 mA cm^{-2} in flow electrolysis cells.

In all, utilizing the vast resources of seawater has emerged as a hopeful avenue to generate hydrogen fuel. Our conviction lies in the advancement of theoretical comprehension and the design of effective catalysts/electrolytes/devices that will facilitate the utilization of SWEto produce hydrogen fuel.This process is envisioned to revolutionize the global energy landscape and lead to a sustainable and environmentally friendly future.

Conflict of Interest

There is no conflict of interest to report.

Funding Information

Y.Y. acknowledges financial support from the National Science Foundation under grant no. CBET-1949840 and ACS PRF (65481-NDio). J.C. acknowledges financial support from the National Natural Science Foundation of China (grant no. 22102105) and a start-up grant from Northeast Normal University (NENU).

References

1. Mufutau, 0. B. Path to Sustainable Energy Consumption: The Possibility of Substituting Renewable Energy for Non-Renewable Energy. *Energy* 2021, *228,* 120519.

2. Thomas,J.M.; Harris, K.D.M. Some of Tomorrow'sCatalystsfor Processing Renewable and Non-Renewable Feedstocks, Diminishing Anthropogenic Carbon Dioxide and Increasing the Production of Energy. *Energy Environ. Sci.* 2016, *9,* 687-708.

3. Liu, J.; Duan,S.; Shi, H.; Wang, T.; Yang, X.; Huang, Y.; Wu, G.; Li, Q.Rationally Designing Efficient Electrocatalysts for Direct Seawater Splitting: Challenges, Achievements, and Promises. *Angew. Chem. Int. Ed.* 2022, *61,* e202210753.

4. Shih, C. F.; Zhang, T.; Li, J.; Bai, C. Powering the Future with Liquid Sunshine. *Joule* 2018, *2,* 1925-1949.

5. Dresp, S.;Dionigi, F.; Klingenhof, M.; Strasser, P. Direct Electrolytic Splitting of Seawater: Opportunities and Challenges. *ACS Energy Lett.* 2019, *4,* 933-942.

DOI: 10.31635/renewables.023.202300034
Citation: *Renewab/es* 2023,, 415-454
Linkto VoR:https:/ /doi.org/10.3'1635/renewables.023-202300034

6. Wang, X.; Wang, Z.; Garcia de Arquer, F. P.; Dinh, C.-T.; Ozden, A.;Li,Y.C.;Nam, D.-H.; Li,J.; Liu,Y.-S.; Wicks, J.;Chen, Z.;Chi, M.; Chen, B.; Wang, Y.; Tam, J.; Howe, J. Y.; Proppe, A.; Todorovic, P.; Li, F.; Zhuang, T.-T.; Gabardo, C. M.; Kirmani, A. R.; Mccallum, C.; Hung, S.-F.; Lum, Y.;Luo,M.; Min, Y.; Xu,A.;O'Brien, C.P.; Stephen, B.; Sun, B.; Ip, A. H.; Richter, L. J.; Kelley, S. O.; Sinton, D.; Sargent, E. H. Efficient Electrically Powered CO_2-to-Ethanol via Suppression of Deoxygenation. *Nat. Energy* 2020, *5,* 478-486.

7. Birdja, Y. Y.; Perez-Gallent, E.; Figueiredo, **M.** C.; Gottle, A J.; Calle-Vallejo, F.; Koper, **M.** T. M. Advances and Challenges in Under- standing the Electrocatalytic Conversion of Carbon Dioxide to Fuels. *Nat. Energy* 2019, *4,* 732-745.

8. Huang,J.K.; Li, F., Ozden,A.;Rasouli, A.S.; de Arquer, F. P.G.;Liu, S.; Zhang, S.; Luo, M.; Wang,X.; Lum, Y.; Xu, Y.; Berterns, K.; Miao, R. K.; Dinh, C.-T.; Sinton, D.; Sargent, E. H. CO_2 Electrolysis to Multicarbon Products in Strong Acid. *Science* 2021, *372,* 1074-1078.

9. Chang, J.; Wang, G.; Zhang, W.; Yang, Y. Atomically Dispersed Catalysts for Small Molecule Electrooxidation in Direct Liquid Fuel Cells. *J. Energy Chem.* 2022, *68,* 439-453.

10. Chang,J.-F.; Xiao,Y.;Luo, Z.-Y.; Ge,J.-J.; Liu, C.-P.; Xing, W.Recent Progress of Non-Noble Metal Catalysts in Water Electrolysis for Hydrogen Production. *Acta Phys. Chim. Sin.* 2016, *32,* 1556-1592.

11. Zhang, H.; Shen, P. K. Recent Development of Polymer Electrolyte Membranes for Fuel Cells. *Chem. Rev.* 2012, *112,* 2780-2832.

12. He, Y.; Liu, S.; Priest, C.; Shi, Q.; Wu, G. Atomically Dispersed Metal-Nitrogen-Carbon Catalysts for Fuel Cells:Advances in Catalyst Design, Electrode Performance, and Durability Improvement. *Chem. Soc. Rev.* 2020, *49,* 3484-3524.

13. Ramaswamy, N.; Mukerjee, S. Alkaline Anion-Exchange Membrane Fuel Cells: Challenges in Electrocatalysis and Interfacial Charge Transfer. *Chem. Rev.* 2019, *119,* 11945-11979.

14. Wang, Y. J.; Wilkinson, D. P.; Zhang, J. Noncarbon Support Materials for Polymer Electrolyte Membrane Fuel Cell Electrocatalysts. *Chem. Rev.* 2011, *111,* 7625-7651.

15. Debe, M. K. Electrocatalyst Approaches and Challenges for Automotive Fuel Cells. *Nature* 2012, *486,* 43-51.

16. Chang, J.; Xiao, Y.; Xiao, M.; Ge, J.; Liu, C.; Xing, W. Surface Oxidized Cobalt-Phosphide Nanorods as an Advanced Oxygen Evolution Catalyst in Alkaline Solution. *ACS Cata/.* 2015, *5,* 6874-6878.

17. Chang, J.; Li, K.; Wu, Z.; Ge, J.; Liu, C.; Xing, W. Sulfur-Doped Nickel Phosphide Nanoplates Arrays: A Monolithic Electrocatalyst for Efficient Hydrogen Evolution Reactions. *ACS Appl. Mater. Interfaces* 2018, 70, 26303-26311.

18. Li, G.; Li, K.;Yang, L; Chang, J.; Ma, R.; Wu, Z.; Ge, J.; Liu, C.; Xing, W. Boosted Performance of Ir Species by Employing TiN as the Support toward Oxygen Ewlution Reaction. *ACS Appl. Mater. Interfaces* 2018, *10,* 38117-38124.

19. Chang,J.; Ko,T.-J.; Je,M.; Chung, H.-S.; Han, S.S.; Shawkat, M. S.; Wang,M.; Park, S.J.; Yu, S. M.; Bae, T.-S.; Moon,M.-W.; Oh, K.H.; Choi, H.; Yang, Y.;Jung, Y. Layer Orientation-Engineered Two-Dimensional Platinum Ditelluride for High-Performance Direct Alcohol Fuel Cells. *ACS Energy Lett.* 2021, 6, 3481-3487.

20. Zou, X.; Zhang, Y. Noble Metal-Free Hydrogen Evolution Catalysts for Water Splitting. *Chem. Soc. Rev.* 2015, *44,* 5148-5180.

21. Tong, W.; Forster, M.; Dionigi, F.; Dresp, S.; Sadeghi Erami, R.; Strasser, P.; Cowan, A. J.; Farras, P. Electrolysis of Low-Grade and Saline Surface Water. *Nat. Energy* 2020, *5,* 367-3n.

22. Yu, J.; Li, B.-Q.; Zhao, C.-X.; Zhang, Q. Seawater Electrolyte-Based Metal-Air Batteries: From Strategies to Applications. *Energy Environ. Sci.* 2020, *13,* 3253-3268.

23- Desai, D.; Beh, E. S.; Sahu, S.; Vedharathinam, V.; van Overmeere, Q.; de Lannoy, C. F.; Jose, A. P.; Volkel, A. R.; Rivest, J.B. Electrochemical Desalination of Seawater and Hypersaline Brines with Coupled Electricity Storage. *ACS Energy Lett.* 2018, *3,* 375-379.

24. Guo, J.; Zheng, Y.; Hu, Z.; Zheng, C.; Mao, J.; Du, K.; Jaroniec, **M.;** Qiao, S.-Z.;Ling, T.Direct Seawater Electrolysis by Adjusting the Local Reaction Environment of a Catalyst. *Nat. Energy* 2023, *8,* 264-272.

25. Xie, H.; Zhao, Z.; Liu, T.; Wu, Y.; Lan, C.; Jiang, W.; Zhu, L.; Wang, Y.; Yang, D.; Shao, Z. A Membrane-Based Seawater Electrolyser for Hydrogen Generation. *Nature* **2022**, *612,* 673-678.

26. Hausmann, J. **N.;** Schlogl, R.; Menezes, P.W.; Driess, **M.** Is Direct Seawater Splitting Economically Meaningful? *Energy Environ. Sci.* **2021**, *14,* 3679-3685.

27. Khan, **M.A.;** Al-Attas, T.; Roy, S.; Rahman, **M. M.;** Ghaffour, N.; Thangadurai, V.;Larter, S.; Hu, J.; Ajayan, P.M.; Kibria, M. G.Seawater Electrolysis for Hydrogen Production: A Solution Looking for a Problem? *Energy Environ. Sci.* 2021, *14,* 4831-4839.

28. Khatun, S.; Hirani, H.; Roy, P. Seawater Electrocatalysis: ActMty and Selectivity. *J. Mater. Chem. A* 2021, *9,* 74-86.

29. Bolar, S.; Shit, S.; Chandra Murmu, **N.;** Kuila, T. Progress in Theoretical andExperimental Investigation on Seawater Electrolysis: Opportunities and Challenges. *Sustain. Energy Fuels* **2021**, *5,* 5915-5945.

30. Mohammed-Ibrahim, J.; Moussab, H. Recent Advances on Hydrogen Production Through Seawater Electrolysis. *Mater. Sci. Energy Technol.* 2020, *3,* 780-807.

31. Zhang, F.; Yu, L; Wu, L; Luo, D.; Ren, Z. Rational Design of Oxygen Evolution Reaction Catalysts for Seawater Electrolysis.*Trends Chem.* 2021, *3,* 485-498.

32. Joya, K. S.; Joya, Y. F.; de Groot, H.J. M. Ni-Based Electrocatalyst for Water Oxidation Developed In-Situ in a HCO_3-/CO_2 System at Near-Neutral pH. *Adv. Energy Mater.* 2014, *4,* 1301929.

33. Li, P.; Zhao, R.; Chen, H.; Wang, H.; Wei, P.; Huang, H.; Liu, Q.; Li, T.; Shi, X.; Zhang, Y.; Liu, M.; Sun, X. Recent Advances in the Development of Water Oxidation Electrocatalysts at Mild pH. *Small* 2019, *15,* e1805103-

34. Dong, Y.; Komarneni, S. Strategies to Develop Earth-Abundant Heterogeneous Oxygen Evolution Reaction Catalysts for pH-Neutral or pH-Near-Neutral Electrolytes. *Small Methods* 2021, *5,* e2000719.

35. Dionigi, F.; Reier, T.; Pawolek, Z.; Gliech, M.; Strasser, P. Design Criteria, Operating Conditions, and Nickel-Iron Hydroxide Catalyst Materials for Selective Seawater Electrolysis. *ChemSusChem* 2016, *9,* 962-972.

36. Zhou, Z.; Pei, Z.; Wei, L; Zhao, S.; Jian, X.; Chen, Y. Electrocatalytic Hydrogen Evolution Under Neutral pH Conditions: Current Understandings, Recent Advances, and Future Prospects. *Energy Environ. Sci.* 2020, *13,* 3185-3206.

37. Auinger, **M.;** Katsounaros, I.; Meier, J. C.; Klemm, S. 0.; Biedermann, P. U.; Topalov, A. A.; Rohwerder, M.; Mayrhofer, K. J. Near-Surface Ion Distribution and Buffer Effects During Electrochemical Reactions. *Phys. Chem. Chem. Phys.* 2011, *13,* 16384-16394.

38. Katsounaros, I.; Meier, J. C.; Klemm, S. O.; Topalov, A. A; Biedermann, P.U.; Auinger, M.; Mayrhofer, K.J. J.TheEffective Surface pH During Reactions at the Solid-liquid Interface. *Electrochem. Commun.* 2011, *13,* 634-637.

DOI: 10.31635/renewables.023.202300034
Citation: *Renewab/es* 2023, 1, 415-454
Linkto VoR:https://doi.org/Jo.31635/renewables.023-202300034

39. Feng, S.; Yu, Y.; Li, J.; Luo, J.; Deng, P.; Jia, C.; Shen, Y.; Tian, X. Recent Progress in Seawater Electrolysis for Hydrogen Evolution by Transition Metal Phosphides. *Cata/. Commun.* 2022, *162,* 106382.

40. Jiang, S.; Suo, H.; Zhang, T.; Liao,C.; Wang, Y.; Zhao, Q.; Lai, W. Recent Advances in Seawater Electrolysis. *Cata(ysts* 2022, *12,* 123.

41. Asghari, E.; Abdullah, M. I.; Foroughi, F.; Lamb,J. J.; Pollet, B. G. Advances, Opportunities, and Challenges of Hydrogen and Oxygen Production from Seawater Electrolysis: An Electrocatalysis Perspective. *Curr. Opin. Electrochem.* 2022, *31,* 100879.

42. Ke, S.-C.; Chen, R.; Chen, G.-H.; Ma, X.-L. Mini Review on Electrocatalyst Design for Seawater Splitting: Recent Progress and Perspectives. *Energy Fuels* 2021, *35,* 12948-12956.

43. Wang, H.-Y.; Weng, C.-C.; Ren, J.-T.; Yuan, Z.-Y. An Overview and Recent Advances in Electrocatalysts for Direct Seawater Splitting. *Front. Chem. Sci. Eng.* 2021, *15,*1408-1426.

44. Wang, C.; Shang, H.; Jin, L; Xu, H.; Du, Y. Advances in Hydrogen Production from Electrocatalytic Seawater Splitting. *Nanoscale* 2021, *13,* 7897-7912.

45. Chang,J.; Wang, G.;Belharsa, A.; Ge, J.; Xing, W.; Yang, Y. Stable $Fe_2P_2S_6$ Nanocrystal Catalyst for High-Effciency Water Electrolysis. *Small Methods* 2020, *4,* 1900632.

46. Chang, J.; Lv, Q.; Li, G.; Ge, J.; Liu, C.; Xing, W. Core-Shell Structured N $_2P_5$/$Ni_3(P0_4)_2$ Hollow Spheres as Difunctional and Efficient Electrocatalysts for Overall Water Electrolysis. *Appl. Cata/. B Environ* 2017, *204,* 486-496.

47. Chang, J.; Liang, L; Li, C.; Wang, **M.;** Ge, J.; Liu, C.; Xing, W. Ultrathin Cobalt Phosphide Nanosheets as Efficient Bifunctional Catalysts for a Water Electrolysis Cell and the Origin for Cell Performance Degradation. *Green Chem.* 2016, *18,* 2287-2295.

48. Chang, J.; Li, S.; Li, G.; Ge, J.; Liu, C.; Xing, W. Monocrystalline $Ni_{12}P_5$Hollow Spheres with Ultrahigh Specific Surface Areas as Advanced Electrocatalysts for the Hydrogen Evolution Reaction. *J. Mater. Chem. A* 2016, *4,* 9755-9759.

49. Chang, J.; Ouyang, Y.; Ge, J.; Wang, J.; Liu, C.; Xing, W. Cobalt Phosphosulfide in the Tetragonal Phase: A Highly Active and Durable Catalyst for the Hydrogen Ewlution Reaction.J. *Mater.Chem. A* 2018, *6,* 12353-12360.

50. Karlsson, R. K.; Cornell, A. Selectivity Between Oxygen and Chlorine Evolution in the Chier-Alkali and Chlorate Processes. *Chem. Rev.* 2016, *116,* 2982-3028.

51. Exner, K. S.; Anton, J.; Jacob, T.; Over, H. Full Kinetics from First Principles of the Chlorine Evolution Reaction over a $Ru0_2$ (110) Model Electrode. *Angew. Chem. Int Ed.* 2016, *55,* 7501-7504.

52. Exner, K. S.; Sohrabnejad-Eskan, I.; Over, H. A Universal Approach to Determine the Free Energy Diagram of an Electrocatalytic Reaction. *ACS Cata/.* **2018,** *8,* 1864-1879.

53. Exner, K. S.;Anton,J.; Jacob, T.; Over, H. Controlling Selectivityin the Chlorine Evolution Reaction over $Ru0_2$-Based Catalysts. *Angew Chem Int Ed* 2014, *53,* 11032-11035.

54. Wu, X.; Zhou,S.; Wang, Z.; Liu,J.; Pei, W.;Yang, P.; Zhao,J.; Qiu,J. Engineering Multifunctional Collaborative Catalytic Interface Enabling Efficient Hydrogen Evolution in All pH Range and Seawater. *Adv. Energy Mater.* 2019, *9,* 1901333.

55. Jin, H.; Wang, X.; Tang, C.; Vasileff, A.; Li, L; Slattery, A.; Qiao, S. Z. Stable and Highly Efficient Hydrogen Evolution from Seawater Enabled by an Unsaturated Nickel Surface Nitride. *Adv. Mater.* 2021, *33,* e2007508.

56. Zang, **W.;** Sun, T.; Yang, T.; Xi, S.; Waqar, **M.;** Kou, Z.; Lyu, Z.; Feng, Y. P.; Wang, J.; Pennycook, S. J. Efficient Hydrogen Evolution of Oxidized **Ni-N_3** Defective Sites for Alkaline Freshwater and Seawater Electrolysis. *Adv. Mater.* 2021, *33,* e2003846.

57. Wu, L; Yu, L; Zhang, F.; McElhenny, B.; Luo, D.; Karim, A.; Chen, S.; Ren, Z. Heterogeneous Bimetallic Phosphide Ni_2P-Fe_2P as an Efficient Bifunctional Catalyst for Water/Seawater Splitting. *Adv. Funct. Mater.* 2020, *31,* 2006484.

58. Huang, C.; Zhou, J.; Duan, D.;Zhou, Q.; Wang, J.; Peng, B.;Yu, L; Yu, Y. Roles of Heteroatoms in Electrocatalysts for Alkaline Water Splitting: A Review Focusing on the Reaction Mechanism. *Chin. J. Cata/.* 2022, *43,* 2091.

59. Seh, Z.W.; Kibsgaard, J.; Dickens, C. F.;Chorkendorff, I.; Norskov, J. K.; Jaramillo, T. F. Combining Theory and Experiment in Electrocatalysis: Insights into Materials Design. *Science* 2017, *355,* 6321.

60. Chang, J.; Wang, G.; Yang, Z.; Li, B.; Wang, Q.; Kuliiev, R.; Orlovskaya, N.; Gu, M.; Du, Y.; Wang, G.; Yang, Y. Dual-Doping and Synergism Toward High-Performance Seawater Electrolysis. *Adv. Mater.* 2021, *33,* e2101425.

61. Wu, Z.Y.; Chen, F.Y.; Li, B.; Yu, S. W.; Finfrock, Y. Z.; Meira, D. M.; Yan,Q.Q.; Zhu,P.; Chen, M. X.;Song,T. W.; Yin, Z.;Liang, H. W.; Zhang, S.; Wang, G.; Wang, H. Non-Iridium-Based Electrocatalyst for Durable Acidic Oxygen Evolution Reaction in Proton Exchange Membrane Water Electrolysis. *Nat. Mater.* 2023, *22,* 100-108.

62. Vos, J. G.; Liu, Z.; Speck, F. D.; Perini, N.; Fu, W.; Cherevko, S.; Koper, M. T. M. Selectivity Trends Between Oxygen Evolution and Chlorine Evolution on Iridium-Based Double Perovskites in Acidic Media. *ACS Cota/.* 2019, *9,* 8561-8574.

63. Hegner, F. S.; Garces-Pineda, F. A.; Gonzalez-Cobos, J.; Rodriguez-Garcia, B.; Torrens, **M.;** Palomares, E.; Lopez, **N.;** Galan-Mascar6s, J.-R. Understanding the Catalytic Selectivity of Cobalt HexacyanoferrateToward Oxygen Evolution in Seawater Electrolysis. *ACS Cata/.* 2021, *11,* 13140-13148.

64. Huang, C.; Zhou, Q.;Duan, D.; Yu, L; Zhang, W.; Wang, Z.;Liu,J.; Peng, B.; An, P.; Zhang, J.; Li, L; Yu, J.; Yu, Y. The Rapid Self-Reconstruction of Fe-Modified Ni Hydroxysulfide for Efficient and Stable Large-Current-Density Water/Seawater Oxidation. *Energy Environ. Sci.* 2022, *15,* 4647-4658.

65. Petrykin, V.;Macounova, K.;Shlyakhtin, 0. A.;Krtil,P.Tailoring the Selectivity for Electrocatalytic Oxygen Evolution on Ruthenium Oxides by Zinc Substitution. *Angew. Chem. Int Ed.* 2010, *49,* 4813-4815.

66. Gayen, P.; Saha, S.; Ramani, V. Selective Seawater Splitting Using Pyrochlore Electrocatalyst. *ACS Appl. Energy Mater.* 2020, *3,* 3978-3983.

67. Wang, N.; Ou, P.; Hung, S. F.; Huang, J. E.; Ozden, A.; Abed, J.; Grigioni, I.; Chen, C.; Miao, **R. K.;** Yan, Y.; Zhang, J.; Wang, Z.; Dorakhan, R.; Badreldin, A.; Abdel-Wahab, A.; Sinton, D.; Liu, Y.; Liang, H.; Sargent, E. H. Strong-Proton-Adsorption Co-Based Electrocatalysts Achieve Active and Stable Neutral Seawater Splitting. *Adv. Mater.* 2023, 35, e2210057.

68. Park, Y. S.; Lee, J.;Jang, **M.** J.; Yang, J.; Jeong, J.; Park, J.; Kim, Y.; Seo, M. H.; Chen, Z.; Choi, S. **M.** High-Performance Anion Exchange Membrane Alkaline Seawater Electrolysis. *J. Mater. Chem. A* 2021, *9,* 9586-9592.

69. Wang, X.H.; Ling, Y.; Wu,B.;Li, B.L; Li, X. L; Lei,J. L.;Li, N. B.; Luo, H. Q. Doping Modification, Defects Construction, and Surface Engineering: Design of Cost-Effective High-Performance Electrocatalysts

DOI: 10.31635/renewables.023.202300034
Citation: *Renewab/es* **2023,** 1, 415-454
Linkto VoR:https://doi.org/10.31635/renewables.023-202300034

and Their Application in Alkaline Seawater Splitting. *Nano Energy* 2021, *87,* 106160.
70. Cui, B.; Hu, Z.;Liu, C.; Liu, S.; Chen, F.;Hu, S.; Zhang,J.;Zhou, W.; Deng, Y.; Qin, Z.; Wu, Z.; Chen, Y.; Cui, L; Hu, W. Heterogeneous Lamellar-Edged Fe-Ni(OH),/NiJS$_2$ Nanoarray for Efficient and Stable Seawater Oxidation. *Nano Res.* 2020, 14, 1149-1155.
71. Yu, L.; Wu, L; McElhenny, B.; Song, S.; Luo, D.; Zhang, F.; Yu, Y.; Chen, S.; Ren, Z. Ultrafast Room-Temperature Synthesis of Porous S-Doped Ni/Fe (Oxy)hydroxide Electrodes for Oxygen Evolution Catal- ysis in Seawater Splitting. *Energy Environ. Sci.* 2020, *13,* 343g-3446.
72. Jimenez-Morales, I.; Cavaliere, S.; Jones, D.; Roziere, J. Strong Metal-Support Interaction Improves Activity and Stability of pt Electrocatalysts on Doped Metal Oxides. *Phys. Chem. Chem. Phys.* 2018, *20,* 8765-8n2.
73. Wei, C.; Rao, **R.R.;** Peng, J.; Huang, B.;Stephens, I.E.L.; Risch, **M.;** Xu, Z. J.; Shao-Horn, Y. Recommended Practices and Benchmark Activity for Hydrogen and Oxygen Electrocatalysis in Water Splitting and Fuel Cells. *Adv. Mater.* 2019, *31,* e1806296.
74. Zeng, L; Zhao, Z.;Lv, F.; Xia, Z.;Lu, S. Y.; Li,J.; Sun, K.; Wang, K.; Sun, Y.; Huang, Q.; Chen, Y.; Zhang, Q.; Gu, L; Lu, G.; Guo, S. Anti-Dissolution Pt Single Site with pt(OH)(OJ)/Co(P) Coordination for Efficient Alkaline Water Splitting Electrolyzer. *Nat.Commun.* 2022,*13,* 3822.
75. Zheng, J. Binary Platinum Alloy Electrodes for Hydrogen and Oxygen Evolutions by Seawater Splitting. *Appl. Surf. Sci.* 2017, *413,* 72-82.
76. Zheng,J. pt-Free NiCo Electrocatalysts for Oxygen Evolution by Seawater Splitting. *Electrochim. Acta* 2017, *247,* 381-391.
TT- Wang, B.; Lu, M.; Chen,D.; Zhang, Q.; Wang, W.; Kang, Y.; Fang, Z.; Pang, G.; Feng, S. NixFeyN@C Microsheet Arrays on Ni Foam as an Efficient and Durable Electrocatalyst for Electrolytic Splitting of Alkaline Seawater. *J. Mater. Chem. A* 2021, 9, 13562-13569.
78. Liu, J.; Yu,**M.;** Wang, X.; Wu, J.; Wang, C.; Zheng, L; Yang, D.; Liu, H.; Yao, Y.; Lu, F.; Wang, W. Investigation of High Oxygen Reduction Reaction Catalytic Performance on Mn-Based Mullite $SmMn_2O_5$. *J. Mater. Chem. A* 2017, *5,* 20922-20931.
79. Zhou, D.; Li, P.; Xu, **W.;** Jawaid, S.; Mohammed-Ibrahim, J.; Liu, W.; Kuang, Y.; Sun, X. Recent Advances in Non-Precious Metal-Based Electrodes for Alkaline Water Electrolysis. *ChemNanoMat* 2020, 6, 336-355.
80. Chinnadurai, D.; Nallal, M.; Kim, H. J.; Li, 0. L.; Park, K. H.; Prabakar, K. Mn3+Active Surface Site Enriched Manganese Phosphate Nano-polyhedrons for Enhanced Bifunctional Oxygen Electrocatalyst. *ChemCatChem* 2020, *12,* 2348-2355.
81. Lei, Z.; Wang, T.; Zhao, **B.;** Cai, W.; Liu, Y.; Jiao, S.; Li, Q.; Cao, **R.;** Liu,M. Recent Progress in Electrocatalystsfor Acidic Water Oxidation. *Adv. Energy Mater.* 2020, *10,* 2000478.
82. Osgood, H.; Devaguptapu, S.V.; Xu,H.; Cho, J.; Wu, G.Transition Metal (Fe, Co, Ni, and Mn) Oxides for Oxygen Reduction and Evolution Bifunctional Catalysts in Alkaline Media. *Nano Today* 2016, *11,* 601-625.
83. Bennett, J. E. Electrodes for Generation of Hydrogen and Oxygen from Seawater. *Int. J. Hydrogen Energy* 1980, *5,* 401-408.
84. Takashima, T.; Hashimoto, K.; Nakamura,R. Mechanisms of pH-Dependent Activity for Water Oxidation to Molecular Oxygen by MnO_2 Electrocatalysts. *J. Am. Chem. Soc.* 2012, *134,* 1519-1527.
85. Izumiya, K.; Akiyama, E.; Habazaki, H.; Kumagai, **N.;** Kawashima, A.; Hashimoto, K. Anodically Deposited Manganese Oxide and Manganese-Tungsten Oxide Electrodes for Oxygen Ewlution from Seawater. *Electrochimica Acta* **1998,** *43,* 3303-3312.
86. El-Moneim, A. A.; Kumagai, **N.;** Hashimoto, K. Mn-Mo-W Oxide Anodes for Oxygen Evolution in Seawater Electrolysis for Hydrogen Production. *Mater. Trans.* 2009, *50,* 1969-19n-
87. Fujimura, K.; Matsui, T.; Habazaki, H.; Kawashima, A.; Kumagai, **N.;** Hashimoto, K. The Durability of Manganese-Molybdenum Oxide Anodes for Oxygen Evolution in Seawater Electrolysis. *Electrochim. Acta* 2000, *45,* 2297-2303.
88. Fujimura, K.; Matsui, T.; Izumiya, K.; Kumagai, **N.;** Akiyama, E.; Habazaki, H.; Kawashima, A.; Asami, K.; Hashimoto, K. Oxygen Evolution on Manganese-Molybdenum Oxide Anodes in Seawater Electrolysis. *Mater. Sci. Eng. A* 1999, *267,* 254-259.
89. Abdel Ghany, N. A.; Kumagai, N.; Meguro, S.; Asami, K.; Hashimoto, K. Oxygen Ewlution Anodes Composed of Anodically Deposited Mn-Mo-fe Oxides for Seawater Electrolysis. *Electrochim. Acta* 2002, *48,* 21-28.
90. El-Moneim, A A.; Bhattarai, J.; Kato, Z.; Izumiya, K.; Kumagai, N.; Hashimoto, K. Mn-Mo-Sn Oxide Anodes for Oxygen Evolution in Seawater Electrolysis for Hydrogen Production. *ECS Trans.* 2010, *25,* 127-137.
91. Suntivich, J.; May, K. J.; Gasteiger, H. A.; Goodenough, J.B.;Shao-Horn, Y. A Perovskite Oxide Optimized for Oxygen Evolution Catalysis from Molecular Orbital Principles.*Science* 2011,*334,* 1383-1385.
92. Shao, D.; Li, P.; Wang, D.; Zhao, C.; Zhao, C. High OER Performance $Ni(OH)_2$ with Hierarchical Structure.*J.SolidState Electrochem.* 2019, *23,* 2051-2060.
93. Sun, Y.; Xu, K.; Wei, Z.; Li, H.; Zhang, T.; Li, X.; Cai, W.; Ma, J.; Fan, H.J.; Li, Y. Strong Electronic Interaction in Dual-Cation-Incorporated $NiSe_2$ Nanosheets with Lattice Distortion for Highly Efficient Overall Water Splitting. *Adv. Mater.* 2018, *30,* e1802121.
94. Dresp, S.; Dionigi, F.; Klingenhof, M.; Merzdorf, T.; Schmies, H.; Drnec, J.; Poulain, A; Strasser, P. Molecular Understanding of the Impact of Saline Contaminants and Alkaline pH on NiFe Layered Double Hydroxide Oxygen Evolution Catalysts. *ACS Cata/.* 2021, *11,* 6800-6809.
95. Wan, S.; Wang, X.; Zhang, G.; Wang, Y.; Chen, J.; Li, Q.; Zhang,Y.; Chen,L.; Wang, X.;Meng, G.; Jiang, K.Electrochemically Activated Ni-Fe Oxyhydroxide for Mimic Saline Water Oxidation. *ACS Sustain. Chem. Eng.* 2022, JO, 11232-11241.
96. Dresp, S.; Dionigi, F.; Loos, S.; Ferreira de Araujo, J.; Spi:iri, C.; Gliech, **M.;** Dau, H.; Strasser, P. Direct Electrolytic Splitting of Seawater: Activity, Selectivity, Degradation, and Recovery Studied from the Molecular Catalyst Structure to the Electrolyzer CellLevel. *Adv. Enery. Mater.* **2018**, *8,* 1800338.
97. Cheng, F.; Feng, X.; Chen, X.; Lin, W.; Rong, J.; Yang, W. Synergistic Action of Co-Fe Layered Double Hydroxide Electrocatalyst and Multiple Ions of Sea Salt for Efficient Seawater Oxidation at Near-Neutral pH. *Electrochim. Acta* 2017, *251,* 336-343.
98. Vos, J. G.; Wezendonk, T. A; Jeremiasse, A. W.; Koper, M. T. M. MnOx/IrOx as Selective Oxygen Evolution Electrocatalyst in Acidic Chloride Solution. *J. Am. Chem. Soc.* 2018, *140,*10270-10281.
99. Bhardwaj, A.A.; Vos, J.G.; Beatty, M. E. S.; Baxter, A.F.; Koper, **M.** T. M.; Yip, **N.** Y.; Esposito, D. V. Ultrathin Silicon Oxide Overlayers Enable Selective Oxygen Evolution from Acidic and Unbuffered pH-Neutral Seawater. *ACS Cata/.* 2021, *11,* 1316-1330.
100. Song, H.J.; Yoon, H.; Ju, B.; Lee, D.-Y.; Kim, D.-W. Electrocatalytic Selective Oxygen Evolution of Carbon-Coated Na_2Co,-x$FexP_2O_7$

DOI: 10.31635/renewables.023.202300034
Citation: *Renewab/es* **2023**, 1, 415-454
Linkto VoR:https://doi.org/10.31635/renewables.023-202300034

Nanoparticles for Alkaline Seawater Electrolysis. *ACS Cata/.* 2019, 10, 702-709.

101. Chen, H.; Zou, Y.; Li, J.; Zhang, K.; Xia, Y.; Hui, B.; Yang, D. Wood Aerogel-Derived Sandwich-Like Layered Nanoelectrodes for Alkaline Overall Seawater Electrosplitting. *Appl. Cata/. B Environ.* 2021, *293,* 120215.

102. Kuang, Y.;Kenney, **M.** J.;Meng, Y.;Hung, W.-H.; Liu,Y.;Huang,J. E.; Prasanna, R.; Li, P.; Li, Y.; Wang, L; Lin, M.-C.; McGehee, M. D.; Sun, X.; Dai, H. Solar-Driven, Highly Sustained Splitting of Seawater into Hydrogen and Oxygen Fuels. *Proc. Natl. Acad. Sci.U. S.* A 2019, 116, 6624-6629.

103. Jadhav, A R.;Kumar, A.; Lee,J.; Yang, T.; Na, S.;Lee, J.;Luo, Y.;Liu, X.; Hwang, Y.; Liu, Y.; Lee, H. Stable Complete Seawater Electrolysis by Using Interfacial Chloride Ion Blocking Layer on Catalyst Surface. *J. Mater. Chem. A* 2020, *8,* 24501-24514.

104. Xu, X.; Song, F.; Hu, X. A Nickel Iron Diselenide-Derived Efficient Oxygen-Evolution Catalyst. *Nat. Commun.* 2016, 7, 12324.

105. Zhou, H.; Yu, F.; Sun,J.; He, R.; Chen, S.;Chu, C.W.; Ren, Z. Highly Active Catalyst Derived from a 30 Foam of $Fe\{PO_3)_2/Ni_2P$ for Extremely Efficient Water Oxidation. *Proc. Natl. Acad. Sci.U. S. A.* 2017, 114, 5607-5611.

106. Keane, T. P.; Nocera, D. G. Selective Production of Oxygen from Seawater by Oxidic Metallate Catalysts. *ACS Omega* 2019, 4,12860-12864.

107. Li, G.; Li, F.; Zhao, Y.; Li, W.; Zhao, Z.; Li, Y.; Yang, H.; Fan, K.; Zhang, P.; Sun, L. Selective Electrochemical Alkaline Seawater Oxidation Catalyzed by Cobalt Carbonate Hydroxide Nanorod Arrays with Sequential Proton-Electron Transfer Properties. *ACS Sustain. Chem. Eng.* 2021, *9,* 905-913-

108. Liu, J.;Liu, X.;Shi,H.; Luo,J.; Wang, L; Liang, J.;Li, S.;Yang, L-M.; Wang, T.; Huang, Y.; Li, *Q.* Breaking the Scaling Relations of Oxygen Evolution Reaction on Amorphous NiFeP Nanostructures with Enha need Activity for Overall Seawater Splitting. *Appl.Cata/. B Environ.* 2022, *302,* 120862.

109. Wang, S.; Yang, P.; Sun, X.; Xing, H.; Hu, J.; Chen, P.; Cui, Z.; Zhu, W.; Ma, Z. Synthesis of 30 Heterostructure Co-Doped Fe,P Electrocatalyst for Overall Seawater Electrolysis. *Appl.Cata/. B Environ.* **2021,** *297,* 120386.

110. Zhao, Y.; Jin, B.; Zheng, Y.; Jin, H.; Jiao, Y.; Qiao, S.-Z. Charge State Manipulation of Cobalt Selenide Catalyst for Overall Seawater Electrolysis. *Adv. Enery. Mater.* **2018,** *8,* 1801926.

111. Wang, C.; Zhu, M.; Cao, Z.; Zhu, P.; Cao, Y.; Xu, X.; Xu, C.; Yin, Z. Heterogeneous Bimetallic Sulfides Based Seawater Electrolysis Towards Stable Industrial-Level Large Current Density. *Appl. Cata/. B Environ.* **2021,** *291,* 120071.

112. Lu, X.; Pan, J.; Lovell, E.; Tan, T. H.; Ng, Y. H.; Amal, R. A Sea-Change: Manganese Doped Nickel/Nickel Oxide Electrocatalysts for Hydrogen Generation from Seawater. *Energy Environ. Sci.* 2018, 11, 1898-1910.

113. Kirk, D.W.; Ledas, A.E. Precipitate Formation During Sea Water Electrolysis. *Int. J. Hydrogen Energy* **1982,** 7.

114. Liu, G.; Xu, Y.; Yang, T.; Jiang, L. Recent Advances in Electrocatalysts for Seawater Splitting. *Nano Mater. Sci.* 2023, 5, 101-106.

115. Wang, X.; Zhai, X.; Yu, Q.; Liu, X.; Meng, X.; Wang, X.; Wang, L. Strategies of Designing Electrocatalysts for Seawater Splitting. *J. Solid State Chem.* 2022, *306,* 122799.

116. Lindquist, G. A; Xu, *Q.;* Oener, S. Z.; Boettcher, S. W. Membrane Electrolyzers for Impure-Water Splitting. *Joule* 2020, 4, 2549-2561.

117. Parsons, R. The Rate of Electrolytic Hydrogen Evolution and the Heat of Adsorption of Hydrogen. *Trans. Faraday Soc.* 1957, *54,* 1053-1063.

118. N9)rskov, J. K.; Bligaard, T.; Logadottir, A.; Kitchin, J. R.; Chen, J. G.; Pandelov, S.; Stimming, U. Trends in the Exchange Current for Hydrogen Evolution. *J. Eledrochem. Soc.* **2005,** *152,* J23-J26.

119. Zhou, *Q.;* Liao, L; Zhou, H.; Li, D.; Tang, D.; Yu, F. Innovative Strategies in Design of Transition Metal-Based Catalysts for L.arge-Current-Density Alkaline Water/Seawater Electrolysis. *Mater. Today Phys.* **2022,** *26,* 100727.

120. Kemppainen, E.; Bodin, A.;Sebok, B.; Pedersen, T.; Seger, B.;Mei, B.; Bae, D.; Vesborg, P. C. K.; Halme, J.; Hansen, O.; Lund, P. D.; Chorkendorff, I. Scalability and Feasibility of Photoelectrochemical H, Evolution: The Ultimate Limit of Pt Nanoparticle as an HER Catalyst. *Energy Environ. Sci.* 2015, *8,* 2991-2999.

121. Chang, J.; Wang, G.; Li, C.; He, Y.; Zhu, Y.; Zhang, W.; Sajid, M.; Kara, A.; Gu, M.; Yang, Y. Rational Design of Septenary High-Entropy Alloy for Direct Ethanol Fuel Cells. *Joule* 2023, *7,* 587-602.

122. Chang, J.; Wang, G.; Chang, X.; Yang, Z.; Wang, H.; Li, B.; Zhang, W.; Kovarik, L; Du, Y.; Orlovskaya, **N.;** Xu, B.; Wang, G.; Yang, Y. Interface Synergism and Engineering of Pd/Co@N-C for Direct Ethanol Fuel Cells. *Nat. Commun.* 2023, 14, 1346.

123. Chang,J.; Wang, G.; Wang,**M.;** Wang,*Q.;*Li,B.; Zhou, H.; Zhu,Y.; Zhang, W.; Omer, **M.;** Orlovskaya, N.; Ma, *Q.;* Gu, M.; Feng, Z.; Wang, G.; Yang, Y. Improving Pd-N-C Fuel Cell Electrocatalysts Through Fluorination-Driven Rearrangements of Local Coordination Environment. *Nat. Energy* 2021, 6, 1144-1153.

124. Chang, J.; Feng, L.; Liu, C.; Xing, W.; Hu, X. Ni,P Enhances the Activity and Durability of the pt Anode Catalyst in Direct Methanol Fuel Cells. *Energy Environ. Sci.* 2014, *7,*1628-1632.

125. Chang,J.; Feng,L.; Liu, C.; Xing, W.;Hu, X. An Effective Pd-Ni,P/C Anode Catalyst for Direct Formic Acid Fuel Cells. *Angew. Chem. Int. Ed.* 2014, *53,* 122-126.

126. Chang, J.; Yang, Y. Recent Advances in Zinc-Air Batteries: Self-Standing Inorganic Nanoporous Metal Film as Air Cathodes. *Chem. Commun.* 2023, *59,* 5823-5838.

127. Guo, L; Yang, Z.;Marcus, K.; Li, Z.;Luo, B.; Zhou, L; Wang, X.;Du, Y.; Yang, Y. MoS_2/TiO_2 Heterostructures as Nonmetal Plasmonic Photocatalysts for Highly Efficient Hydrogen Evolution. *Energy Environ. Sci.* 2018, 11, 106-114.

128. Zheng, J.; Zhao, Y.; Xi, H.; Li, C. Seawater Splitting for Hydrogen Evolution by Robust Electrocatalysts from Secondary M (M = Cr, Fe, Co, Ni, Mo) Incorporated pt_ *RSC Adv.* 2018, *8,* 9423-9429.

129. Xiu, L; Pei, W.; Zhou, S.; Wang, Z.; Yang, P.; Zhao, J.; Qiu, J. Multilevel Hollow MXene Tailored Low-Pt Catalyst for Efficient Hydrogen Evolution in Full-pH Range and Seawater. *Adv.Fund. Mater.* 2020, *30,*1910028.

130. Ye, S.; Xiong, W.; Liao, P.; Zheng, L; Ren, X.;He, C.; Zhang, *Q.;*Liu, J. Removing the Barrier to Water Dissociation on Single-Atom pt sites Decorated with a CoP Mesoporous Nanosheet Array to Achieve Improved Hydrogen Evolution. *J. Mater. Chem. A* 2020, *8,* 11246-11254.

131. Chen, C.H.; Wu,D.; Li, Z.; Zhang,R.; Kuai, C.G.; Zhao, X. R.;Dong, C. K.; Qiao, S. Z.; Liu, H.; Du, X. W. Ruthenium-Based Single-Atom Alloy with High Electrocatalytic Activity for Hydrogen Evolution. *Adv. Energy Mater.* 2019, *9,* 1803913.

132. Wu, D.; Chen, D.; Zhu, J.; Mu, S. Ultralow Ru Incorporated Amorphous Cobalt-Based Oxides for High-Current-Density Overall

DOI: 10.31635/renewables.023.202300034
Citation: *Renewab/es* **2023,** 1, 415-454
Linkto VoR:https://doi.org/10.31635/renewables.023-202300034

Water Splitting in Alkaline and Seawater Media. *Small* 2021, 17, e2102m.

133. Niu, X.; Tang, Q.; He, B.; Yang, P. Robust and Stable Ruthenium Alloy Electrocatalysts for Hydrogen Evolution by Seawater Splitting. *Electrochim. Acta* 2016, *208,*180-187.

134. Li, H.; Tang, Q.; He, B.; Yang, P. Robust Electrocatalysts from an Alloyed Pt-Ru-M (M = Cr, Fe, Co, Ni, Mo)-Decorated Ti Mesh for Hydrogen Evolution by Seawater Splitting. *J. Mater. Chem. A* 2016, *4,* 6513-6520.

135. Jiang, X.; Dong, Z.; Wang,J.; Zhang, N.; Xu,G.-R.; Zhang, W.; Lai, J.; Li, Z.; Wang, L. Self-Assembly of Functionalized Echinops-like Rh Porous Nanostructure Electrocatalysts for Highly Efficient Seawater Splitting. *J. Mater. Chem. C* 2021, *9,* 8314-8322.

136. Liu, Y.; Hu, X.; Huang, B.; Xie, Z. Surface Engineering of Rh Catalysts with N/S-Codoped Carbon Nanosheets Toward High-Performance Hydrogen Evolution from Seawater. *ACS Sustain. Chem. Eng.* 2019, 7,18835-18843.

137. Gao, Y.; Xue, Y.; Qi, L.; Xing, C.; Zheng, X.; He, F.; Li, Y. Rhodium Nanocrystals on Porous Graphdiyne for Electrocatalytic Hydrogen Evolution from Saline Water. *Nat. Commun.* 2022, *13,* 5227.

138. Zhang, W.; Chang, J.; Wang, G.; Li, Z.; Wang, M.; Zhu, Y.; Li, B.; Zhou, H.; Wang, G.; Gu, M.; Feng, Z.; Yang, Y. Surface Oxygenation Induced Strong Interaction Between Pd Catalyst and Functional Support for Zinc-Air Batteries. *Energy Environ. Sci.* 2022, *15,* 1573-1584.

139. Wang, G.; Chang, J.; Koul, S.; Kushima, A.; Yang, Y. CO_2 Bubble- Assisted pt Exposure in PtFeNi Porous Film for High-Performance Zinc-Air Battery. *J. Am. Chem. Soc.* 2021, *143,* 11595-11601.

140. Zhang, W.; Chang, J.; Yang, Y. Strong Precious Metal-Metal Oxide Interaction for Oxygen Reduction Reaction: A Strategy for Efficient Catalyst Design. *SusMat* 2023, *3,* 2-20.

141. Wang, G.; Aubin, **M.;** Mehta, A.; Tian,H.; Chang, J.; Kushima, A; Sohn, Y.; Yang, Y. Stabilization of Sn Anode Through Structural Reconstruction of a Cu-Sn Intermetallic Coating Layer. *Adv. Mater.* 2020, *32,* 2003684.

142. Xu, W.; Chang, J.; Cheng, Y.; Liu, H.; Li, J.; Ai, Y.; Hu, Z.-N.; Zhang, X.; Wang, Y.; Liang, Q.; Yang, Y.; Sun, H.-b. A Multi-Step Induced Strategy to Fabricate Core-Shell pt-Ni Alloy as Symmetric Electrocatalysts for Overall Water Splitting. *Nano Res.* 2021, *15,* 965-971.

143- Yuan, W.; Cui, Z.; Zhu, S.; Li, Z.; Wu, S.; Liang, Y. Structure Engineering of Electrodeposited NiMo Films for Highly Efficient and Durable Seawater Splitting. *Electrochim. Acta* 2021, *365,* 137366.

144. Jiang, N.; Meng, H.-M.; Song, L-J.; Yu, H.-Y. Study on Ni-Fe-C Cathode for Hydrogen Evolution from Seawater Electrolysis. *IntJ. Hydrogen Energy* 2010, *35,* 8056-8062.

145. Zhao, Y.; Jin, B.; Vasileff, A.; Jiao, Y.; Qiao, S.-Z. Interfacial Nickel Nitride/Sulfide asa Bifunctional Electrode for Highly Efficient Overall Water/Seawater Electrolysis. *J. Mater. Chem. A* 2019, 7, 8117-8121.

146. Ma, Y.-Y.; Wu, C.-X.; Feng, X.-J.; Tan, H.-Q.; Yan, L-K.; Liu, Y.; Kang, Z.-H.; Wang, E.-B.; Li, Y.-G. Highly Efficient Hydrogen Evolution from Seawater by a Low-Cost and Stable CoMoP@C Electrocatalyst Superior to pt/C. *Energy Environ. Sci.* 2017, 10, 788-798.

147. Lin, Y.; Sun, K.; Chen, X.; Chen, C.; Pan, Y.; Li, X.; Zhang, J.High- Precision Regulation Synthesis of Fe-Doped Co_2PNanorod Bundles as Efficient Electrocatalysts for Hydrogen Evolution in All-pH Range and Seawater. *J. Energy Chem.* 2021, *55,* 92-101.

148. Gao, S.; Li, G.D.; Liu, Y.; Chen, H.; Feng, L.L; Wang, Y.; Yang, M.; Wang, D.; Wang, S.; Zou, X. Electrocatalytic H_2 Production from Seawater over Co, N-Codoped Nanocarbons. *Nanoscale* 2015, 7, 2306-2316.

149. Huang, W.; Zhou, D.; Qi, G.; Liu, X. Fe-Doped MoS_2 Nanosheets Array for High-Current-Density Seawater Electrolysis. *Nanotechnology* 2021, *32,* 415403.

150. Zhang, Q.; Guan, J. Single-Atom Catalysts for Electrocatalytic Applications. *Adv. Funct. Mater.* 2020, *30,* 2000768.

151. Lv, Q.; Han, J.; Tan, X.; Wang, W.; Cao, L; Dong, B. Featherlike NiCoP Holey Nanoarrys for Efficient and Stable Seawater Splitting. *ACS Appl. Energy Mater.* 2019, *2,* 3910-3917.

152. Jin, H.; Liu, X.; Vasileff, A.; Jiao, Y.; Zhao, Y.; Zheng, Y.; Qiao, S. Z. Single-Crystal Nitrogen-Rich Two-Dimensional Mo_5N_6 Nanosheets for Efficient and Stable Seawater Splitting. *ACS Nano* 2018, *12,* 12761-12769.

153. Zhu,J.; Xia, L; Yu, R.; Lu, R.; Li,J.; He, R.; Wu, Y.; Zhang, W.; Hong, X.; Chen, W.; Zhao, Y.; Zhou, L.; Mai, L; Wang, Z. Ultrahigh Stable Methanol Oxidation Enabled by a High Hydroxyl Concentration on pt Clusters/MXene Interfaces. *J Am Chem Soc* 2022, *144,* 15529-15538.

154. Zhang, J.; Zhao, Y.; Guo, X.; Chen, C.; Dong, C.-L; Liu, R.-S.; Han, C.-P.; Li, Y.; Gogotsi, Y.; Wang, G. Single Platinum Atoms Immobilized on an MXene as an Efficient Catalyst for the Hydrogen Evolution Reaction. *Nat. Cata/.* 2018, 1, 985-992.

155. Han, L.; Peng, X.; Wang, H. T.; Ou, P.; Mi, Y.; Pao, C. W.; Zhou, J.; Wang, J.; Liu, X.; Pong, W. F.; Song, J.; Lin, Z.; Luo, J.; Xin, H. L Chemically Coupling SnO_2 Quantum Dots and MXene for Efficient CO_2 Electroreduction to Formate and Zn-CO_2 Battery. *Proc. Natl. Acad. Sci. U. S. A.* 2022, 119, e2207326119.

156. Yao, Y.; Zhu, Y.; Pan, C.; Wang, C.; Hu, S.; Xiao, W.; Chi, X.;Fang, Y.; Yang, J.; Deng, H.; Xiao, S.; Li, J.; Luo, Z.; Guo, Y. Interracial sp C-O-Mo Hybridization Originated High-Current Density Hydrogen Evolution. *J. Am. Chem. Soc.* 2021, *143,* 8720-8730.

157. Kuhn,A. Y.; Chan, C.Y.pH Changes at Near-Electrode Surfaces.J. *Appl. Electrochem.* **1983,** *13,*189-207.

158. Hammar, L.; Wranglen, G. Cathodic and Anodic Efficiency Losses in Chlorate Electrolysis. *Electrochim. Acta* 1964, *9,* 1-16.

159. Kenney, M. J.; Gong, M.; Li, Y.; Wu, J. Z.;Feng, J.; Lanza, M.; Dai, H. Nickel Films for Water Oxidation High-Performance Silicon Photoanodes Passivated with Ultrathin. *Science* 2013, *342,* 836-840.

160. Esswein, A.J.; Surendranath, Y.; Reece, S.Y.; Nocera, D.G. Highly Active Cobalt Phosphate and Borate Based Oxygen Evolving Cata- lysts Operating in Neutral and Natural Waters. *Energy Environ. Sci.* 20n, *4,* 499-504.

161. Gerken, J. B.; McAlpin, J. G.; Chen, J. Y. C.; Rigsby, M. L.; Casey, W. H.; Britt, R. D.; Stahl, S. S. Electrochemical Water Oxidation with Cobalt-Based Electrocatalysts from pH 014: The Thermodynamic Basis for Catalyst Structure, Stability, and Activity. *J. Am. Chem. Soc.* 2011, *133,* 14431-14442.

162. Kanan, **M. W.;** Nocera, D. G. In Situ Formation of an Oxygen-Evolving Catalyst in Neutral Water Containing Phosphate and Co^{2+}. *Science* **2008,** *321,*1072-1075.

163. Surendranath, Y.; Dinca, **M.;** Nocera, D. G. Electrolyte-Dependent Electrosynthesis and Activity of Cobalt-Based Water Oxidation Catalysts. *J.Am. Chem. Soc.* **2009,** *131,* 2615-2620.

164. Ma, T.; Xu, W.; Li, B.; Chen, X.; Zhao, J.; Wan, S.; Jiang, K.; Zhang, S.; Wang, Z.; Tian, Z.; Lu, Z.; Chen, L. The Critical Role of Additive Sulfate for Stable Alkaline Seawater Oxidation on Nickel-Based Electrodes. *Angew. Chem. Int. Ed.* 2021, 60, 22740-22744.

DOI: 10.31635/renewables.023.202300034
Citation: *Renewab/es* **2023,** 1, 415-454
Linkto VoR:https://doi.org/10.31635/renewables.023-202300034

165. Dresp, S.; Ngo Thanh, T.; Klingenhof, **M.;** Bruckner, S.; Hauke, P.; Strasser, P. Efficient direct seawater electrolysers using selective alkaline NiFe-LDH as OER Catalyst in Asymmetric Electrolyte Feeds. *Energy Environ. Sci.* 2020, *13,* 1725-1729.

166. Gupta, S.; Forster, **M.;** Yadav, A.; Cowan, A.J.; Patel, **N.;** Patel, **M.** Highly Efficient and Selective Metal Oxy-Boride Electrocatalysts for Oxygen Evolution from Alkali and Saline Solutions. *ACS Appl. Energy Mater.* 2020, *3,* 7619-7628.

167. Chen, Y.; Shen, L; Wang, C.; Feng, S.; Zhang, N.; Zhang, K.; Yang, B. Utilizing Tannie Acid and Polypyrrle to Induce Reconstruction to Optimize the Activity of MOF-Derived Electrocatalyst for Water Oxidation in Seawater. *Chem. Eng.* J. 2022, *430,* 132632.

168. Wu, Y.; Tian, Z.; Yuan, S.; Qi, Z.; Feng, Y.; Wang, Y.; Huang, R.; Zhao, Y.; Sun, J.; Zhao, W.; Guo, W.; Feng, J.; Sun, J. Solar-Driven Self-Powered Alkaline Seawater Electrolysis via Multifunctional Earth-Abundant Heterostructures. *Chem. Eng.* J. 2021, *411,* 128538.

169. Ko, J.S.; Johnson, J. K.; Johnson, P. I.; Xia, Z. Decoupling Oxygen and Chlorine Evolution Reactions in Seawater Using Iridium-based Electrocatalysts. *ChemCatchem* 2020, *12,* 4526-4532.

170. Enkhtuvshin, E.; Kim, K. M.; Kim, Y.-K.; Mihn, S.; Kim, S. J.; Jung, S.Y.; Thu Thao, N. T.; Ali, G.; Akbar, M.; Chung,K. Y.; Chae, K.H.; Kang, S.; Lee, T. W.; Kim, H. G.; Choi, S.; Han, H. Stabilizing Oxygen Intermediates on Redox-Flexible Active Sites in Multimetallic Ni-Fe-Al-Co Layered Double Hydroxide Anodes for Excellent Alkaline and Seawater Electrolysis. J. *Mater. Chem. A* 2021, *9,* 27332-27346.

171. Hung, W. H.; Xue, B. Y.; Lin, T. M.; Lu, S. Y.; Tsao, I. Y. A Highly Active Selenized Nickel-Iron Electrode with Layered Double Hydroxide for Electrocatalytic Water Splitting in Saline Electrolyte. *Mater. Today Energy* 2021, *19,* 100575.

172. Yang, J.; Wang,Y.;Yang,J.; Pang, Y.; Zhu, X.;Lu, Y.; Wu,Y.; Wang, J.; Chen, H.; Kou, Z.; Shen, Z.; Pan, Z.; Wang, J. Quench-Induced Surface Engineering Boosts Alkaline Freshwater and Seawater Oxygen Ewlution Reaction of PorousNiC0$_2$ 0$_4$ Nanowires. *Small* 2022, *18,* e2106187.

173. Zhang, S.; Wang, W.; Hu, F.; Mi, Y.; Wang, S.; Liu, Y.; Ai, X.; Fang, J.; Li, H.; Zhai, T. 2D CoOOH Sheet-Encapsulated Ni_2P into Tubular Arrays Realizing 1000 mA cm^{-2}-Level-Current-Density Hydrogen Evolution Over 100 h in Neutral Water. *Nanomicro Lett.* 2020, *12,* 140.

174. Wen, M.; Cao, Y.; Wu, B.; Xiao, T.; Cao, R.; Wang, Q.; Liu, X.; Xue, H.; Yu, Y.; Lin, J.; Xu, C.; Xu, J.; OuYang, B. PD-L1 Degradation Is Regulated by Electrostatic Membrane Association of Its Cytoplasmic Domain. *Nat. Commun.* 2021, *12,* 5106.

175. Chen, I. P.; Hsiao, C. H.; Huang, J. Y.; Peng, Y. H.; Chang, C. Y. Highly Efficient Hydrogen Evolution from Seawater by Biofunctionalized Exfoliated MoS_2 Quantum Dot Aerogel Electrocatalysts That Is Superior to pt_ *ACS Appl. Mater. Interfaces* 2019, *11,* 14159-14165.

176. Zheng, J. Seawater Splitting for High-Efficiency Hydrogen Evolution by Alloyed ptNi x Electrocatalysts. *Appl. Surf. Sci.* 2017, *413,* 360-365.

1n. Kato, Z.; Sato, **M.;** Sasaki, Y.; Izumiya, K.; Kumagai, **N.;** Hashimoto, K. Electrochemical Characterization of Degradation of Oxygen Evolution Anode for Seawater Electrolysis. *Electrochim. Acta* 2014, *116,* 152-157.

178. Senthilkumar, S.T.; Park, S.O.; Kim, J.;Hwang, S.M.; Kwak,S. K.; Kim, Y. Seawater Battery Performance Enhancement Enabled by a Defect/Edge-Rich, Oxygen Self-Doped Porous Carbon Electrocatalyst. *1. Mater. Chem. A* 2017, *5,* 14174-14181.

179. Yu, L.; Zhu, Q.;Song, S.;McElhenny, B.; Wang, D.; Wu, C.; Qin, Z.; Bao, J.; Yu, Y.; Chen, S.; Ren, Z. Non-Noble Metal-Nitride Based Electrocatalysts for High-Performance Alkaline Seawater Electrolysis. *Nat. Commun.* 2019, *10,* 5106.

DOI: 10.31635/renewables.023.202300034
Citation: *Renewab/es* **2023**, 1, 415-454
Linkto VoR:https://doi.org/10.31635/renewables.023-202300034